A STUDY ON THE EQUILIBRIUM

GROSSULAR + CLINOCHLORE = 3 DIOPSIDE + 2 SPINEL + 4 H_2O

by

XIAOMIN WANG

A THESIS SUBMITTED IN PARTIAL FULFILMENT OF

THE REQUIREMENTS FOR THE DEGREE OF

MASTER OF SCIENCE

in

THE FACULTY OF GRADUATE STUDIES

Department of Geological Sciences

We accept this thesis as conforming

to the required standard

THE UNIVERSITY OF BRITISH COLUMBIA

June, 1986

In presenting this thesis in partial fulfilment of the requirements for an advanced degree at the The University of British Columbia, I agree that the Library shall make it freely available for reference and study. I further agree that permission for extensive copying of this thesis for scholarly purposes may be granted by the Head of my Department or by his or her representatives. It is understood that copying or publication of this thesis for financial gain shall not be allowed without my written permission.

Department of Geological Sciences

The University of British Columbia
2075 Wesbrook Place
Vancouver, Canada
V6T 1W5

Date: June, 1986

ABSTRACT

The equilibrium grossular + clinochlore = 3 diopside + 2 spinel + 4 H_2O was investigated using cold seal pressure vessels from 500°C to 700°C at 0.5 kilobar to 4.0 kilobars. All phases used in the experiments were synthesized from oxides. Good brackets with stable assemblages diopside + spinel or grossular + clinochlore were made at conditions far from the equilibrium. Assemblages diopside + clinochlore were found at conditions close to the equilibrium over the entire pressure range. Analysis of internal consistency by linear programming indicates that the experimental results from this study are fully consistent with the UBCDATABASE and Helgeson's database and the experiments, with UBCDATABASE may safely be used as an indication of the metamorphic conditions of metarodingites. Run product diopside, the only possible solid solution phase in this study was extensively examined. X-ray refinement demonstrates that the cell parameters of the diopside are well within the range for pure diopside and Ca-Tschermak pyroxene. Scanning electron microscope and electron microprobe analyses showed that these diopsides contain aluminum interpreted as substitution of both Ca-Tschermak and Mg-Tschermak pyroxene. This interpretation satisfies the mass-balance requirements of these assemblages. Theoretical thermodynamic prediction of the equilibrium allowing for solid solutions in pyroxene indicates that diopside should be the main component, which is consistent with the

experiments in that the equilibrium curve according to the experimental brackets did not show measurable displacement caused by the low diopside activity. Thermodynamic calculation using diopside activity calculated from microprobe analysis data shows a significant shift in the equilibrium curve. Comparison of experimental results with natural minerals results in contradiction. Natural diopsides (clinopyroxene) found in similar assemblages at similar conditions contain much less aluminum. Undetected metastable zonation of aluminum or even aluminum-rich inclusions are probably the main causes for this.

Table of Contents

ABSTRACT ii

LIST OF TABLES vi

LIST OF FIGURES vii

ACKNOWLEDGEMENTS ix

I. INTRODUCTION 1

II. EXPERIMENTAL METHOD 4

A. PROCEDURES 4

B. STARTING MATERIALS 7

C. SYNTHESIS 9

1. Spinel 9

2. Diopside 11

3. Clinochlore 13

4. Grossular 13

D. EXPERIMENTAL RESULTS 19

III. CLINOPYROXENE COMPOSITION 30

A. OPTICAL MICROSCOPE 31

B. X-RAY DIFFRACTION (X.R.D.) 31

C. SCANNING ELECTRON MICROSCOPE (S.E.M.) 32

1. Sample preparation 33

2. Observation 34

D. ELECTRON MICROPROBE 38

1. Sample preparation 38

2. Analysis procedure 38

3. Interpretation of data 40

E. COMPOSITION OF CLINOPYROXENES FROM RODINGITES ..52

IV. THERMODYNAMIC ANALYSIS 53

A. PRECALCULATION 53

B. EXPERIMENTAL CONSTRAINTS ON THERMODYNAMIC PROPERTIES 55

C. CLINOPYROXENE SOLID SOLUTION 57

D. DIOPSIDE ACTIVITIES AND DISPLACED EQUILIBRIUM ..65

V. CONCLUSION 69

REFERENCES 72

APPENDIX 1 80

APPENDIX 2 84

LIST OF TABLES

Table I. Oxide weight percentage of minerals studied.....10

Table II. D-spacings and refined cell parameters for synthetic diopside.....12

Table III. Comparison of cell parameters of synthetic and natural diopsides.....16

Table IV. D-spacings and refined cell parameters for synthetic clinochlore.....17

Table V. Experimental results for the equilibrium Grossular+Clinochlore=3Diopside+2Spinel+4H_2O.....21

Table V(continued). Experimental results for the equilibrium Grossular+Clinochlore=3Diopside+2Spinel+4H_2O.....22

Table VI. D-spacings and refined cell paramenters for diopside (clinopyroxene) from run product.....33

Table VII. Standards used for microprobe analyses.....40

Table VIII. Duplicate of the microprobe analyses of standard diopside.....41

Table IX. The results of mass balance calculation according to the microprobe analyses.....50

Table X. Thermodynamic properties for phases considered in this study.....56

Table XI. Range of thermodynamic properties that are consistent with experimental results.....57

LIST OF FIGURES

Fig.1 Calibration of ratios of X.R.D. peak heights from starting material XRR to XRE.....8

Fig.2 Representative x-ray powder diffraction pattern for the synthetic diopside.....14

Fig.3 X-ray powder diffraction standard pattern for diopside.....15

Fig.4 Precalculated curve of the equilibrium Grossular + Clinochlore = 3 Diopside + 2 Spinel + 4 H_2O and the experimental brackets.....20

Fig.5-a Illustration of phase relations in the reaction Grossular+Clinochlore=3Diopside+2Spinel+4H_2O at high temperature.....24

Fig.5-b Illustration of phase relations in the reaction Grossular+Clinochlore=3Diopside+2Spinel+4H_2O at low temperature.....25

Fig.6 Illustration of the starting material compositions for experiments XRBulk-1 to XRBulk-10.....26

Fig.7 The scanning electron microscope E.D.S. chemical spectrum of synthetic diopside.....35

Fig.8 The scanning electron microscope E.D.S. chemical spectrum of diopside from run XRE-10.....35

Fig.9 The scanning electron microscope E.D.S. chemical spectrum of diopside from run XRR-3.....36

Fig.10 The scanning electron microscope E.D.S. chemical spectrum of diopside from run XRE-10.....36

Fig.11 The scanning electron microscope E.D.S. chemical spectrum of diopside from run XRR-4.....37
Fig.12 The scanning electron microscope E.D.S. chemical spectrum of diopside from run XRE-10.....37
Fig.13 The relation between Al_2O_3 and CaO (mol) in run product diopside from microprobe analyses.....42
Fig.14 The relation between Al_2O_3 and MgO (mol) in run product diopside from microprobe analyses.....43
Fig.15 The relation between Al_2O_3 and (CaO+MgO) (mol) in run product diopside from microprobe analyses.....44
Fig.16 The relation between Al_2O_3 and SiO_2 (mol) in run product diopside from microprobe analyses.....45
Fig.17 The relation between CaO and SiO_2 (mol) in run product diopside from microprobe analyses.....46
Fig.18 The relation between MgO and SiO_2 (mol) in run product diopside from microprobe analyses.....47
Fig.19 The relation between CaO and MgO (mol) in run product diopside from microprobe analyses.....48
Fig.20 Calculated P_{H_2O}-T diagram for dehydration equilibria among phases found in metarodingites.....54
Fig.21 The range of thermodynamic properties that are internally consistent.....58
Fig.22 Comparison of the equilibrium curves derived from UBCDATABASE, Helgeson's database and this study.....59
Fig.23 The displaced equilibria with different diopside activities.....67

ACKNOWLEDGEMENTS

I express my deepest gratitude to the following persons without whose contribution this thesis would not be possible. Dr. H.J. Greenwood, my supervisor, for his enthusiasm, suggestions, invaluable efforts and patient guidance through the course of this research; my committee members, Drs. T.H. Brown and E.P. Meagher for their helpful suggestions, advice and careful reviews of the early manuscript of this thesis; Dr. R.G. Berman for his help and advice in thermodynamic analysis work; Drs. J.M. Rice and S.A. Rawson of University of Oregon for their kindness of sending their unpublished analysis data used; the technical staff, notably Mr. B. Cranston, Mr. L. Hammerstrom, Mrs. S.J. Horsky and Mr J.B. Knight for their patient laboratory instructions and preparations; my fellow graduate students, especially C. DeCapitani and Bear McPhail for their constructive suggestions and helpful discussions.

This research work was partly supported through the Natural Science and Engineering Research Council operating grant number A-4222 held by Dr. H.J. Greenwood and fellowship awarded by the Ministry of Education of People's Republic of China.

I. INTRODUCTION

Rodingites are metasomatic rocks consisting mainly of diopside, chlorite and hydrogrossular which occur in mafic bodies adjacent to and within ultramafic rocks undergoing serpentinization. Metamorphism of rodingites may result in mineral parageneses that can be used in conjunction with diagnostic assemblages in the adjacent metaperidotite to place limits on temperatures and pressures of metamorphism.

The term "rodingite" was first introduced to describe altered gabbros in the Dun Mountain serpentinites of New Zealand (Bell, Clark and Marshall, 1911). Since then, rodingites have been found and reported in almost every major alpine ultramafic complex over the world (Benson, 1913-1918; Turner, 1930; Wells, Hotz and Carter, 1949; Miles, 1950; Carter and Wells, 1953; Suzuki, 1953; Bloxam, 1954; Jaffe, 1955; Bilgrami and Howie, 1960; Chesterman, 1960; Schlocker, 1960; Coleman, 1961-1967; Seki and Kuriyagawa, 1962; Muller, 1963; Dal Piaz, 1967, 1969; Vuagnat, 1967).

The significance of rodingites to metamorphic petrologists is twofold (Rice, 1983). First of all, the formation of rodingite is related exclusively to low-temperature serpentinization, so the presence of rodingite in some medium- and high-grade ultramafic rocks indicates that the terrane was formerly under a condition appropriate for serpentinization. Secondly, changes in mineral assemblages that take place in the rodingite during

later progressive metamorphism may be used in conjunction with those affecting the surrounding ultramafic rocks to delineate isograds and place limits on intensive variables such as temperature, pressure and fluid composition during the metamorphism.

Thermodynamic calculations of equilibria among minerals commonly found in metarodingites have been reported by Rice (1983). In that paper, the stable μ_{CO_2}-μ_{H_2O} topologies relating minerals were first established according to observed natural parageneses. Available thermodynamic data were then used to calculate the inferred metarodingite equilibria in terms of temperature, pressure and composition of a CO_2-H_2O fluid phase. The resulting petrogenetic model was in agreement with observed natural assemblages in both low- and high-pressure terranes and indicated that certain rodingite parageneses can be used to place limits on temperatures and pressures of metamorphism.

This study is the first report on experimental work related directly to metarodingites. Phases considered in this study are grossular, clinochlore, diopside, spinel and water (H_2O). The system which describe these phases is CaO-MgO-Al_2O_3-SiO_2-H_2O. One important equilibrium:

Grossular + Clinochlore = 3 **Diopside** + 2 **Spinel** + 4 H_2O

was studied and experimental reversals were obtained. It was found that many runs under conditions near the equilibrium

ended with diopside + clinochlore instead of either diopside + spinel or grossular + clinochlore. The cause is attributed to solid solution in diopside toward the Ca-Tschermak and Mg-Tschermak components. The diopside from each run was examined by optical microscope, x-ray diffraction, scanning electron microscope and electron microprobe. The diopsides were found to be very aluminum-rich, which is not common in the diopside from rodingite assemblages. Ca-Tschermak and Mg-Tschermak substitution in diopside are shown by thermodynamic calculation to displace the equilibrium studied from the expected position for pure end-member phases.

II. EXPERIMENTAL METHOD

A. PROCEDURES

All experiments were carried out using standard cold seal pressure vessels of either Stellite K-25 or Rene 41 alloys. Furnaces used were placed either horizontally (for 0.5 to 2.0 kilobar runs) or vertically (for 4.0 kilobar runs). The results from both types of furnaces were in good agreement.

Temperature was measured by sheathed chromel-alumel thermocouples mounted in an external well designed to hold the thermocouple tip close to the sample. Calibrations of the thermocouple were made between 400°C and 800°C at one atmosphere for each furnace with a specific bomb and thermocouple. It was found that the temperature gradients were less than ±1°C over the two to three centimeter length of the sample capsule. During runs, temperatures were controlled by fully proportional controllers which usually control the temperature of bomb with variations less than ±1°C. Temperature measurements were made daily using a temperature compensated digital thermometer with a resolution of 1°C. As a check, a potentiometer with an estimated resolution of 0.1°C was occassionally used to measure temperature precisely. An automatic data recording system using an IBM-XT computer and DAS A to D interface was used to measure temperature automatically once every half hour for the duration of the run. No systematic temperature

difference was noticed between measurements taken with digital thermometer, L&N potentiometer, or computer. Temperatures given in the table of experimental results are the averages of the daily measurements. The total cumulative errors including calibration and measurement and variation are estimated to be less than ±5°C.

Either methane (for runs at less than 2.0 kilobars) or distilled water (for runs with 4.0 kilobars) was used as pressure media. Pressure measurements were made daily with either an Ashcroft Maxisafe gauge with a resolution of 15 bars or a Heise Bourdon tube gauge with a resolution of 5 bars. If the pressure dropped more than 3%, the experiment was repeated. The pressures listed in the experimental result table are the averages of daily measurements and the total errors of pressure were estimated to be less than ±20 bars.

Most of runs were investigated with two adjacent capsules of starting mixtures having different proportions of low- and high-temperature assemblages. The exceptions are the runs having conditions quite far from equilibrium for which only one capsule of starting material was used. The two commonly used mixtures were 20wt% low-temperature assemblage plus 80wt% high-temperature assemblage, and the other 80wt% low-temperature assemblage plus 20wt% high-temperature assemblage. For each capsule, approximately 20 milligrams of starting mixture were sealed with excess distilled water (30wt%) and then weighed. The seal was

checked by placing the sealed capsule in an oven at temperature of 100°C for 30 to 40 minutes and reweighing. Loss of weight indicated failure of the seal and a new capsule was prepared. The furnace was preheated to the desired temperature before the pressure vessel was inserted. After insertion the temperature was stablized within about 30 to 60 minutes. After the required duration, the pressure vessel was removed, placed in a steel cooling jacket and quenched by blowing compressed air around the vessel. Usually, the temperature dropped to less than 100°C within 5 minutes. After the residual pressure was released, the capsule was removed, weighed, punctured and reweighed to make sure there was no loss of any material during the run. After the charge was dried in the oven at 100°C for 30 minutes, the capsule was opened for examination. Run charges were examined under the optical microscope and with x-ray diffraction. Then they were examined under scanning electron microscope and microprobe if neccessary. Because most of the runs showed incomplete reaction, an x-ray diffraction intensity technique was used to obtain height ratios of certain peaks of different phases to determine the extent and direction of reaction. This was done as follows: for each of two starting mixtures, six x-ray diffraction patterns were made using different slides with different amount of materials to obtain the average values of the peak ratios based on the known composition (80wt% low-temperature assemblage plus 20wt% high-temperature assemblage or 20wt%

low-temperature assemblage plus 80wt% high-temperature assemblage, Fig 1). The same method was applied to each run charge with incomplete reaction to find the peak ratios. The ratios from starting material and from run product were compared to determine the extent and direction of reaction. Only the runs with large ratio changes (greater than 30%) were considered to have reacted.

B. STARTING MATERIALS

All phases considered in this study were synthesized from oxide mixtures. A Lindberg furnace was used for the preparation of the oxides.

Periclase (MgO) was prepared by baking MgO (Fisher Certified Reagent Lot#741694) for 24 hours at 800°C and 1 hour at 1000°C.

Cristobalite (SiO_2) was made from $SiO_2.nH_2O$ by baking at 1300°C for 24 hours. For better crystallization the SiO_2 was baked for another 24 hours at 1200°C.

γ-Al_2O_3 was prepared from aluminum chloride ($AlCl_3.6H_2O$) (Fisher Certified Reagent Lot#429332) by heating it in a fume hood using a gas burner for 1 hour until frothing stops. The Al_2O_3 was then baked at 650°C for 96 hours.

Lime (CaO) was made from calcium carbonate ($CaCO_3$) by baking at 500°C for 24 hours, followed by at 800°C for 12 hours.

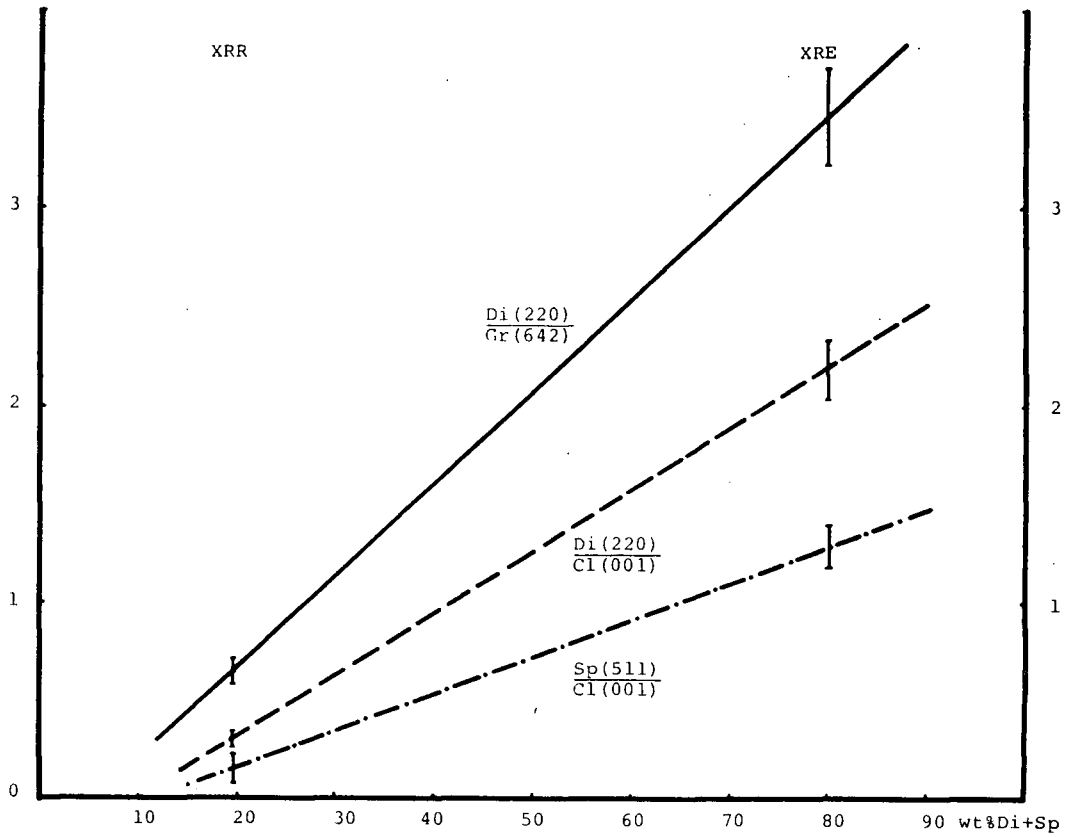

Fig 1 Calibration of ratios of peak heights from starting material XRR (80wt% grossular + clinochlore, 20wt% diopside + spinel) to XRE (80wt% diopside + spinel, 20wt% grossular + clinochlore). Vertical bars show the standard deviation of mean from 6 measured peak ratios.

Each prepared oxide was ground, under alcohol, in an agate mortar by hand for several hours to make sure that the grain size was less than 1 micron. The oxide was then dried in a furnace and stored in dessicator for further use.

C. SYNTHESIS

Phase syntheses were conducted using either a Lindberg furnace at one atomsphere or in pressure vessels.

Each oxide was carefully weighed according to the desired weight proportion for each mineral (see Table I). To reduce weighing errors, 5 grams of mixture for each mineral was mixed. The mixture was ground by hand under alcohol for at least 2 hours. To ensure homogeneity the mixture was periodically dried and collected into the bottom of the mortar. After drying in an oven at 100°C for about 30 minutes, the oxide mixtures were stored in a dessicator.

1. SPINEL

Spinel was synthesized by two methods. One atomsphere synthesis was made in a platinum capsule and directly put in a Lindberg furnace. For this synthesis two cycles of heating and grinding were used in order to obtain a high percentage of yield (Engi, 1983). For the first cycle, the mixture was heated at 1000°C for 1 hour and then it was taken out from furnace and ground for 1 hour by hand under alcohol in an agate mortar. For the second cycle the mixture was heated to

Table I

Oxide weight percentage of the mineral involved

Mineral	Formula	MgO	CaO	Al_2O_3	SiO_2
Gros	$Ca_3Al_2Si_3O_{12}$	0.00	37.35	22.64	40.02
Diop	$CaMgSi_2O_6$	18.61	25.90	0.00	55.49
Clin	$Mg_5Al_2Si_3O_{10}(OH)_8$	41.66	0.00	21.08	37.26
Spin	$MgAl_2O_4$	28.33	0.00	71.67	0.00

1200°C for 24 hours. The hydrothermal synthesis was made using a gold capsule sealed with about 150 milligrams of the mixture plus approximately 20-30wt% distilled water. The synthesis conditions of 795°C and 1.0 kilobar were maintained for 12 days. Different conditions of syntheses were used because of considerations of order-disorder phenomena in spinels. It has been found that magnesium and aluminum cation distribution in the tetrahedral and octahedral sites of the spinel structure may be sensitive both to temperature of formation and to cooling rate (Barth and Posnjak, 1932; O'Neill and Navrotsky,1984) There are techniques using powder diffraction available to measure the degree of order-disorder in spinel (Furuhashi, et al. 1973). These techniques measure the difference between the theoretical and observed intensities of different peaks. The theoretical intensities are calculated based on the scattering factors of the elements involved. Because magnesium and aluminum have similar scattering factors the calculated intensities are not very sensitive to ordering in the structure (Lindsley, 1976). Therefore these techniques are not suitable for measuring order-disorder in the Mg-Al

spinel of this study. But one would expect samples quenched from high temperatures to be disordered rather than ordered. Both syntheses were successful and their products were examined under optical microscope, x-ray diffraction and scanning electron microscope. It was found that spinels by both methods were identical with respect to optics, x-ray powder diffraction, and scanning electron microscopy. The synthetic spinel typically crystallized as euhedral crystals with (1 1 1) and (1 1 0) faces(plates 1,2). The grain size ranged from 2 microns to more than 10 microns. The crystals are optically isotropic, with no sign of inhomogeneity. No other phase was detected in either of the synthesis charges.

2. DIOPSIDE

Diopside was synthesized at 795°C and 1 kilobar for 15 days. Attempts to synthesize diopside at one atmosphere failed because of the slow crystallization rate. The synthesis product was examined under the optical microscope, x-ray diffraction and scanning electron microscope and no impurity was found. The synthetic diopside was subhedral to euhedral, with a grain size of 2 x 5 microns (plate 3). Cell parameter refinement was carried out using four x-ray diffraction scans (two with increasing 2Θ and two with decreasing 2Θ). Silicon metal was used as an internal standard (a=5.4305 A). CuKα radiation and a scanning rate 1/4 degree 2Θ per minute was used. Eleven diffraction lines were selected. The mean of the peak positions were obtained

Table II

D-spacings and refined cell parameters for synthetic diopsides, $CaMgSi_2O_6$

h k l	Synthetic[1] d(calc)	d(obs)	I(/100)	Synthetic[2] d(obs)	standard[3] d
0 2 1	3.344	3.344	15	3.346	3.350
2 2 0	3.234	3.232	30	3.232	3.230
2 2-1	2.991	2.990	100	2.990	2.991
3 1 0	2.952	2.949	32	2.950	2.952
3 1-1	2.894	2.892	37	2.893	2.893
1 3-1	2.565	2.564	25	2.565	2.566
3 1 1	2.302	2.303	20	2.300	2.304
3 3 0	2.156	2.156	12	2.155	2.157
3 3-1	2.133	2.134	20	2.131	2.134
4 2-1	2.108	2.109	12	-----	2.109
0 4 1	2.041	-----	--	2.040	2.043
1 3-2	1.968	1.970	10	-----	1.970
1 5 0	-----	-----	--	1.754	1.755
5 3-1	-----	-----	--	1.624	1.625
a(A)	9.755(4)			9.748	9.761
b(A)	8.928(6)			8.924	8.926
c(A)	5.247(7)			5.251	5.258
β	105°52'			105°47'	105 °47'
V(A^3)	439.51(45)			439.5	440.80

[1] Synthetic diopside from this study.
[2] Synthetic diopside from Nolan and Edgar (1963).
[3] standard diopside from Mineral Powder diffraction File, Data Book by JCPDS.

and the cell parameters were calculated using the program of Evans, et al (1963). The results are shown in Table II. Also shown in this table are cell refinement results of synthetic diopside from Nolan and Edgar (1963) and diopside standard from Mineral Powder Diffraction File, Data Book by JCPDS, card #11-654 (1980). Table III shows some diopside cell refinement parameters by various authors. Our cell refinement data are in very good agreement with others. The X.R.D. pattern of synthetic diopside is comparable with the

pattern of JCPDS diopside standard (Fig 2 and Fig 3).

3. CLINOCHLORE

Clinochlore was synthesized from the oxide mixture plus approximately 30wt% distilled water at 680°C and 4.0 kilobars for 21 days. Synthetic clinochlore was fine grained and the size ranged from 1 micron to 4 microns. Under optical microscope and scanning electron microscope, well formed platy crystals were observed (plate 4). Trace spinel was found with the optical microscope using index oil but this impurity was not detected by x-ray diffraction. The amount of spinel was estimated to be much less than 1% judging from the comparative charts for visual estimation of volume percentage(Terry and Chilingar, 1955). The change in clinochlore composition caused by the extraneous spinel, is probably not significant (see also McPhail, 1985). The results of cell parameter refinement are listed in Table IV. Also provided are cell refinement results of synthetic clinochlore by Chernosky (1974). Both results are in very good agreement.

4. GROSSULAR

Grossular was synthesized under two different conditions: at 745°C and 1 kilobar for 17 days, and at 680°C at 4.0 kilobars for 21 days. Examination under the microscope showed that both synthesis products had additional phase impurities (anisotropic crystal) estimated

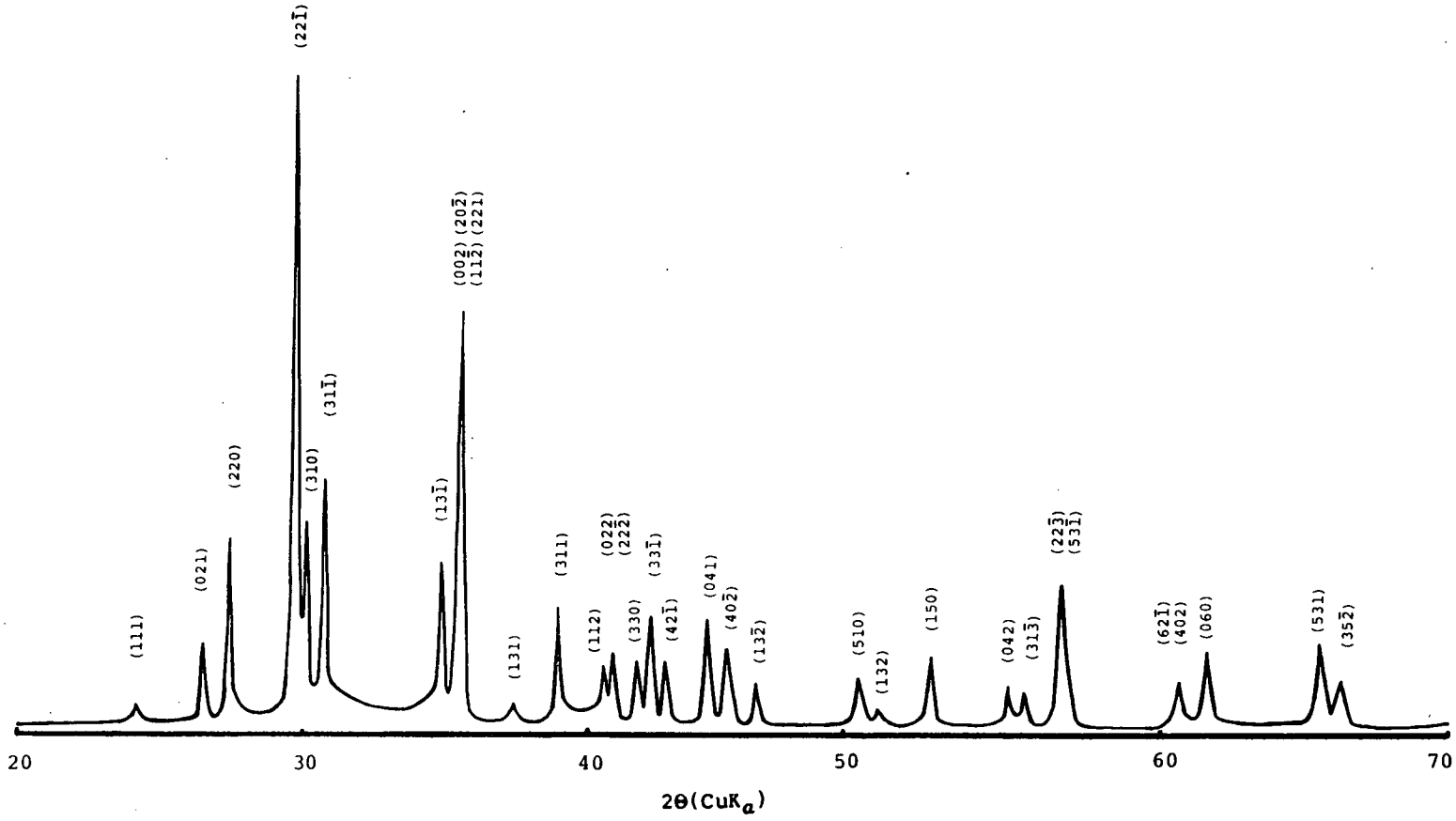

Fig 2 Representative x-ray powder diffraction pattern for a synthetic diopside.

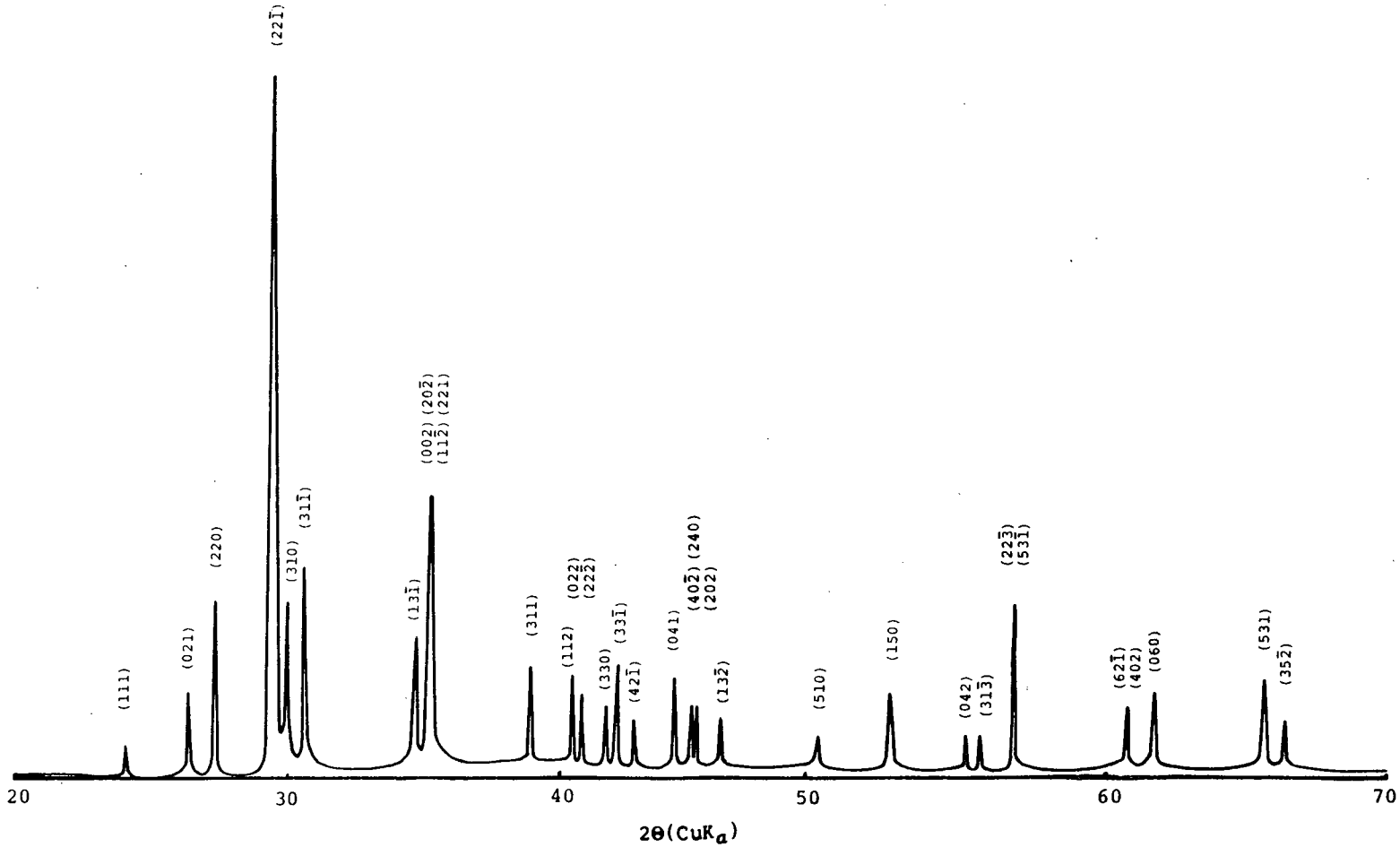

Fig **3** X-ray powder diffraction standard pattern for diopside, data from Mineral Powder Diffraction File, Data Book by JCPDS, card # 11-654.

Table III

Cell parameters of synthetic and natural diopsides

Samples	Reference	a (A)	b (A)	c (A)	β	V (A^3)
Synthetic	Rutstein, et al.(1969)	9.752(2)	8.926(2)	5.246(2)	105°50′	439.68(15)
Synthetic	Present study	9.754(4)	8.927(5)	5.246(7)	105°52′	439.51(45)
Synthetic	Clark, et al.(1962)	9.745(1)	8.925(1)	5.248(1)	105°52′	
Synthetic	Sakata,(1957)	9.743	8.923	5.251	105°56′	
Synthetic	Nolan and Edgar,(1963)	9.748	8.924	5.251	105°47′	439.5
Natural	Viswanathan,(1966)	9.754(14)	8.916(8)	5.24(9)	105°49′	
Natural	Clark et al.(1969)	9.746(4)	8.899(5)	5.251(6)	105°39′	438.6
Run Diop	This study	9.725(4)	8.891(5)	5.260(5)	105°55′	437.13(31)
Syn. CaTs	Okamura et al.(1974)	9.609	8.652	5.274	106°3′	421.35

Table IV

D-spacings and refined cell parameters for synthetic clinochlore, $Mg_5Al_2Si_3O_{10}(OH)_8$ and chlorite $Mg_{4.75}Al_{2.5}Si_3O_{10}(OH)_8$

	Clin[1]			Clin[2]	chl[3]
h k l	d(calc)	d(obs)	I(/100)	d(obs)	d(obs)
0 0 1	14.299	-----	--	14.132	-----
0 0 2	7.149	-----	--	7.135	-----
0 0 3	4.766	4.771	xx[4]	4.757	4.752
0 2 0	4.609	-----	--	-----	4.592
1 1 0	4.581	4.587	40	4.588	-----
-1 1 1	4.505	-----	--	4.493	4.500
0 2 1	4.387	-----	--	4.373	4.384
1-1 1	-----	-----	--	4.242	-----
0 2 2	3.874	-----	--	3.883	3.862
1 1 2	3.682	-----	--	3.674	-----
0 0 4	3.575	3.577	xx	3.572	3.560
0 0 5	2.860	2.860	60	2.864	2.846
1 1 4	2.682	-----	--	2.691	-----
2 0-1	2.655	2.653	12	2.656	2.653
2 0-2	2.582	2.581	45	2.584	2.579
2 0 1	2.541	2.540	100	2.540	2.538
-2 0 3	2.440	2.440	75	2.441	2.437
0 0 6	2.383	2.383	36	2.385	2.380
2 0-4	2.261	2.261	28	2.260	2.258
1 3 4	2.071	2.071	11	-----	-----
0 0 7	2.043	2.042	18	2.041	2.034
2 0 4	2.008	2.009	58	2.008	2.004
2 0-6	1.889	1.889	20	1.889	1.885
2 0 5	1.830	1.830	20	1.831	1.826
0 0 8	1.787	-----	--	-----	1.781
2 0-7	-----	-----	--	1.724	-----
2 0 6	1.669	1.670	11	1.671	-----
2 0-8	1.573	1.573	32	1.573	1.568
0 6 0	1.536	1.536	53	1.539	1.532
0 6 2	1.502	1.502	15	1.502	1.501
0 6 3	1.462	1.463	18	1.463	-----
1 1 9	1.454	-----	--	1.455	-----
0 010	1.430	1.430	10	-----	1.424
3 3 3	1.411	-----	--	1.412	-----
2 0 8	1.402	1.402	24	1.402	1.397
------					
a(A)	5.320(1)			5.324(1)	5.317(1)
b(A)	9.218(1)			9.224(3)	9.192(2)
c(A)	14.409(2)			14.420(5)	14.349(2)
β	97°5'(1')			97°6'(1')	97 °8'(1')
V(A^3)	701.26(16)			702.69	695.83

[1] Synthetic clinochlore from this study.
[2] Synthetic clinochlore from Chernosky, (1974).
[3] Synthetic chlorite from McPhail, (1985).
[4] Peak intensity more than 100 renormalized.

to be less than 5% by volume. This may have been the result of too low a pressure used for syntheses. Attempts to identify these impurities by x-ray diffraction and scanning electron microscope showed it to be wollastonite. The fate of the released aluminum is unknown as no aluminum rich impurity was found. Such a small proportion of impurity should not have much effect on the composition of the synthetic grossular. Synthetic grossular was subhedral to euhedral and ranged in size from 2 microns to 10 microns (plate 5,6). Under the light microscope it appeared isotropic and homogeneous.

In natural rodingites, hydrogrossular is the most common mineral present and is often the most abundant mineral within volcanic rocks altered to rodingites (Coleman, 1966). Hydrogrossular with formula $Ca_3Al_2(SiO_4)_{3-x}(H_4O_4)_x$ was found to be the result of a continuous solid solution between $Ca_3Al_2Si_3O_{12}$ and $Ca_3Al_2(H_4O_4)_3$ at low temperature (Flint, et al., 1941). Silica-free $Ca_3Al_2(H_4O_4)_3$ decomposes above approximately 250°C. Yoder (1950) studied the stable fields for grossular and hydrogrossular and reported that hydrogrossular is stable at temperatures only below about 600°C. Shoji (1974) found that the hydrogen content in the grossular-hydrogrossular series decreases with increasing temperature and the d-spacing of the (4 2 0) plane can be used to determine the H_2O content in hydrogrossular. The d-spacing value of the (4 2 0) plane varies from about 2.650 (A) for grossular to 2.680 (A) for

hydrogrossular. Careful determination of the d-spacing of the (4 2 0) plane for the grossular synthesized in this study shows that the value (2.6498 (A)) is in very good agreement with the value reported by Shoji (1974). It is believed therefore that synthetic grossular from this study is on composition and no hydrogrossular component is involved.

D. EXPERIMENTAL RESULTS

Experimental reversals of the equilibrium;

Grossular + Clinochlore = 3 Diopside + 2 Spinel + 4 H_2O

were made at pressures of 0.5, 1.0, 2.0 and 4.0 kilobars. The experimental conditions and results are listed in Table V and illustrated in Fig 4. A few runs at conditions far from equilibrium achieved complete reaction (100% grossular + clinochlore or 100% diopside + spinel). For most of the runs, the peak height ratios from x-ray diffraction were used to indicate the reaction direction and to estimate extent of reaction. For high temperature runs, the common assemblages were diopside + spinel + minor clinochlore, i.e. grossular seems to disappear easily. For low temperature runs, grossular + clinochlore + minor diopside was the common phase assemblage, i.e. spinel disappeared easily. When runs were put at conditions assumed to be close to the equilibrium, the final assemblage was clinochlore + diopside

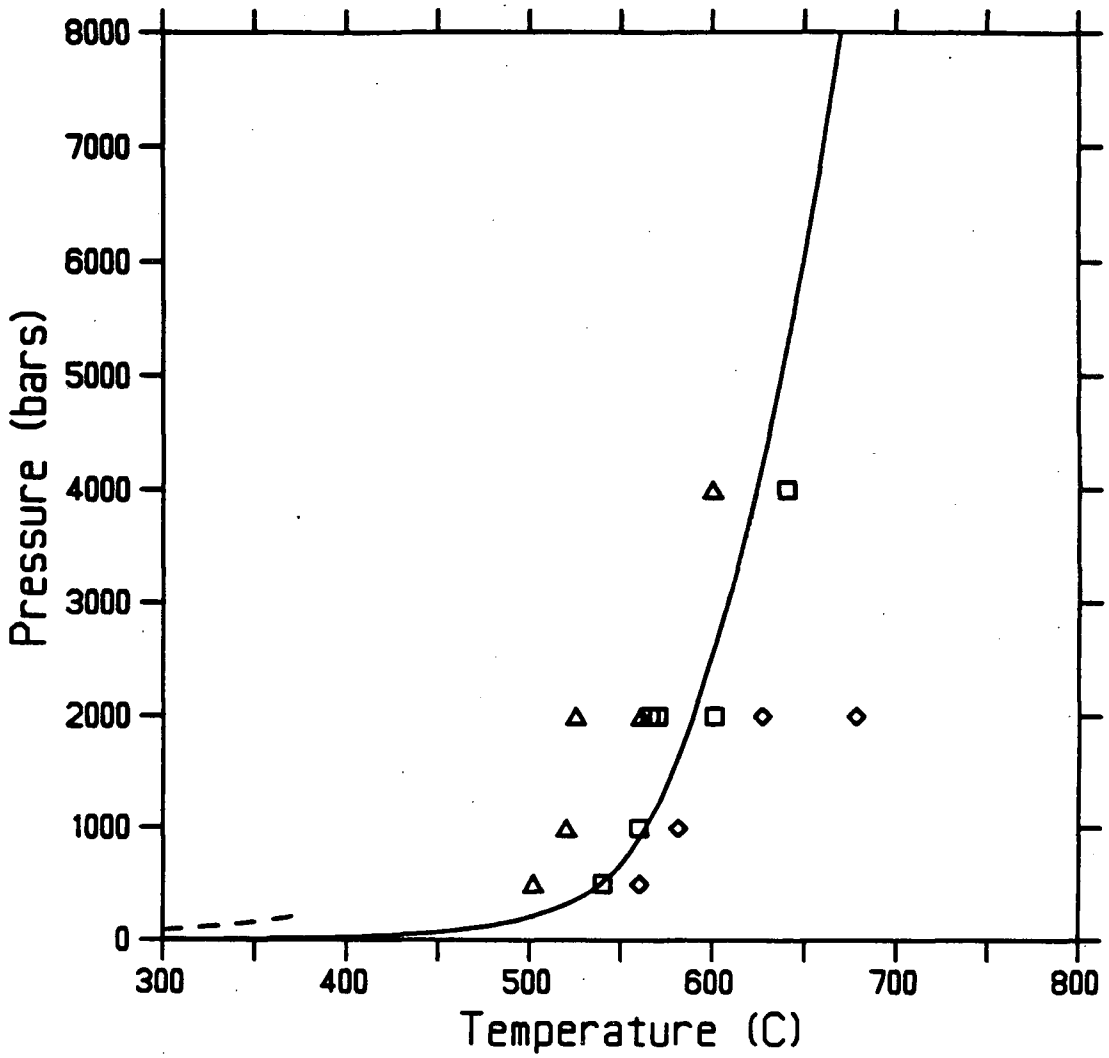

Fig 4 Precalculated curve of the equilibrium grossular + clinochlore = 3 diopside + 2 spinel + 4 H_2O by PTSYSTEM using phase properties from UBCDATABASE and the experimental brackets of this study.
△ -- assemblage grossular + clinochlore stable.
◇ -- assemblage diopside + spinel stable.
□ --abnormal assemblage diopside + clinochlore.

Table V

Experimental results for the equilibrium
Grossular + Clinochlore = 3 Diopside + 2 Spinel + 4 H_2O

Run #	P(bar)	T(°C)	Duration	Results
XRR-1	2000	678	384(hrs)	100% Di + Sp
XRE-1	2000	525	336	80% Gr + Clino
XRR-2	2000	627	360	mainly Di + Sp, minor Clino
XRE-2	2000	566	504	no reaction
XRR-3	2000	601	552	Di + Clino
XRE-3	2000	601	552	Di + Sp stable
XRR-4	2000	580	588	mainly Di + Clino, minor Gr
XRE-4	2000	580	588	Di + Sp stable
XRR-5	2000	561	552	Gr + Clino stable
XRE-5	2000	561	552	Gr + Clino grow 40%
XRR-7	2000	570	576	Gr + Clino stable
XRE-7	2000	570	576	mainly Di + Clino, minor Gr
XRR-6	1000	560	600	no obvious reaction
XRE-6	1000	560	600	Gr + Clino grow
XRR-9	1000	520	384	80% Gr + Clino
XRE-9	1000	520	384	60% Gr + Clino
XRR-10	1000	581	720	Di + Sp grow
XRE-10	1000	581	720	Di + Clino
XRR-8	500	502	840	100% Gr + Clino
XRE-8	500	502	840	95% Gr + Clino, minor Di
XRR-11	500	540	672	Di + Sp grow
XRE-11	500	540	672	Mainly Gr + Clino ???
XRR-17	500	560	648	Mainly Di + Clino
XRE-17	500	560	648	Mainly Di + Sp
XRR-18	4000	600	600	Mainly Gr + Clino
XRE-18	4000	600	600	Mainly Gr + Clino
XRR-19	4000	640	672	Mainly Di + Clino
XRE-19	4000	640	672	Mainly Di + Clino
XR-13*	2000	600	672	Mainly Di + Clino
XR-14*	1000	570	672	Mainly Di + Clino
XR-20	2000	600	552	Mainly Di + Clino
XRBulk-1	1000	590	1152	Mainly Di + Clino
XRBulk-3	1000	590	1152	Mainly Di + Clino

* Runs with starting material of 50wt% reactant and 50wt% product.

Table V (continued)

Experimental results for the equilibrium
Grossular + Clinochlore = 3 Diopside + 2 Spinel + 4 H_2O

Run #	P(bar)	T(°C)	Duration	Results
XRBulk-5	1000	590	1152	Mainly Di + Clino
XRBulk-7	1000	590	1152	Mainly Di + Minor Clino
XRBulk-9	1000	590	1152	Mainly Di + Minor Clino
XRBulk-2	1000	530	1152	Mainly Gr + Clino + Minor Di
XRBulk-4	1000	530	1152	Mainly Di + Clino + Di + (unknown)
XRBulk-6	1000	530	1152	Mainly Gr + Clino + Minor Di
XRBulk-8	1000	530	1152	Mainly Gr + Di + Minor Clino
XRBulk-10	1000	530	1152	Mainly Gr + Di + Minor Clino + Minor Sp

instead of clinochlore + grossular or diopside + spinel. This was first found in experiments at 2.0 kilobars and the repeated experiments at 2.0 kilobars showed the same results. Similar results were obtained from 0.5, 1.0 and 4.0 kilobar runs. Therefore only wide reversal brackets were obtained for each pressure condition.

Some special experiments were conducted after the assemblage diopside + clinochlore was found. One experimental product (XRR-3) containing only diopside + clinochlore was used as new starting material. It is assumed that the phases diopside and clinochlore from this run are the stable phases at this temperature and pressure conditions. Relative proportions of diopside and clinochlore were estimated according to peak intensities of the X.R.D.

pattern. Appropriate amounts of spinel and grossular were then added to the diopside and clinochlore mixture for 1:1 ratio of product and reactant (50% reactants and 50% products in weight) of the reaction grossular + clinochlore = 3 diopside + 2 spinel + 4 H_2O. After grinding under alcohol for 2 hours, the sample was loaded under the same conditions as that of the run from which produced diopside + clinochlore.

After 552 hours duration, the run (XR-20) products were examined and found to be 100% reacted to diopside + clinochlore (see table V).

For the experimental runs, the calculated wt% of each phase was mixed into the starting material. It is possible thus to obtain starting assemblage such as grossular + clinochlore + minor diopside, and diopside + spinel + minor clinochlore (Fig 5a, 5b).

Ten synthesis runs were made to test this possibility. Oxides were used as starting materials for the synthetic runs. The compositions of the mixtures were designed to be off the bulk composition of the reaction for stoichiometric phases. The original bulk composition was prepared to balance the reaction between the stoichiometric phases. Four new mixes were prepared so as to guarantee that their compositions would lie in the four sectors defined by the crossing stoichiometric tie-lines (see Fig 6).

Two run conditions were used for the special synthesis runs (see Table V). Long durations of the runs were

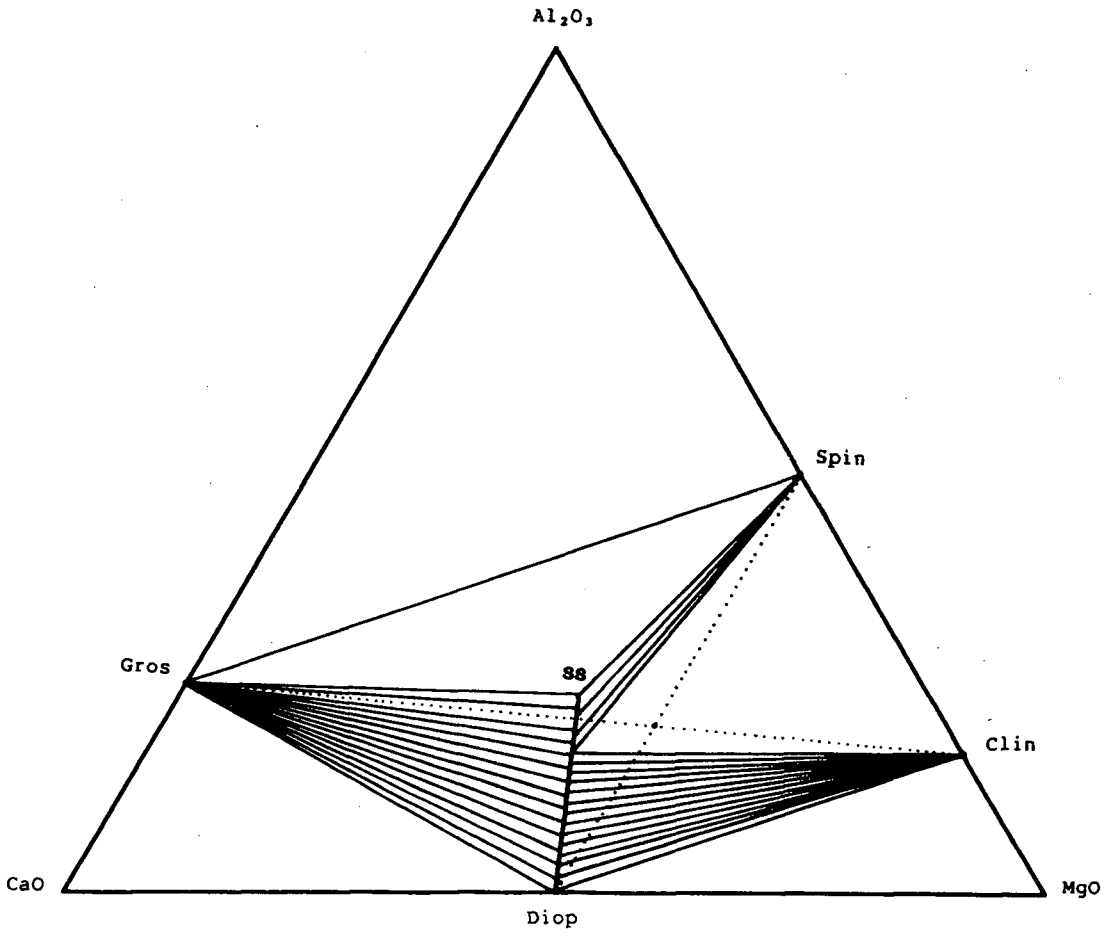

(a)

Fig 6 Illustrations of phase relations in the reaction grossular + clinochlore = 3 diopside + 2 spinel + 4 H_2O at (a) high temperature and (b) low temperature. Diopside is an Al-bearing solid solution. Dotted lines are the tie lines for the reaction without considering solid solution in diopside. The intersection point of these tie lines represents the reaction bulk composition and the starting materials used for the experiments. Point ss in (a) represents the mean composition of run diopsides from microprobe analyses.

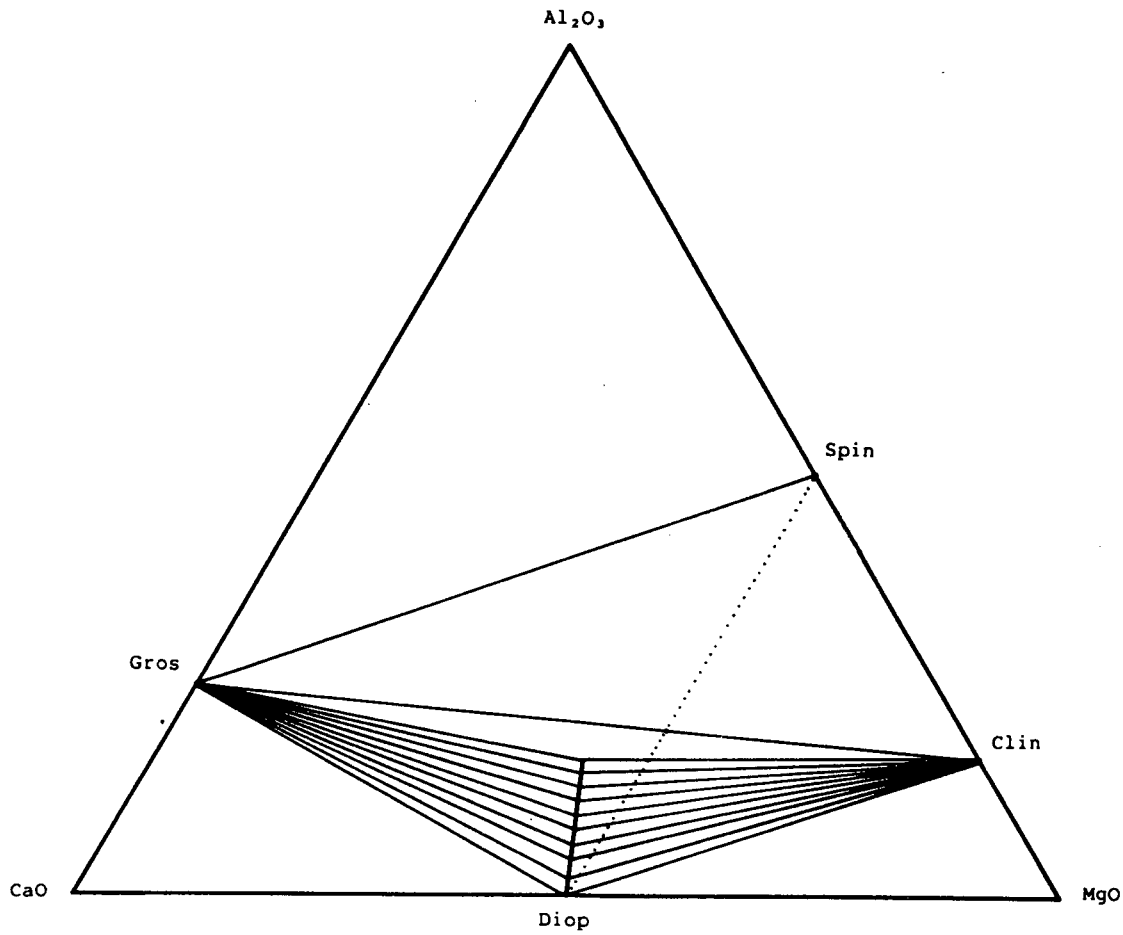

(b)

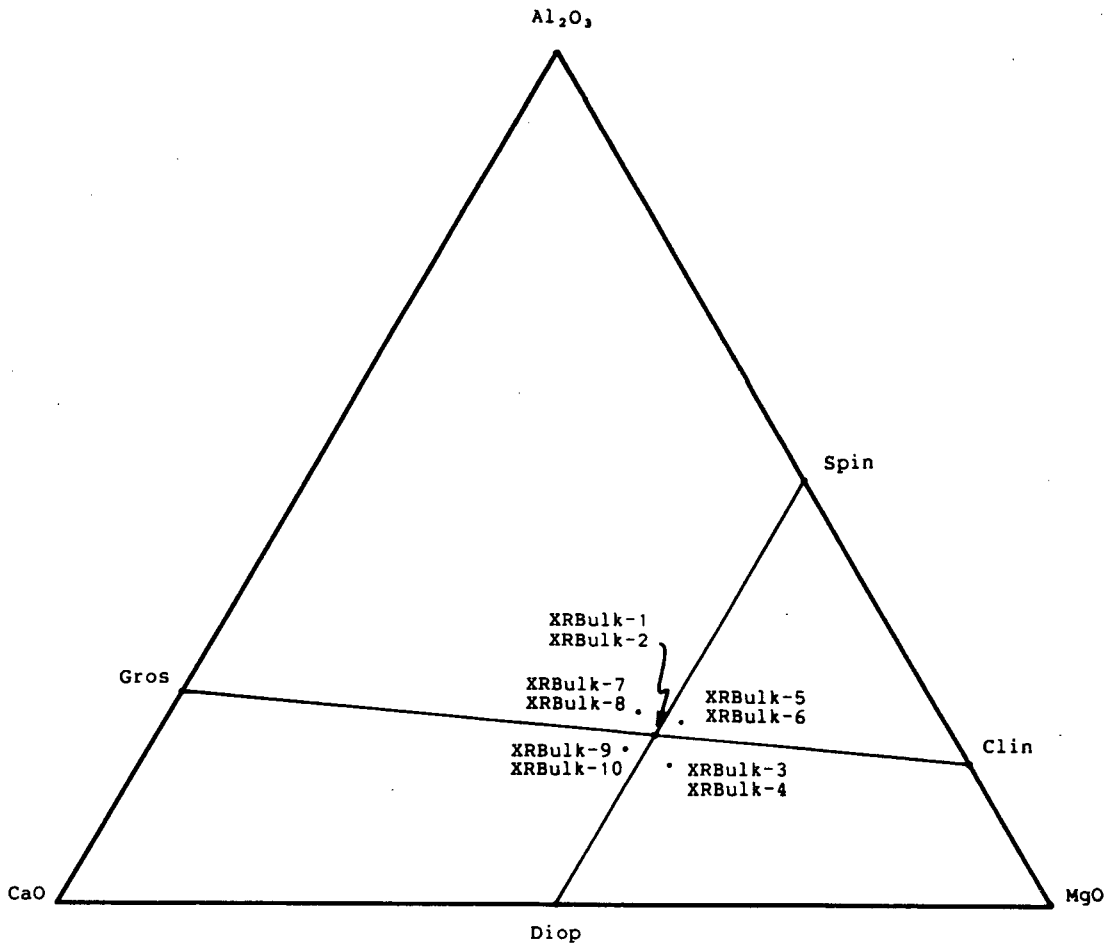

Fig 6 Illustration of the starting material compositions for experiments XRBulk-1 to XRBulk-10. The solid lines within the triangle are the tie line for the stoichiometric reaction and their intersection represents the bulk composition for that reaction. The starting material compositions for other experiments are shown as XRBulk-3 to XRBulk-10.

maintained to ensure a complete reaction. The results of these synthesis runs show that their run products are no different from those of the equilibrium runs made earlier. The experiments all concluded with either diopside + clinochlore or the low temperature assemblage grossular + clinochlore. Only one run (XRBulk-4) showed three unidentified peaks in the X.R.D. patterns which could be an indication of unknown phases.

The above results suggest that non-stoichiometric behaviour may occur in one or more of the phases involved. Spinel is the only phase that may not exhibit solid solution in the chemical system studied.

Grossular ($Ca_3Al_2Si_3O_{12}$) was treated as a stoichiometric phase although pyrope-grossular can be a complete solid solution at very high temperature and high pressure. The mixing properties of grossular-pyrope solid solution have been discussed by various authors e.g. Chinner et al. (1960); Saxena (1968); Boyd (1970); Wilken (1977); Ganguly and Kennedy (1974); Hensen et al. (1975). Synthesis studies of garnet along this join were made by Yoder and Chinner (1960). The stabilities of garnet with this composition are strongly dependent on the pressure of formation. At 29 kilobars and 1250°C, a complete range of solid solution can be crystallized. But at 10 kilobar water pressure and 950°C, only garnets within the narrow range Gr_{100}-$Gr_{94}Py_6$ are stable. This solid solution was also studied theoretically and experimentally by Ganguly and

Kennedy (1974); Hensen, Schmid and Wood (1975). it was demonstrated that pyrope-grossular solid solution exhibited a significant positive deviation from ideality. The deviation increases with decreasing temperature. The temperature of critical mixing marks the top of the pyrope-grossular solvus. The values of 694±50°C (Ganguly and Kennedy, 1974) and 629±90°C (Hensen et al, 1975) are both higher than the temperature used in this study. Also it was demonstrated earlier that the synthetic grossular is in composition as shown by checking the d-spacing value of (4 2 0) plane with X.R.D. Therefore it seems reasonable to treat grossular as a stoichiometric phase at the temperature and pressure conditions used for this study.

Changes in chlorite composition with increasing pressure were reported by Fawcett and Yoder (1966). It was concluded that the composition of chlorite coexisting with other phases varies with pressure, becoming more aluminous at higher pressure. Careful studies of this shift in chlorite composition were made by McPhail (1985) by measuring (004) and higher order basal peaks of chlorite against forsterite and spinel peaks before and after the experiments. No shifts in the peak position for chlorite were noticed. Similar work was done by Chernosky (1974) with clinochlore using the same methods in which he showed that clinochlore from different temperatures and pressures showed no non-stoichiometric phenomena. In this study, the same attention was paid and no peak shift was detected for

clinochlore. Clinochlore in this study therefore was considered to have the same composition ($Mg_5Al_2Si_3O_{10}(OH)_8$) throughout the course of the experiments.

A variety of techniques were used to study the variation in composition of diopside. It was found that the diopside has a high aluminum content which may be described by substitution of Ca-Tschermak or/and Mg-Tschermak molecule.

III. CLINOPYROXENE COMPOSITION

The experimental results of the previous chapter suggest that the clinopyroxene may not be stoichiometric end-member diopside because many runs concluded with 'diopside' + clinochlore instead of either diopside + spinel or grossular + clinochlore. Grossular, spinel, and clinochlore have been concluded to be stoichiometric, leaving only errors in bulk composition of the run or variation in clinopyroxene composition as the source of the problem. Ten test experiments (XRBulk-1 to XRBulk-10 see Table V), with different bulk compositions, have eliminated the possibility of first of these problems, leading to the conclusion that the clinopyroxene contains aluminum.

Research on aluminum in clinopyroxene has been extensive, indicating mostly that high Al-content is the result of high pressure, Al-rich bulk compositions, or both. The solid solutions between $CaMgSi_2O_6$, $CaAl_2SiO_6$, $MgAl_2SiO_6$ and $Mg_2Si_2O_6$ have been studied very extensively (Clark, et al., 1962; Neufville and Schairer, 1962; Kushiro and Yoder, 1965; 1966; MacGregor, 1965; O'Hara et al., 1971; Herzberg, 1972, 1976a, 1976b; Gupta et al., 1973; Yang, 1973; Okamura et al., 1974; Presnall, 1976; Yoshikawa, 1977; Onuma and Kimura, 1978; Holland, 1979; Jenkins and Newton, 1979; Akasaka and Onuma, 1980; Gasparik, 1980a, 1980b, 1984). The system diopside, Ca-Tschermak, Mg-Tschermak and enstatite is complex, forming binary and ternary solid solution systems. Diopside and Ca-Tschermak pyroxene form a continuous solid

solution at high pressure and temperature (Clark et al., 1962). Limited solid solution also occurs between diopside and Mg-Tschermak pyroxene (deNeufville and Schairer, 1962).

In this study, diopsides from the starting materials and from each run were examined under the light microscope, x-ray diffraction, scanning electron microscope and electron microprobe to determine if they were Al-bearing.

A. OPTICAL MICROSCOPE

Each experimental product was examined with the optical microscope under immersion oils. In some case, the sample was dispersed with an ultrasonic equipment before examination. The crystals from both synthesis and equilibrium experiments were commonly too small to measure many optical parameters, being anisotropic, prismatic grains less than 5 microns long. Attempts to determine diopside compositions from refractive index failed because of the insensitivity of refractive index to composition.

B. X-RAY DIFFRACTION (X.R.D.)

Experimental products were examined by powder X-ray diffraction using copper radiation on a Philips XRD unit. Routine identification of mineral phases was done with diffractometer settings of 2 degree 2θ per minute and chart speed of 2 centimeters per minute.

Samples were prepared by dispersing the charge using either ultrasonic separation in alcohol or grinding under

alcohol in an agate motar. The sample was mounted on a quartz slide, allowed to dry, and X-rayed.

The synthetic stoichiometric end-member diopside was very well crystallized, with peak positions and intensities comparable with standard diopside (see Fig 2 and Fig 3). Cell parameter refinements were made using eleven peaks in the program of Evans, et al (1963) (see Table II).

Each experimental run producing diopside was also examined by powder diffraction. Cell parameter refinements were carried out to trace the variation of diopside composition. The run products usually contained four phases (due to incomplete reaction) resulting in many peak overlaps. Consequently only seven peaks could be measured precisely for cell refinement. The results of this cell parameter refinement are listed in Table VI.

The results of cell parameter refinement show that the cell parameters of run product diopside are well within the cell parameter range between the join diopside and Ca-Tschermak pyroxene as reported by Clark (1962).

C. SCANNING ELECTRON MICROSCOPE (S.E.M.)

All examinations were carried out using a SEMCO Nanolab-7 scanning electron microscope. Samples were mounted on graphite stubs and coated with carbon or gold depending on whether composition or morphology was being studied.

Table VI

D-spacings and refined cell parameters for diopside (clinopyroxene) from run product

	Run product diopside			Synthetic diopside
h k l	d(calc)	d(obs)	I(/100)	d(obs)
0 2 1	3.338	3.340	22	3.344
2 2 0	3.222	3.222	65	3.234
2 2-1	2.985	2.984	100	2.991
3 1 0	2.942	2.943	45	2.952
3 1-1	2.889	2.889	52	2.894
1 3-1	2.558	2.558	70	2.565
3 1 1	2.297	2.297	25	2.302
a(A)	9.725(3)			9.755
b(A)	8.891(5)			8.928
c(A)	5.257(5)			5.247
β	105°58'			105°52'
V(A^3)	437.13(30)			439.51

1. SAMPLE PREPARATION

Graphite discs were polished using polishing papers and glass and then attached to the metal stub with double sided tape. The experimental products were put into individual glass vials with alcohol and ultrasonically dispersed. Good dispersion was neccessary for chemical analysis to avoid signals from neighbouring grains. To achieve this separation, a small glass micropipette was used to transfer the suspension of grains in alcohol to the graphite stubs. The loaded stubs were checked with the binocular microscope to ensure the correct dispersion before coating.

A Denton Vacuum DV-515 coater was used for carbon coating to a thickness of about 25 nm. Carbon coated samples were used for qualitative chemical analyses and gold coated samples were used for photography.

2. OBSERVATION

A SEMCO Nanolab-7 scanning electron microscope with a Kevex E.D.S. attachment was operated at 15 KV accelerating potential at a usual working distance of 15-18 mm.

Synthetic end-member diopside was examined for morphology and chemistry as reference material for the equilibrium experimental products. Photos were taken and qualitative chemical analyses were made using EDS (Fig 7)

Synthetic diopsides are euhedral to subhedral prismatic crystals. Although the EDS could not give quantitative analysis, the following features may be noted. The chemical spectra show that the diopside is very uniform in composition with all grains having very similar spectra. The peak ratios of Mg/Si and Ca/Si are very similar from one grain to another.

Diopside from equilibration experiments was easily identified by crystal shape, morphology and chemical analysis on the basis of results on end-member synthetic diopside. Grains of diopside at least 4 microns apart from other grains of any phase were chosen for chemical analysis. It was found that if any other phase lay within 4 microns of the diopside, its chemical spectrum would show the effects of the neighbour.

Assemblages commonly found in the run products were diopside + spinel, Clinochlore + grossular, diopside + spinel + minor clinochlore, clinochlore + grossular + minor diopside and diopside (clinopyroxene) + clinochlore (plates

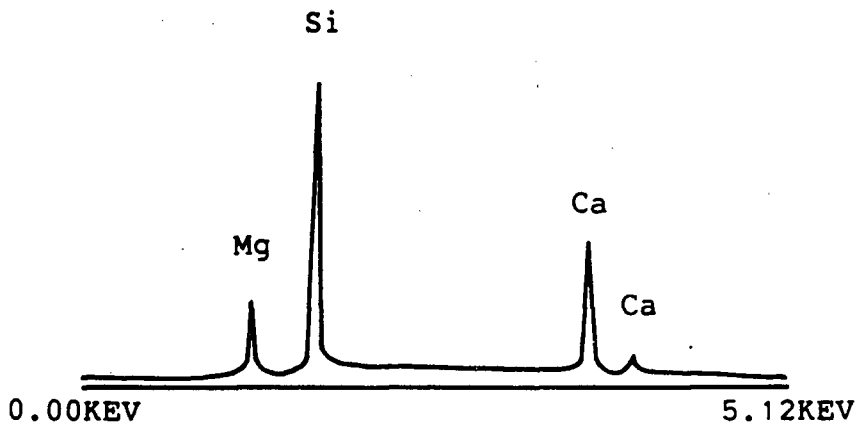

Fig 7 The Scanning Electron Microscope E.D.S. chemical spectrum of synthetic diopside (105 Sec., 8764 Int., Vertical scale(full) 1024, 15 KV accelerating voltage)

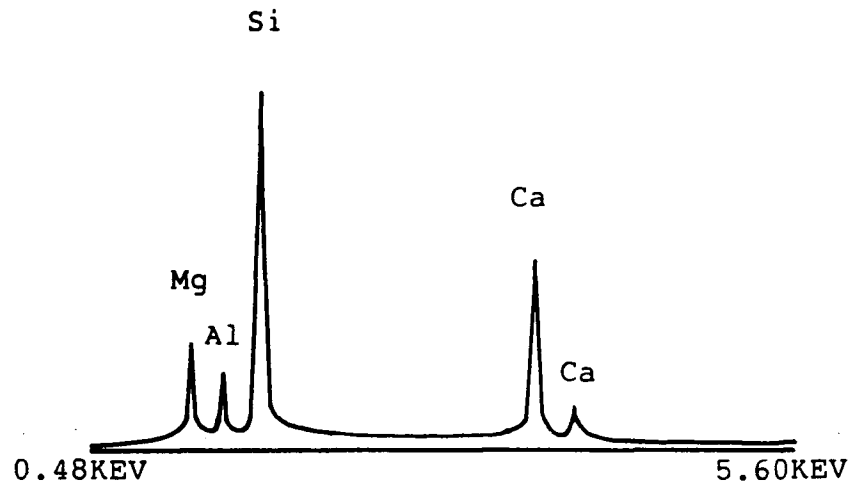

Fig 8 The Scanning Electron Microscope E.D.S. chemical spectrum of diopside from run XRE-10(70 Sec., 13093 Int., Vertical scale(full) 1024, 15 KV accelerating voltage)

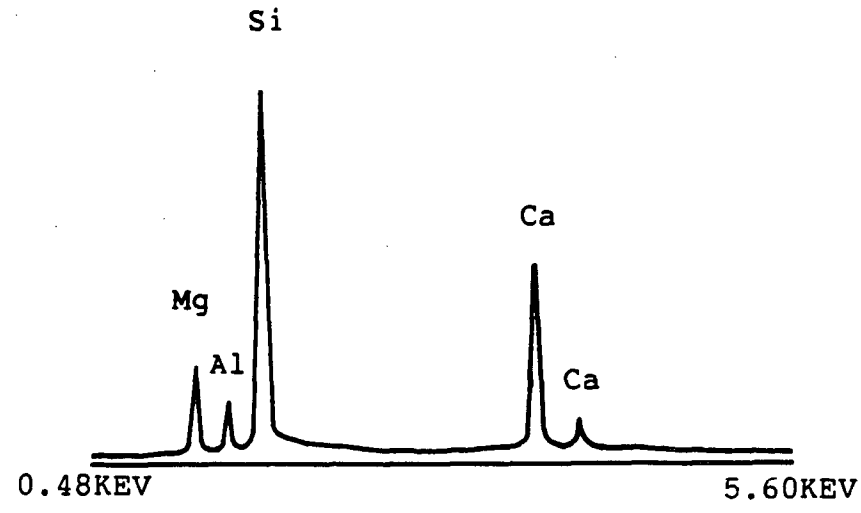

Fig 9 The Scanning Electron Microscope E.D.S. chemical spectrum of diopside from run XRR-3(78 Sec., 10112 Int., Vertical scale(full) 1024, 15 KV accelerating voltage)

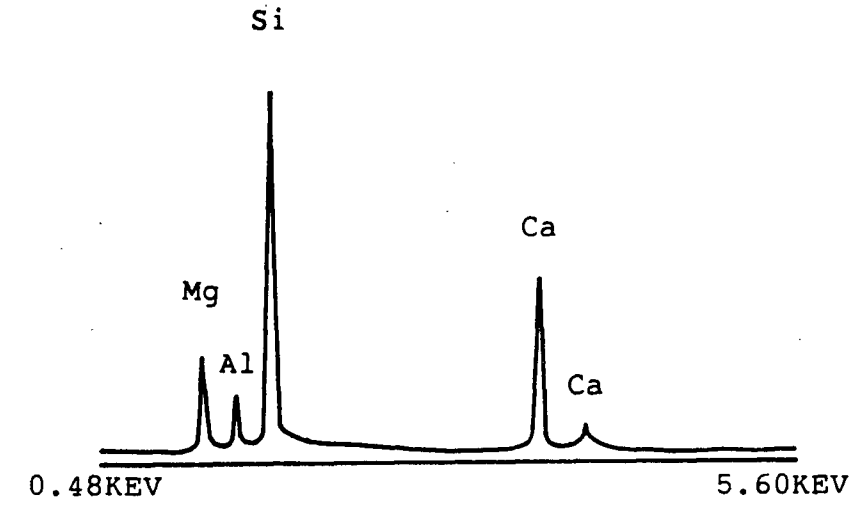

Fig 10 The Scanning Electron Microscope E.D.S. chemical spectrum of diopside from run XRE-10(73 Sec., 9346 Int., Vertical scale(full) 1024, 15 KV accelerating voltage)

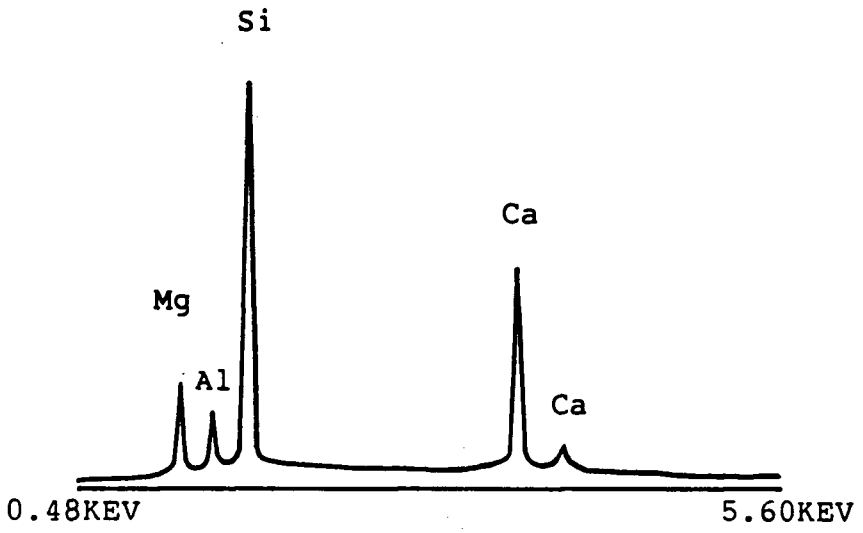

Fig11 The Scanning Electron Microscope E.D.S. chemical spectrum of diopside from run XRR-4(62 Sec., 13527 Int., Vertical scale(full) 1024, 15 KV accelerating voltage)

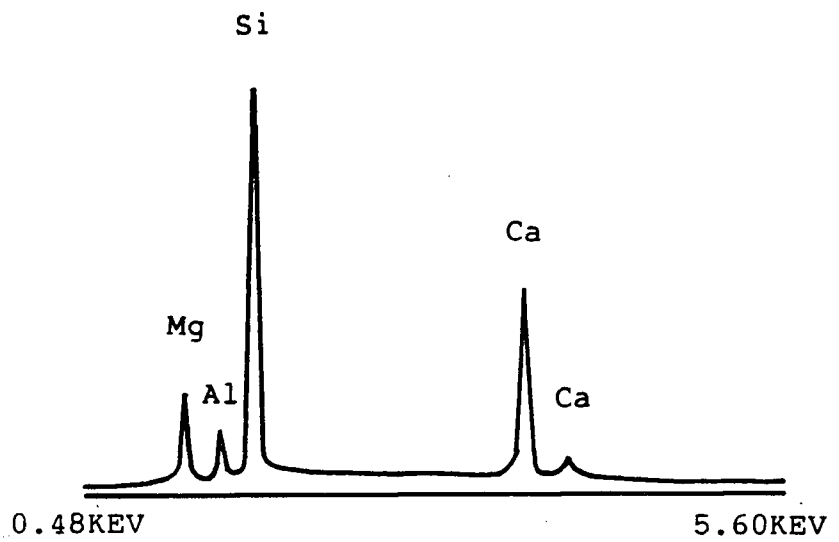

Fig12 The Scanning Electron Microscope E.D.S. chemical spectrum of diopside from run XRE-10(80 Sec., 22193 Int., Vertical scale(full) 2048, 15 KV accelerating voltage)

7-12). No differences of morphology were found between these diopside crystals and the synthetic end-member diopsides. The chemical spectra show clearly that some diopsides contain aluminum. A reproducible aluminum peak was obtained from most of these diopsides(Fig 8 to Fig 12).

The qualitative scanning electron microscope E.D.S. data show that the diopsides in equilibrium with clinochlore contain aluminum, in agreement with deductions from chemography. The electron microprobe was used to obtain more quantitative analyses of diopside.

D. ELECTRON MICROPROBE

1. SAMPLE PREPARATION

Samples were prepared for microprobe analysis in the same way as for the S.E.M. examination, using graphite stubs of 0.25 inch diameter. Using the same technique as for the SEM sample preparation, the charge was loaded onto the graphite stubs and carbon coated to a thickness of 25 nm.

2. ANALYSIS PROCEDURE

An A.R.L. SEMQ microprobe was used for all the analyses. Specimen current was set at 40 nA on aluminum at an accelerating potential of 15 KV with a 300 μm aperture. Counting time for both background and peak was 10 seconds. Analyses using the minimum size beam were unsatisfactory because of Na loss in standardization on jadeite and beam

instability on the small grains available. A small raster about 2 microns was succesfully used.

Oxides determined in the analyses were Al_2O_3, SiO_2, CaO and MgO. Standardization was made on synthetic diopside of similar size and shape to the unknown. Synthetic end-member jadeite provided by H.J. Greenwood and synthetic end-member diopside from this study were used as standards (see Table VII). Because the grains of synthetic standard minerals and run products were all very small (less than the x-ray excitation volume), the shape and the size of the grains selected were very important factors in achieving good analyses. It was easily shown that differences in size and orientation between standard and unknown minerals can significantly affect the analyses. To reduce this effect, grains of similar shape, orientation and size were chosen. Both standard and unknown mineral grains had to be well separated from other grains.

Great care was needed to acquire good analyses. Aside from the above precautions it was found that the beam would shift slowly off the center of the grain as the spectrometers moved. This caused loss of counts and low totals. Runs with less than 80% or more than 120% total weight percentage were not used even for calculating element ratios. To check the repeatability and reliability, many analyses were made on the same grain. No differences were noticed from data obtained on different days. Table VIII shows the duplicate analyses of standard diopside. Appendix

Table VII

Standards used for microprobe analyses

Oxides	Composition	Sources
MgO	$CaMgSi_2O_6$	Synthetic endmember diopside from this study
CaO	$CaMgSi_2O_6$	Synthetic endmember diopside from this study
SiO_2	$CaMgSi_2O_6$	Synthetic endmember diopside from this study
Al_2O_3	$NaAlSi_2O_6$	Synthetic endmember jadeite from H.J. Greenwood

1 shows the analysis results in formula total and weight total. Analyses on diopsides from different run products did not show any obviously regular variation of the aluminum content. Al_2O_3 in clinopyroxene varies from 0.3 to 0.7 per formula unit. MgO and CaO are both less than 1.0 per formula unit, which is the value in diopside.

3. INTERPRETATION OF DATA

The presence of aluminum and the deficiencies of magnesium and calcium in clinopyroxene indicate that the solution can be described by substitution of Tschermak "molecules". If only Ca-Tschermak substituted for diopside according to the AlAl--MgSi substitution, then calcium should not change in value and would remain around 1.0. Magnesium and silicon contents would decrease while aluminum increased. The deficiencies in both magnesium and calcium suggest that substitutions by both Ca-Tschermak and Mg-Tschermak occured.

Table VIII

Duplicate of the microprobe analyses of standard diopside

Time	MgO	Al_2O_3	SiO_2	CaO	Total	wt%total
Grain A						
#1	.9957	.0037	1.9773	1.0453	4.0211	97.96
#2	.9933	.0034	1.9891	1.0231	4.0093	104.36
Grain B						
#1	.9965	.0057	1.9944	1.0063	4.0029	112.49
#2	1.0514	.0051	1.9828	.9753	4.0146	115.36
#3	1.0207	.0041	1.9975	.9782	4.0005	110.94

In an attempt to see more clearly the relations between element oxides, various plots were made using different oxide values in the formula. For example, Al_2O_3 versus SiO_2, Al_2O_3 versus CaO, Al_2O_3 versus MgO and MgO versus CaO were plotted (see Fig 13 to Fig 19). The plots show that the data points are relatively scattered. Theoretically if a run reached equilibrium and the analytical errors could be eliminated, then all the points should plot at one point. The differences in composition seen in this study are certainly beyond analytic error.

Although the data for aluminum and silicon vary from one analysis to another, the plot of Al_2O_3 versus SiO_2 (Fig 16) shows that the data can be very well fitted in a linear equation. Linear regression shows that the relation between Al_2O_3 and SiO_2 can be expressed as SiO_2(formula) = -0.5298 * Al_2O_3(formula) + 1.9914. If only Tschermak molecule substitutions were involved, then theoretically the constants in this equation should be 0.5 and 2.0 respectively. The closeness of the values indicates that

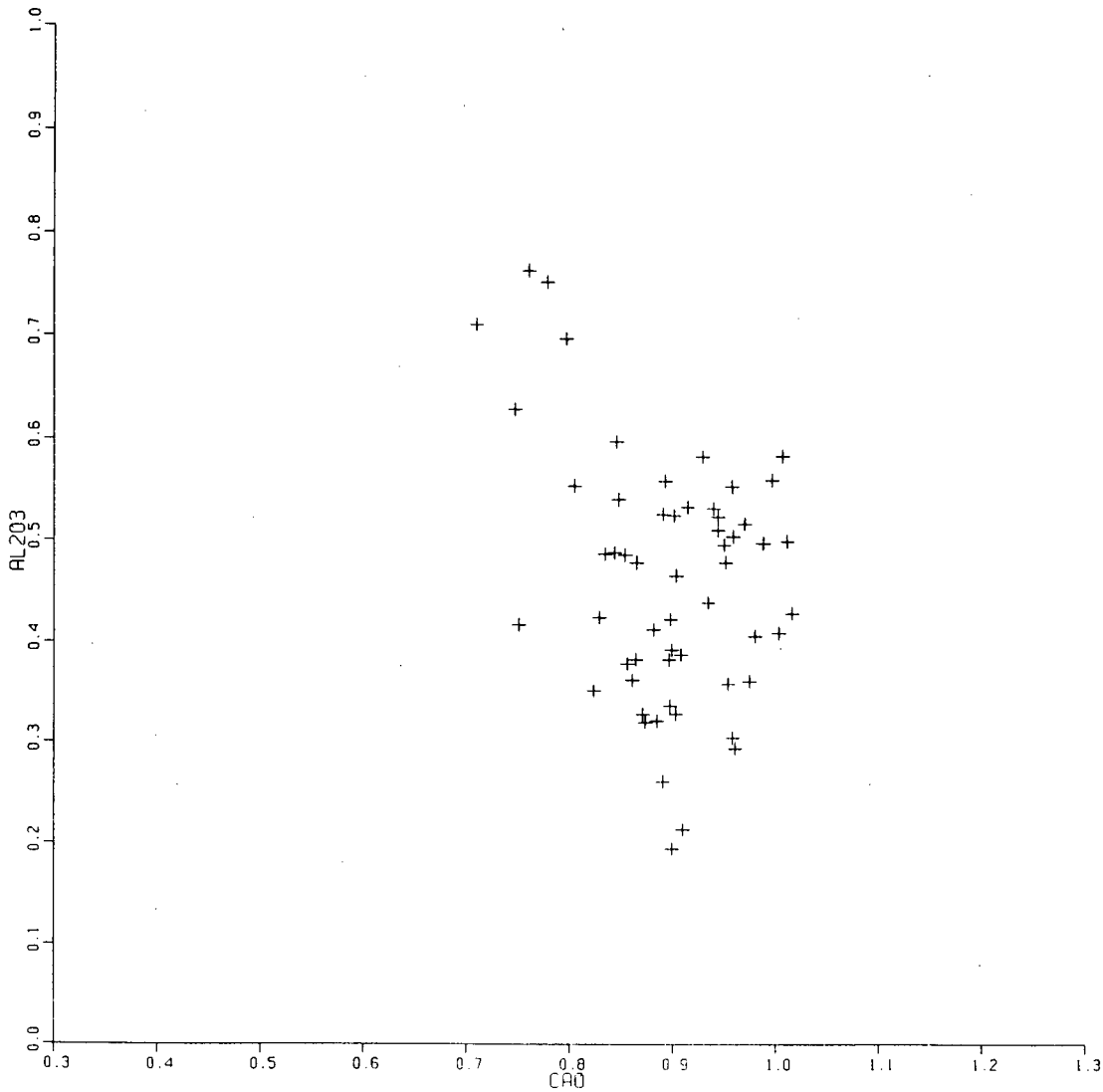

Fig 13 The relation between Al_2O_3 and CaO (mol) in run product diopside from microprobe analyses

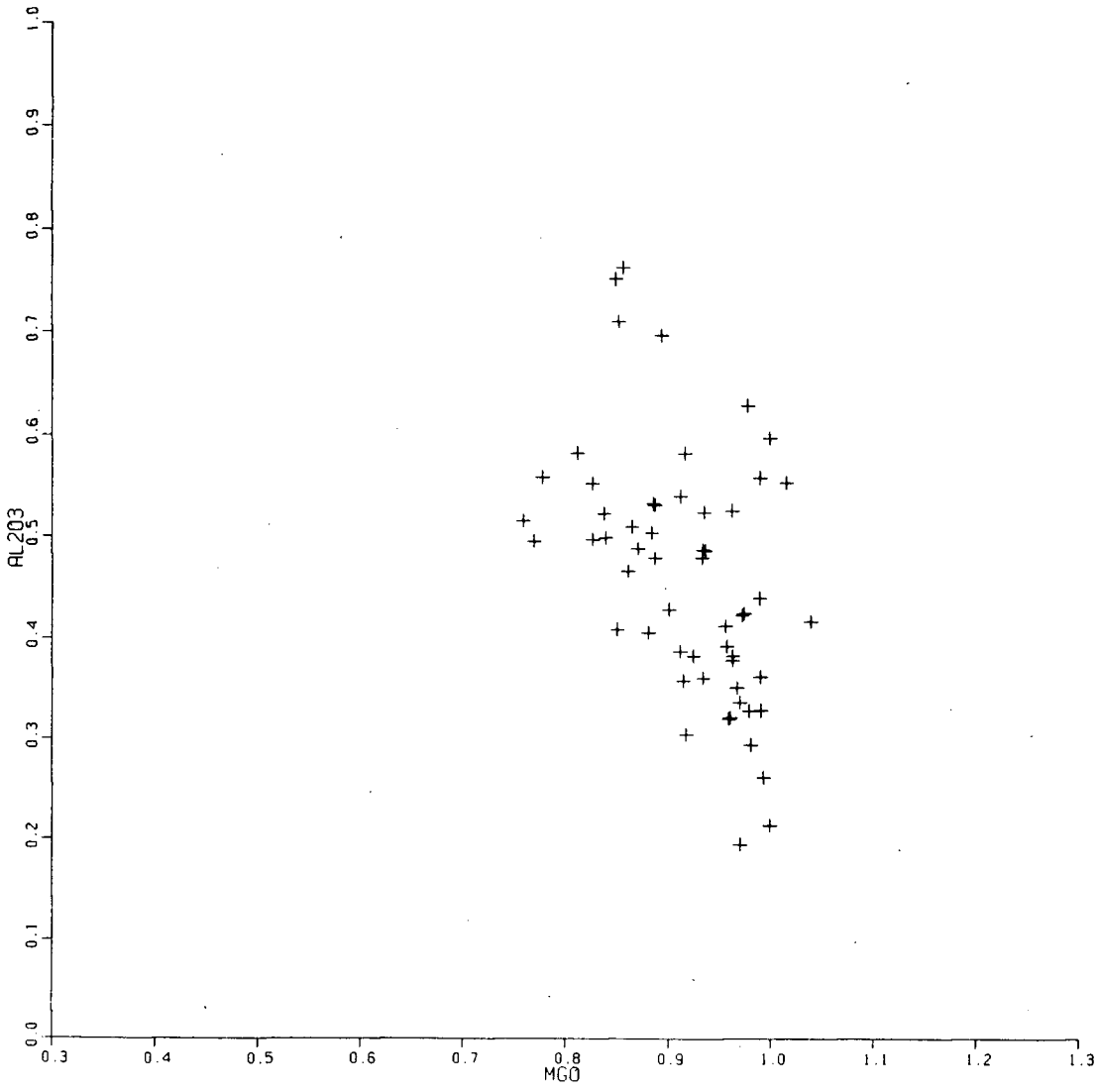

Fig 14 The relation between Al_2O_3 and MgO (mol) in run product diopside from microprobe analyses

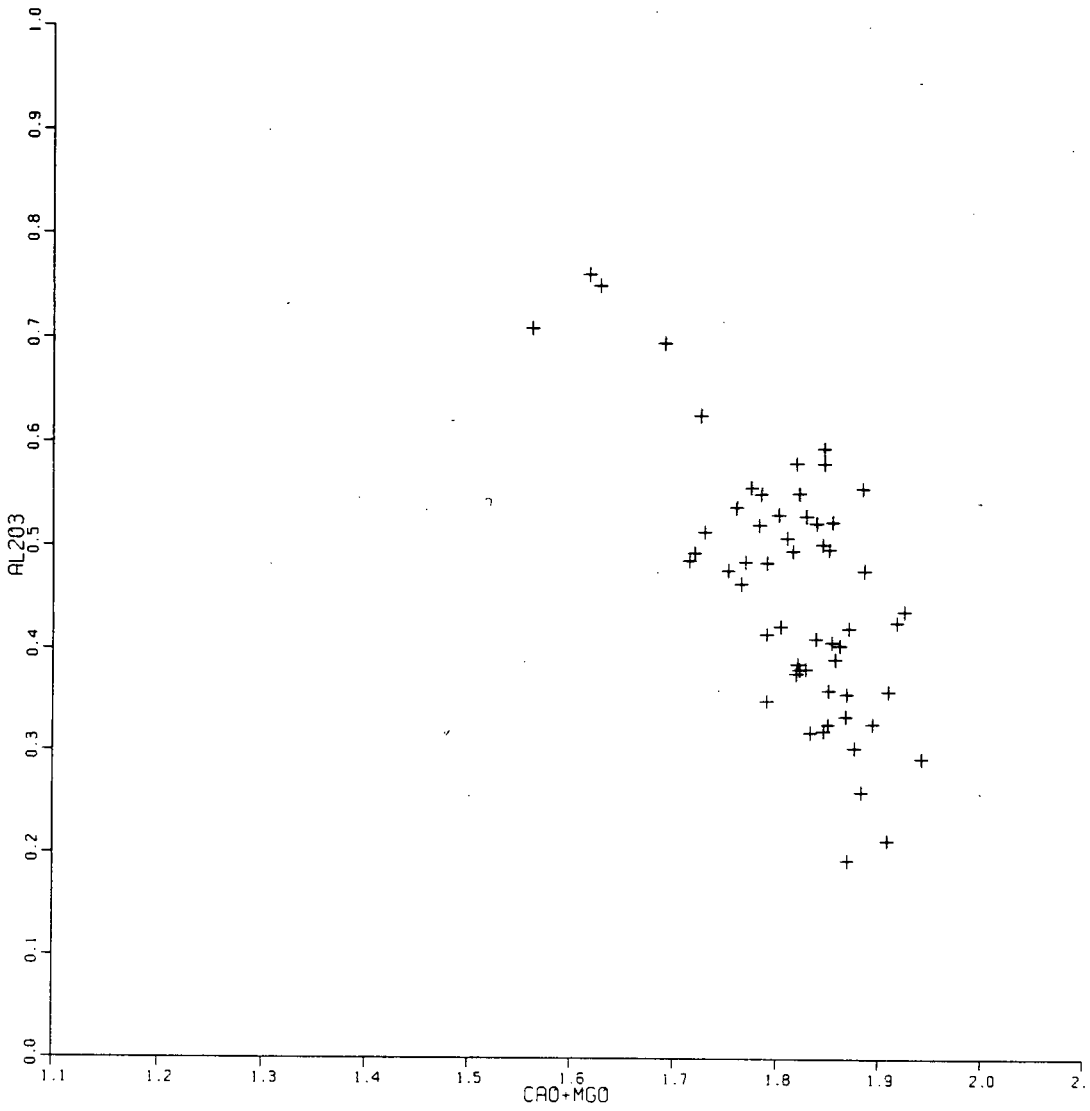

Fig 15 The relation between Al_2O_3 and (CaO+MgO) (mol) in run product diopside from microprobe analyses.

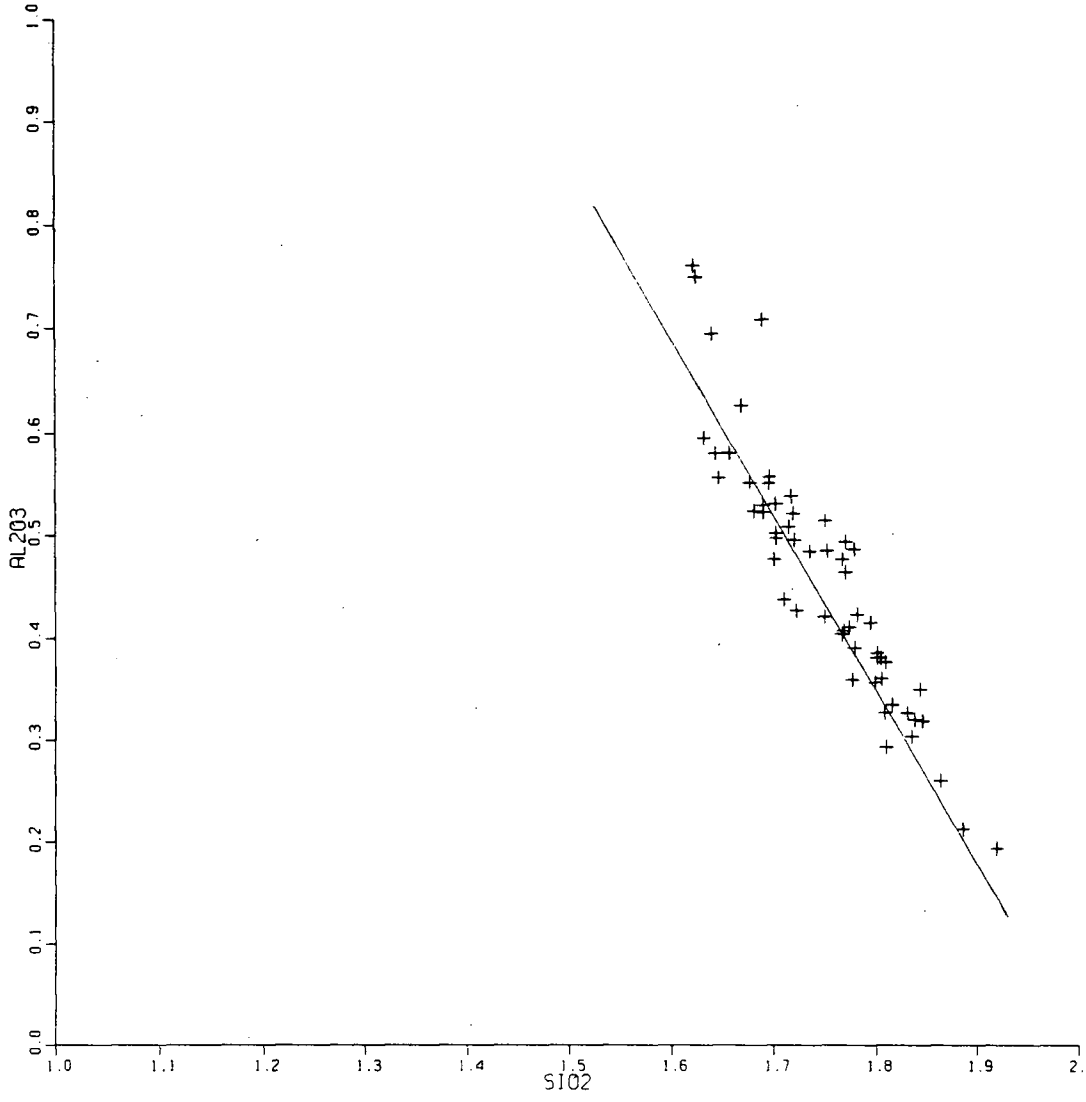

Fig 16 The relation between Al_2O_3 and SiO_2 (mol) in run product diopside from microprobe analyses. The straight line is the relation between Al_2O_3 and SiO_2 for Tschermak's substitution.

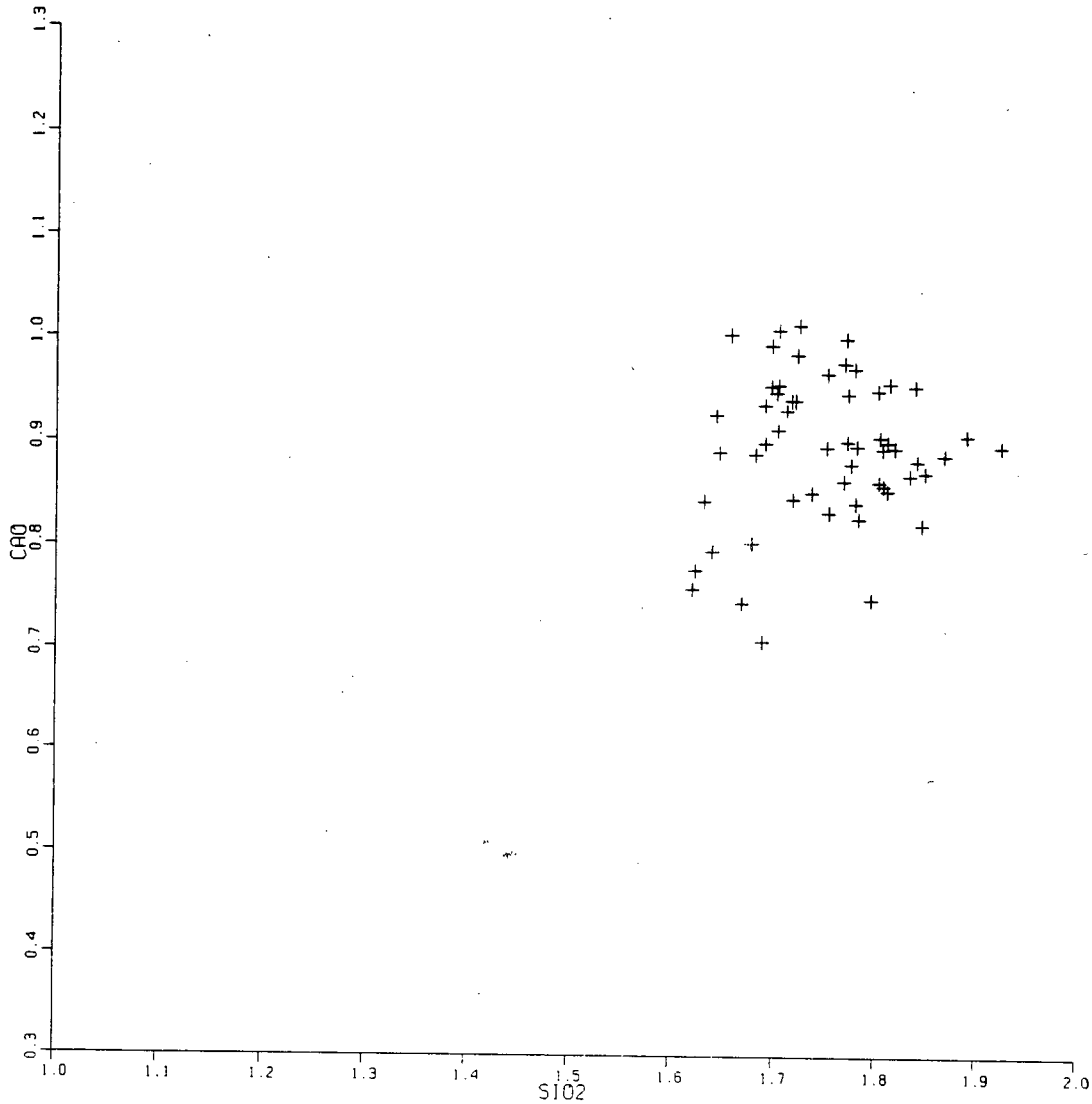

Fig17 The relation between CaO and SiO_2 (mol) in run product diopside from microprobe analyses

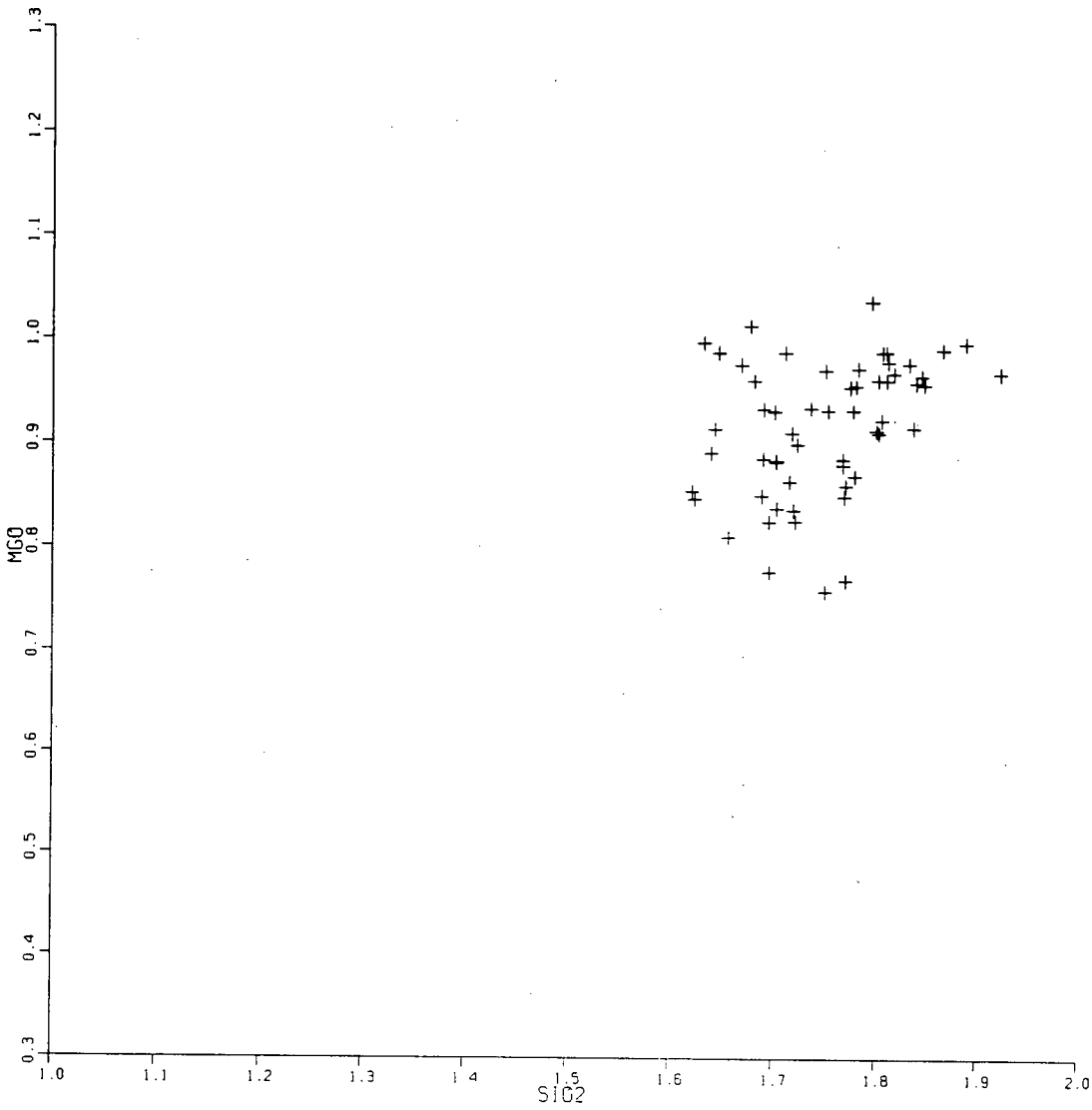

Fig 18 The relation between MgO and SiO_2 (mol) in run product diopside from microprobe analyses

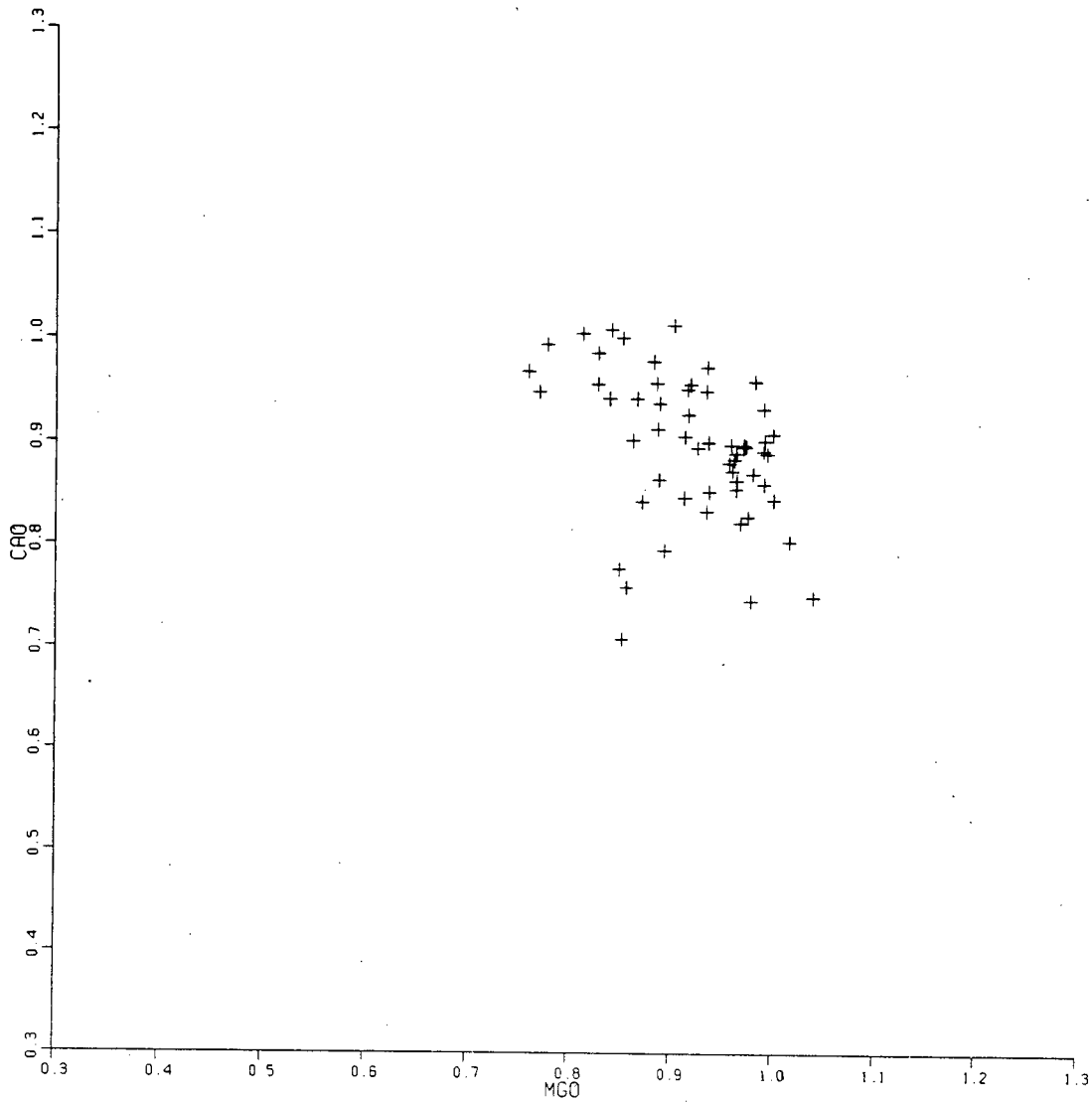

Fig 19 The relation between CaO and MgO (mol) in run product diopside from microprobe analyses

this is probably the case.

The question arises as to the relative proportion of Ca-Tschermak and Mg-Tschermak molecule substitution. All the oxides have been partitioned and balanced between the solution phases of Ca-Tschermak, Mg-Tschermak and diopside. The analytical data show that the average calcium deficiency is greater than that of magnesium. This could be caused by more Mg-Tschermak than Ca-Tschermak molecules substituting for diopside molecules, but this seems unlikely to be the case.

Ohashi et al. (1975) and Ohashi and Finger (1976) report that there is a magnesium and calcium cation distribution problem between M1 site and M2 site in the diopside structure. For our analytical results, it may be reasonable to assume that some magnesium substituted for calcium in the M2 site, ie. assume $Ca^{++} + Mg^{++}(M2) = 1.0$. Then half of the aluminum could be treated as substituting for magnesium in M1 site while the other half substituted for silicon in the tetrahedral site. According to this partition model, mass-balance calculations were made and the results are listed in Table IX. The results are consistent ie. the atom totals in M1 are very close to 1.0 formula unit and the atom totals in the tetrahedral space are very close to 2.0 formula units. This may be the evidence for having achieved an appropriate model for the substitution.

It has been reported (Gasparik et al., 1980a) that aluminous pyroxenes are very difficult to equilibrate and

Table IX

The results of mass balance calculation according to the microprobe analyses

Analysis data by microprobe				Data distributed among the different sites			
CaO	MgO	Al_2O_3	SiO_2	M2	M1	T	Activity
0.9514	0.9328	0.4783	1.6992	1.0000	1.1233	1.9383	0.5755
1.0062	0.8111	0.5818	1.6552	1.0000	1.1082	1.9461	0.5368
0.9016	0.9350	0.5240	1.6887	1.0000	1.0986	1.9507	0.5145
1.0104	0.8391	0.4986	1.7013	1.0000	1.0988	1.9506	0.5942
1.0152	0.9009	0.4281	1.7209	1.0000	1.1301	1.9349	0.6509
0.9579	0.9174	0.3046	1.8339	1.0000	1.0276	1.9862	0.6956
0.8641	0.9629	0.3823	1.7998	1.0000	1.0181	1.9909	0.5736
1.0025	0.8503	0.4082	1.7674	1.0000	1.0569	1.9715	0.6501
0.9875	0.8266	0.4969	1.7193	1.0000	1.0625	1.9677	0.5776
0.8345	0.9338	0.4865	1.7510	1.0000	1.0115	1.9943	0.4886
0.7601	0.8557	0.7630	1.6199	1.0000	0.9973	2.0014	0.3075
0.7781	0.8482	0.7521	1.6227	1.0000	1.0023	1.9987	0.3204
0.7094	0.8512	0.7103	1.6870	1.0000	0.9157	2.0421	0.2964
0.9796	0.8809	0.4053	1.7658	1.0000	1.0631	1.9684	0.6380
0.9396	0.8872	0.5309	1.6885	1.0000	1.0922	1.9539	0.5311
0.8555	0.9625	0.3776	1.8078	1.0000	1.0068	1.9966	0.5698
0.8970	0.9697	0.3357	1.8147	1.0000	1.0345	1.9825	0.6296
0.8474	0.9118	0.5394	1.7159	1.0000	1.0289	1.9856	0.4670
0.8962	0.9246	0.3819	1.8032	1.0000	1.0117	1.9941	0.5945
0.8707	0.9787	0.3275	1.8297	1.0000	1.0131	1.9935	0.6150
0.8845	0.9605	0.3210	1.8366	1.0000	1.0055	1.9971	0.6286
0.9288	0.9157	0.5816	1.6416	1.0000	1.1353	1.9324	0.4986
0.8435	0.8705	0.4877	1.7772	1.0000	0.9579	2.0210	0.4862
0.8929	0.9893	0.5576	1.6452	1.0000	1.1610	1.9240	0.4961
0.9438	0.8375	0.5224	1.7176	1.0000	1.0425	1.9788	0.5329
0.9437	0.8648	0.5097	1.7135	1.0000	1.0633	1.9683	0.5438
0.9960	0.7772	0.5583	1.6946	1.0000	1.0523	1.9738	0.5394
0.7962	0.8928	0.6965	1.6381	1.0000	1.0372	1.9863	0.3597
0.9145	0.8855	0.5323	1.7008	1.0000	1.0661	1.9669	0.5131
0.9573	0.8259	0.5524	1.6941	1.0000	1.0594	1.9703	0.5232
0.7466	0.9776	0.6280	1.6669	1.0000	1.0382	1.9809	0.3688
0.9093	0.9986	0.2138	1.8856	1.0000	1.0148	1.9925	0.7286
0.8990	0.9699	0.1947	1.9195	1.0000	0.9663	2.0168	0.7323
0.8229	0.9669	0.3507	1.8421	1.0000	0.9651	2.0174	0.5614
0.8730	0.9588	0.3196	1.8444	1.0000	0.9916	2.0042	0.6202
0.9532	0.9146	0.3578	1.7978	1.0000	1.0467	1.9767	0.6537
0.8976	0.9720	0.4223	1.7485	1.0000	1.0807	1.9596	0.5750
0.8603	0.9896	0.3614	1.8040	1.0000	1.0306	1.9847	0.5862
0.9029	0.9901	0.3281	1.8074	1.0000	1.0570	1.9714	0.6411
0.9586	0.8840	0.5035	1.7011	1.0000	1.0943	1.9529	0.5600
0.9074	0.9119	0.3869	1.8002	1.0000	1.0127	1.9937	0.5985
0.9696	0.7589	0.5156	1.7490	1.0000	0.9863	2.0068	0.5440
0.8533	0.9359	0.4857	1.7341	1.0000	1.0320	1.9769	0.5020
0.8906	0.9621	0.5251	1.6798	1.0000	1.1152	1.9423	0.5093
0.9500	0.7691	0.4950	1.7692	1.0000	0.9666	2.0167	0.5439
0.9603	0.9805	0.2939	1.8091	1.0000	1.0877	1.9560	0.7105
0.9743	0.9339	0.3603	1.7757	1.0000	1.0883	1.9558	0.6702
0.8812	0.9558	0.4118	1.7726	1.0000	1.0429	1.9785	0.5677
0.7504	1.0388	0.4161	1.7933	1.0000	0.9973	2.0013	0.4768
0.8990	0.9574	0.3919	1.7783	1.0000	1.0523	1.9742	0.5936
0.8650	0.8866	0.4782	1.7656	1.0000	0.9907	2.0047	0.5090
0.8454	0.9988	0.5963	1.6307	1.0000	1.1423	1.9288	0.4465
0.8045	1.0151	0.5526	1.6757	1.0000	1.0959	1.9520	0.4434
1.0587	0.9070	0.3218	1.7758	1.0000	1.1266	1.9367	0.7630
0.8900	0.9926	0.2612	1.8628	1.0000	1.0132	1.9934	0.6770
0.9343	0.9891	0.4389	1.7092	1.0000	1.1428	1.9286	0.5929
0.8287	0.9741	0.4241	1.7805	1.0000	1.0148	1.9925	0.5234
1.0349	0.9568	0.2868	1.7891	1.0000	1.1351	1.9325	0.7750

may form inhomogeneous crystals because of the slow diffusion of aluminum. It would not be surprising according to Gasparik's results to find an aluminum-free center of diopside seed crystals with an aluminum-rich clinopyroxene overgrowth. Fujii (1977) has also experimentally determined the compositions of orthopyroxene and clinopyroxene coexisting with forsterite and spinel at 16 kbar and 1100 to 1375°C, using both glass and crystalline mixture of synthetic clinoenstatite, diopside and spinel as the starting material. Run time ranged from six hours at 1375°C to four days at 1100°C. The run products were analyzed under electron microprobe. It was found that in the run products of homogenization experiments, the pyroxene grains were not completely equilibrated, as the composition of the cores of large grains were close to the composition of the starting material. However, the analyses of small grains were similar to those of the rims of the large grains. Although an examination of such zoned grains was impossible in this study because of the small grain size, this could be the main reason for the variation of aluminum content. Although the analysis beam was always put as near the center of the grain as possible, the shifting beam makes it probable that different zones were analysed in different grains, in different proportions.

E. COMPOSITION OF CLINOPYROXENES FROM RODINGITES

Clinopyroxenes from rodingite have been analysed by many petrologists (Bell, Clarke and Marshall, 1911; Challis, 1965; Frost, 1975; Evans, Trommsdorff and Richter, 1979; Rawson, 1984; Rice, personal communication). Rawson (1984), studing the rodingites from the north-central Klamath Mountains, California (pressure condition 5 to 7 kbars), found that clinopyroxene in rodingites is a complex solid solution of Mg, Mn, Fe and Al in diopside. Ca contents range from 0.931 to 0.993 cations per formula unit. X_{Mg} for pyroxene is between 0.94 and 0.81. Tschermak's substitution of aluminum, ferric iron and titanium appears to increase with metamorphic grade. Aluminum is the only cation substituting in the tetrahedral site in these pyroxenes. The mineral assemblages and electron microprobe analyses of the clinopyroxenes from these assemblages are shown in Appendix 2. Also presented are the clinopyroxene compositions from the Paddy-Go-Easy Pass, Washington rodingites (P=3kbars?) by Rice (personal communication).

Compositions of clinopyroxene from rodingites show that aluminum contents are usually low, although some of the samples contain as high as 11.48 wt% of Al_2O_3 (0.48 cation per formula unit) (528A1-MB). The average value of Al_2O_3 is about 2 to 3 wt%. It seems clear that diopsides from natural rodingites metamorphosed under conditions similar to those in the experiments reported here contain much less aluminum than the experimentally produced diopsides.

IV. THERMODYNAMIC ANALYSIS

A. PRECALCULATION

Thermodynamic calculations of reactions among phases found in metarodingite were made in detail by Rice (1983). The thermodynamic properties used in that calculation were mainly from Helgeson et al.(1978). The calculated phase relations are shown in Fig 20. The following expression was used by Rice (1983) for equilibria involving CO_2 and H_2O:

$$RT(\nu_{CO_2} \ln f_{CO_2} + \nu_{H_2O} \ln f_{H_2O}) = RT \ln K$$

$$= -\Delta H_r^o - \Delta V_s (P-1) + T_e \Delta S_r^o - \int_{T_o}^{T_e} \Delta Cp_r \, dT$$

$$+ T_e \int_{T_o}^{T_e} \Delta Cp_r \, d\ln T$$

where ν_{gas} is the stoichiometric coefficient of the volatile species in the reaction. T_o is the thermodynamic reference temperature (298.15°K), and T_e is the equilibrium temperature. ΔH_r^o, ΔS_r^o, ΔV_s , and ΔCp refer to the standard reaction enthalpy, third-law entropy, solid-phase volume change, and heat capacity at the reference temperature and 1 bar pressure.

Program P-T System by Perkins, Brown and Berman (1986) was used for this study to calculate the phase equilibrium. Thermodynamic properties (heat capacities, enthalpies, entropies and volumes) for the phases involved were adopted

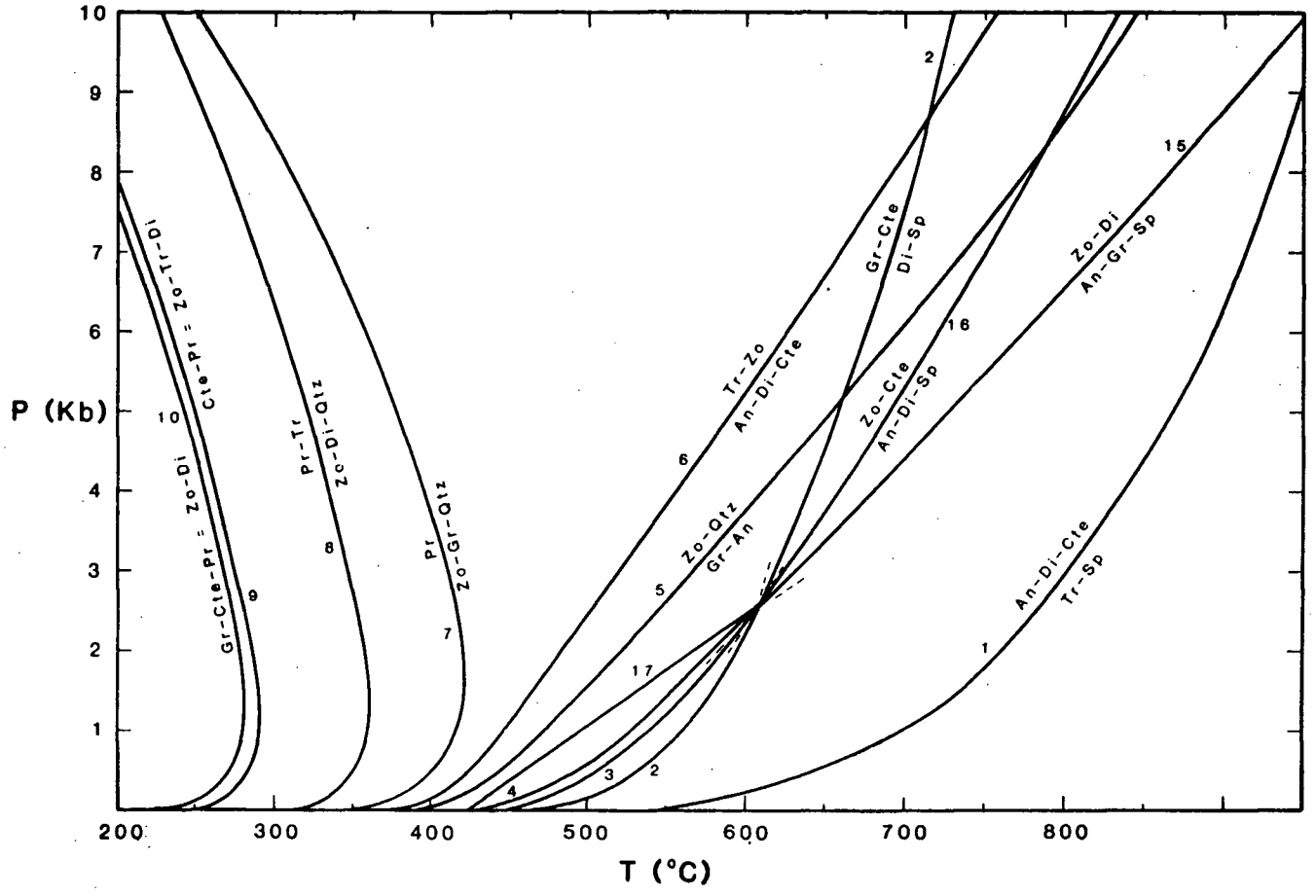

Fig 20 Calculated P_{H_2O}-T diagram for dehydration equilibria among phases found in metarodingites. Taken from Rice (1983). An=anorthite, Cte=chlorite, Di=diopside, Gr=grossular, Pr=prehnite, Qtz=quartz, Sp=spinel, Tr=trmolite, Zo=zoisite.

from UBCDATABASE, described by Berman, Brown, and Greenwood (1986).

The heat capacity function and the coefficients used in this study are from Berman and Brown (1985):

$$Cp = K_0 + K_1/T^{0.5} + K_2/T^2 + K_3/T^3$$

Table X lists all the thermodynamic properties and heat capacity function coefficients for the phases considered here. The equilibrium curves calculated as described above are shown in Fig 22, where it will be seen that they are close to the curves calculated by Rice (1983) using Helgeson and others' (1978) data.

B. EXPERIMENTAL CONSTRAINTS ON THERMODYNAMIC PROPERTIES

Critically-limiting experimental results were selected for the constraint of sets of ΔS^o_r (298, 1 bar) and ΔH^o_r (298, 1 bar). These data were analyzed by linear programming (Berman, Engi, Greenwood, and Brown, 1986). Fig 21 shows the range of thermodynamic properties, derived from experimental results without any constrains of thermodynamic properties from UBCDATABASE, that are internally consistent for the reaction. Also shown in this figure are the values of ΔS^o_r (298, 1 bar) and ΔH^o_r (298, 1 bar) calculated from UBCDATABASE and Helgeson's database. Linear programming solutions to problems of this kind can also result from

Table X

Thermodynamic properties for phases considered in this study (all from UBCDATABASE)

Phase				
Clinochlore	ΔH_f^o (J)	S^o(J/K)	V (cm^3)	
	-8921085	429.77	209.82	
$Mg_5Al_2Si_3O_{10}(OH)_8$	K_0	K_1	K_2	K_3
	1214.28	-11217.13	0.0	-1256253184
Diopside	ΔH_f^o (J)	S^o(J/K)	V (cm^3)	
	-3201898	142.50	66.18	
$CaMgSi_2O_6$	K_0	K_1	K_2	K_3
	305.41	-1604.93	-7165973	921837568
Grossular	ΔH_f^o (J)	S^o(J/K)	V (cm^3)	
	-6632395	255.00	125.30	
$Ca_3Al_3Si_3O_{12}$	K_0	K_1	K_2	K_3
	573.43	-2039.41	-18887168	2319311872
Spinel	ΔH_f^o (J)	S^o(J/K)	V (cm^3)	
	-2302436	83.67	39.74	
$MgAl_2O_4$	K_0	K_1	K_2	K_3
	235.90	-1766.58	-1710415	40616928
Water	ΔH_f^o (J)	S^o(J/K)	V (cm^3)	
H_2O	-241816	188.72	24450.30	

optimizing some objective function, which may be any linear combination of the thermodynamic properties of the phases. For example, one may find the maximum or minimum of the S^o and ΔH_f^o of any phase, or the ΔS_r^o and ΔH_r^o of the reaction. The limits on ΔS_r^o and $\Delta H^o{}_r$ for the reaction that are consistent with the experiments are listed in Table XI.

Table XI

Range of thermodynamic properties that are consistent with experimental results

Clinochlore		Reaction	
maximum S	627.77(J/K)	minimum ΔS	466.99(J/K)
minimum S	65.42(J/K)	maximum ΔS	1029.34(J/K)
maximum H	-8755376.(J)	minimum ΔH	209941.(J)
minimum H	-9233983.(J)	maximum ΔH	688548.(J)

The reaction curves were calculated and plotted (Fig 22) using these two sets of ΔS_r^o (298, 1 bar) and ΔH_r^o (298, 1 bar) values. Also shown are the equilibrium calculated with coefficients from UBCDATABASE and the curve calculated by Rice (1983) using the Helgeson's database (1978). Fig 21 and Fig 22 both indicate that the experimental results from this study are fully consistent with UBCDATABASE and Helgeson's database.

C. CLINOPYROXENE SOLID SOLUTION

The previous calculations were made on the assumption that all phases present are pure endmembers. The possible solid solutions were ignored.

In previous chapters, it was demonstrated that diopsides from some run products contain aluminum and could be described by substitution of the Ca-Tschermak and Mg-Tschermak "molecules".

Wood and Holloway (1984) have discussed the solid solution of pyroxenes and their mixing properties. In the four-component system $CaO-MgO-Al_2O_3-SiO_2$, orthopyroxene

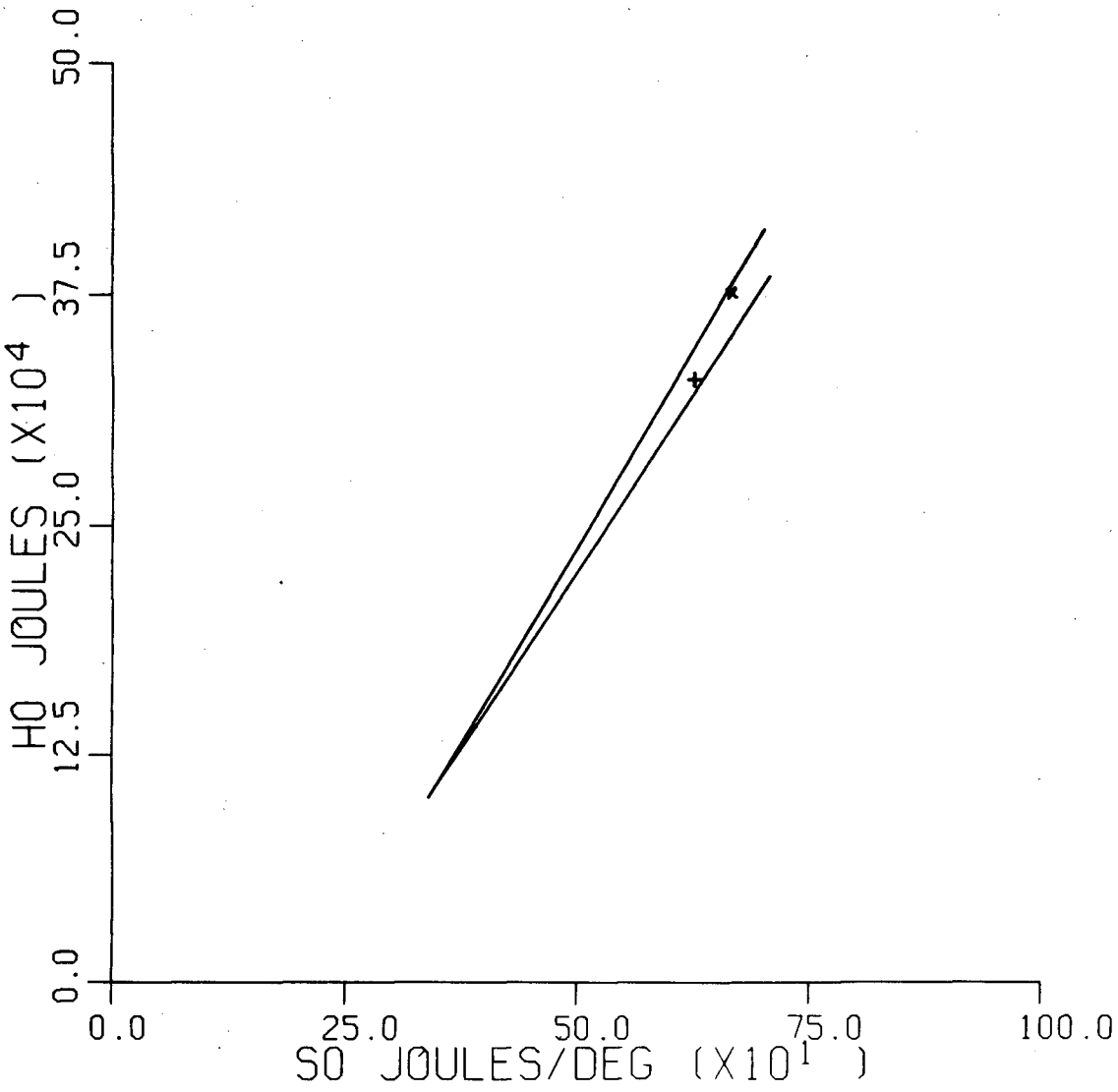

Fig 21 The range of thermodynamic properties, derived from experimental results with linear programming, that are internally consistent.
× -- ΔS_r^o and ΔH_r^o values calculated from UBCDATABASE.
+ -- ΔS_r^o and ΔH_r^o values calculated from Helgeson's database.

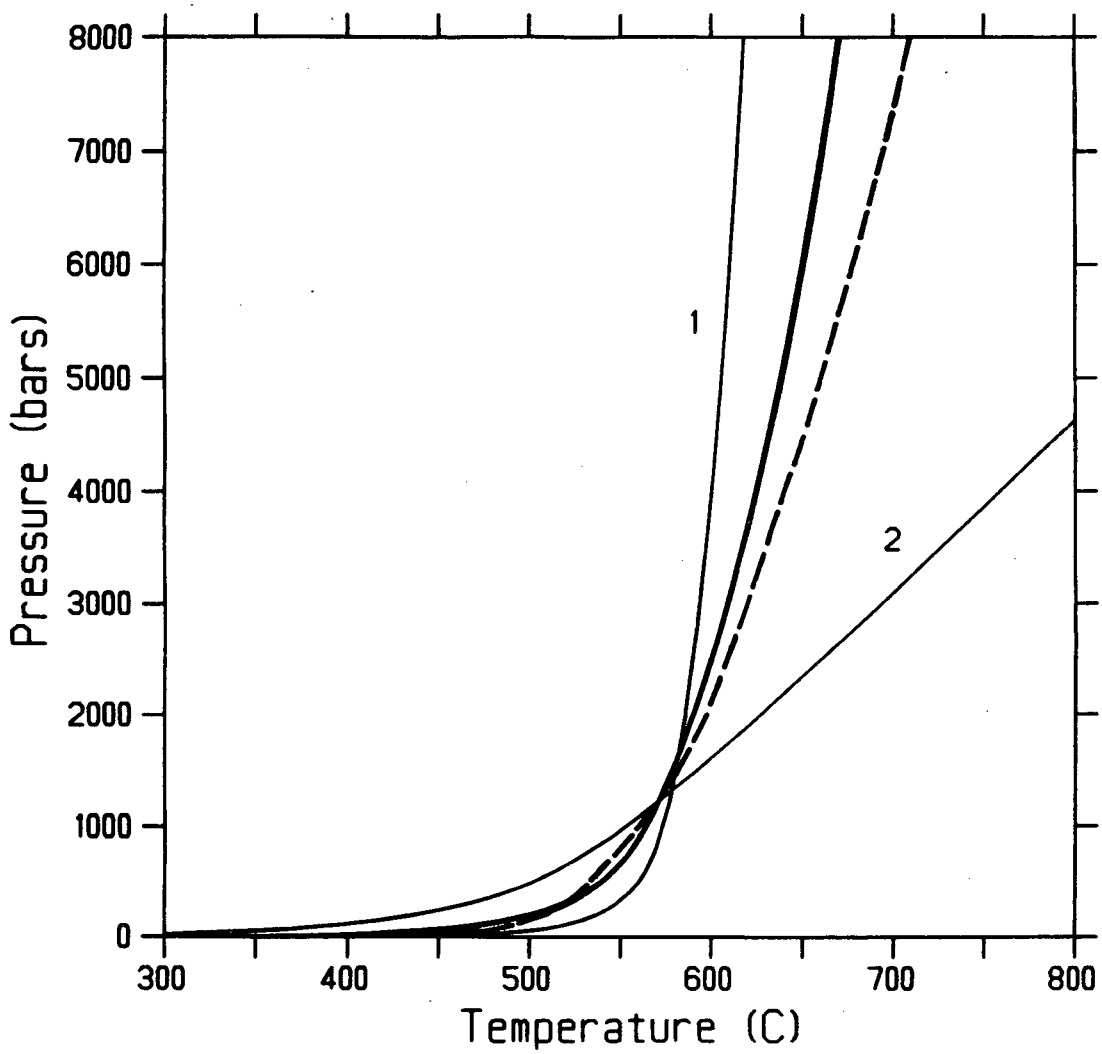

Fig 22 The upper (curve #1) and lower (curve #2) limits of equilibrium from consistent analysis of experimental results taken without reference to other constraining data. The heavy solid curve is the precalculated equilibrium using UBCDATABASE and the heavy dashed curve is calculated from Helgeson's database by Rice (1983).

compositions can be represented in the ternary $CaMgSi_2O_6$, $Mg_2Si_2O_6$ and $MgAl_2SiO_6$. Clinopyroxene compositions may readily be represented by the compositions $CaMgSi_2O_6$, $Mg_2Si_2O_6$ and $CaAl_2SiO_6$.

Holland et al.(1979, 1980) have derived mixing properties of $CaMgSi_2O_6$-$Mg_2Si_2O_6$ clinopyroxene and orthopyroxene solid solutions. These mixing properties are consistent with experimental determinations of the two-pyroxene miscibility gap and with enthalpy of solution data. For the reaction:

$$Mg_2Si_2O_6(\text{orthopyroxene}) = Mg_2Si_2O_6(\text{Clinopyroxene})$$

they derived standard state (pure phase at P and T) temperature-independent enthalpy and entropy changes of 1625 Cal and 0.66 Cal/K (6799.00 Joules and 2.76 J/K) respectively.

The free energy of solution in the binary system, $Mg_2Si_2O_6$-$CaMgSi_2O_6$ can be represented as

$$G_{mix} = RT\,(X_{Mg_2Si_2O_6} * \ln X_{Mg_2Si_2O_6} + X_{CaMgSi_2O_6} * \ln X_{CaMgSi_2O_6}) + W_G * X_{CaMgSi_2O_6} * X_{Mg_2Si_2O_6}$$

where the first two terms on the right hand side are ideal entropy contributions and the last term is the excess free energy due to Mg-Ca mixing on the larger cation position M_2.

The interaction parameter, W_G , defined in terms of excess enthalpy W_H , entropy W_S and W_V , is as follows:

$$W_G = W_H - T*W_S + P*W_V$$

Holland et al. (1979) have adopted a temperature-independent W_G value of 8126 Cal/Mol (34000 Joules/Mol) for the orthopyroxene solid solution although this value was poorly constrained by the data. For the clinopyroxene binary, a W_H value of 5913 Cal/Mol (24739.99 J/Mol), W_S of 0.0 and W_V of 0.025 Cal/Mol (0.10 J/Mol) were derived.

Mixing properties of the $CaMgSi_2O_6$-$Mg_2Si_2O_6$ orthopyroxene and clinopyroxene binaries and of the $Mg_2Si_2O_6$-$MgAl_2SiO_6$ orthopyroxene join have also been derived by combining mixing parameters for each of the individual sites (Saxena and Ghose, 1971) with "cross-site" or reciprocal terms as described by Wood and Nicholls (1978). The orthopyroxene and clinopyroxene solid solution may be considered as containing three binary solution sites, M_1(Al-Mg), M_2(Ca-Mg), and T(Al-Si). The solution of $MgAl_2SiO_6$ component in orthopyroxene was treated following Wood and Banno (1973). In this treatment, Al-Si mixing on tetrahedral sites does not contribute to the free energy of solution independently, because of coupled substitutions in M_1 and M_2. Neglecting tetrahedral sites for both pyroxenes we can express entropy of mixing as follows:

$$S_{mix} = -R(X_{CaM_2} \ln X_{CaM_2} + X_{MgM_2} \ln X_{MgM_2})$$

$$- R*(X_{AlM_1} \ln X_{AlM_1} + X_{MgM_1} *\ln X_{MgM_1})$$

This expression assumes random mixing and neglects the possibility of short range order.

Excess free energy contributions consist of terms for each of the sites discussed above and a reciprocal term ΔG_i for the internal equilibrium:

$$MgAl_2SiO_6 + CaMgSi_2O_6 = CaAl_2SiO_6 + Mg_2Si_2O_6.$$

This yields for the free energy of mixing

$$G_{mix} = -T*S_{mix} + X_{CaM_2} *X_{MgM_2} *W_{Gm_2}$$

$$+ X_{AlM_1} *X_{MgM_1} *W_{Gm_1} + X_{MgM_2} *X_{AlM_1} *\Delta Gi^{o}$$

for clinopyroxene and

$$G_{mix} = -T*S_{mix} + X_{CaM_2} *X_{MgM_2} *W_{Gm_2}$$

$$+ X_{AlM_1} *X_{MgM_1} *W_{Gm_1} + X_{CaM_2} *X_{AlM_1} *\Delta Gi^{o}$$

for orthopyroxene. ΔGi^{o} refers to the standard free energy change of the internal equilibrium.

The W_G's for M_2 sites are simply those given by Holland et al.(1979, 1980) for diopside-enstatite solid solutions. The excess free energy due to Mg-Al interactions on the orthopyroxene M_1 site must, to be consistent with the MAS system, be set to zero. (Wood and Holloway, 1984).

Substantial positive excess enthalpies of mixing in synthetic $CaMgSi_2O_6$-$CaAl_2SiO_6$ clinopyroxenes from heat of solution measurement were found by Newton et al.(1977). Wood (1979) indicated that the excess enthalpies of solution would be consistent with phase equilibrium measurements on pyroxene coexisting with anorthite and quartz provided Al and Si were completely disordered. Phase equilibrium data reported by Gasparik and Lindsley (1980b) tend to suggest, however, that these pyroxenes exhibit large negative deviations from ideality which can not readily be made consistent with Newton et al's enthalpy measurement.

Wood and Holloway (1984) have opted to use the simple model outlined above with an empirical Al-Mg interaction parameter in their paper. Reversals of clinopyroxene composition in the CMAS system suggested that a temperature-independent Mg-Al interaction parameter of 1800 Cal/Gram atom (7531.20 Joules/Gram atom) is an appropriate fit parameter.

Using the Margules parameters from the preceding discussion, thermodynamic calculation was made considering solid solution between joins orthopyroxene $CaMgSi_2O_6$ and $Mg_2Si_2O_6$, clinopyroxene $CaMgSi_2O_6$, $Mg_2Si_2O_6$ and $CaAl_2SiO_6$.

The program THERIAK by C. Decapitani (personal communication) was used for the calculation. This program is a free energy minimization algorithm that accepts UBCDATABASE thermodynamic parameters, including Margules parameters for solid solutions, and computes the proportions and compositions of all coexisting phases for a given bulk composition at any chosen pressure and temperature.

The reaction:

Grossular + Clinochlore = 3 Diopside + 2 spinel + 4 H_2O,

was examined, allowing for solid solution in pyroxene as outlined above. This resulted in determining the equilibrium temperatures to be 583°C and 558°C at 2000 bars and 1000 bars respectively. These temperatures are almost identical to those found from the calculation without considering solid solution in pyroxenes. This can be explained by examining the composition of the equilibrium phases. At the low temperature side, the assemblage grossular + clinochlore is stable and no solid solution was allowed for in this study. The compositions obtained are the ideal formulae with $Ca_3Al_2Si_3O_{12}$ for grossular and $Mg_5Al_2Si_3O_{10}(OH)_8$ for clinochlore. The mineral assemblage for the high temperature side consists of clinopyroxene and spinel. Composition of clinopyroxene is temperature and pressure dependent, but on the whole, diopside is the main component of the pyroxene, comprising more than 98mol% of pyroxene. This is almost pure

diopside and its activity in pyroxene is more than 0.96. The remaining 2mol% are components of clinoenstatite and Ca-Tschermak. The computed equilibrium composition for clinopyroxene along the equilibrium curve is low in aluminum with a value of about 0.3mol%.

D. DIOPSIDE ACTIVITIES AND DISPLACED EQUILIBRIUM

In the reaction:

$$\text{Grossular} + \text{Clinochlore} = 3\ \text{Diopside} + 2\ \text{Spinel} + 4\ H_2O$$

the equilibrium will be displaced from the pure end-member reaction if any phase is not a pure end-member. The experimental evidence is that all phases are of end-member composition except diopside which appears to contain aluminum. This substitution of Al reduces the free energy of diopside by an amount $\Delta\mu_{Di}$, where

$$\Delta\mu_{Di} = R*T * \ln a_{Di}^{Cpx}$$

in which a_{Di}^{Cpx} is the activity of diopside in clinopyroxene, which is evaluated below. This reduction in free energy of diopside component stabilizes the high-temperature assemblage, displacing the equilibrium curve to lower temperature.

The experimental results indicate that diopsides from the run products are aluminum-bearing. We must therefore

consider the activity of diopside in the diopsidic clinopyroxene. Assuming other phases in this reaction are pure and setting their activities to 1.0, we will have

$$\Delta G = \Sigma \mu_i^a = \Sigma \mu_i^o + R^*T\ \Sigma \ln a_i^a$$

$$= 3\ \mu_{di}^o + 2\ \mu_{sp}^o + 4\ \mu_{H_2O}^o - \mu_{gr}^o$$

$$- \mu_{clin}^o + R^*T\ \ln a_{Di}^{Cpx}$$

$$= 0$$

Using the above equation we can calculate the position of the equilibrium curve with different diopside activities as shown in Fig. 23. The displacement of equilibrium curves with different diopside activity values is significant. Equilibrium temperature decreases as the diopside activity values decrease. This leads to having a larger stable field of the high temperature assemblage diopside + spinel + H_2O.

The equilibrium curve with diopside activity value of 0.96 which is from the calculation using program THERIAK is also plotted in Fig 23. Diopside activity in clinopyroxene from experiments can also be calculated from the microprobe analyses of diopside. As discussed in Chapter 3, the M_1 sites in the diopside structure were occupied mainly by Mg^{++} and some Al^{3+} . M_2 sites were occupied mainly by Ca^{++} and some Mg^{++} . The tetrahedral sites were filled with Si^{4+} and

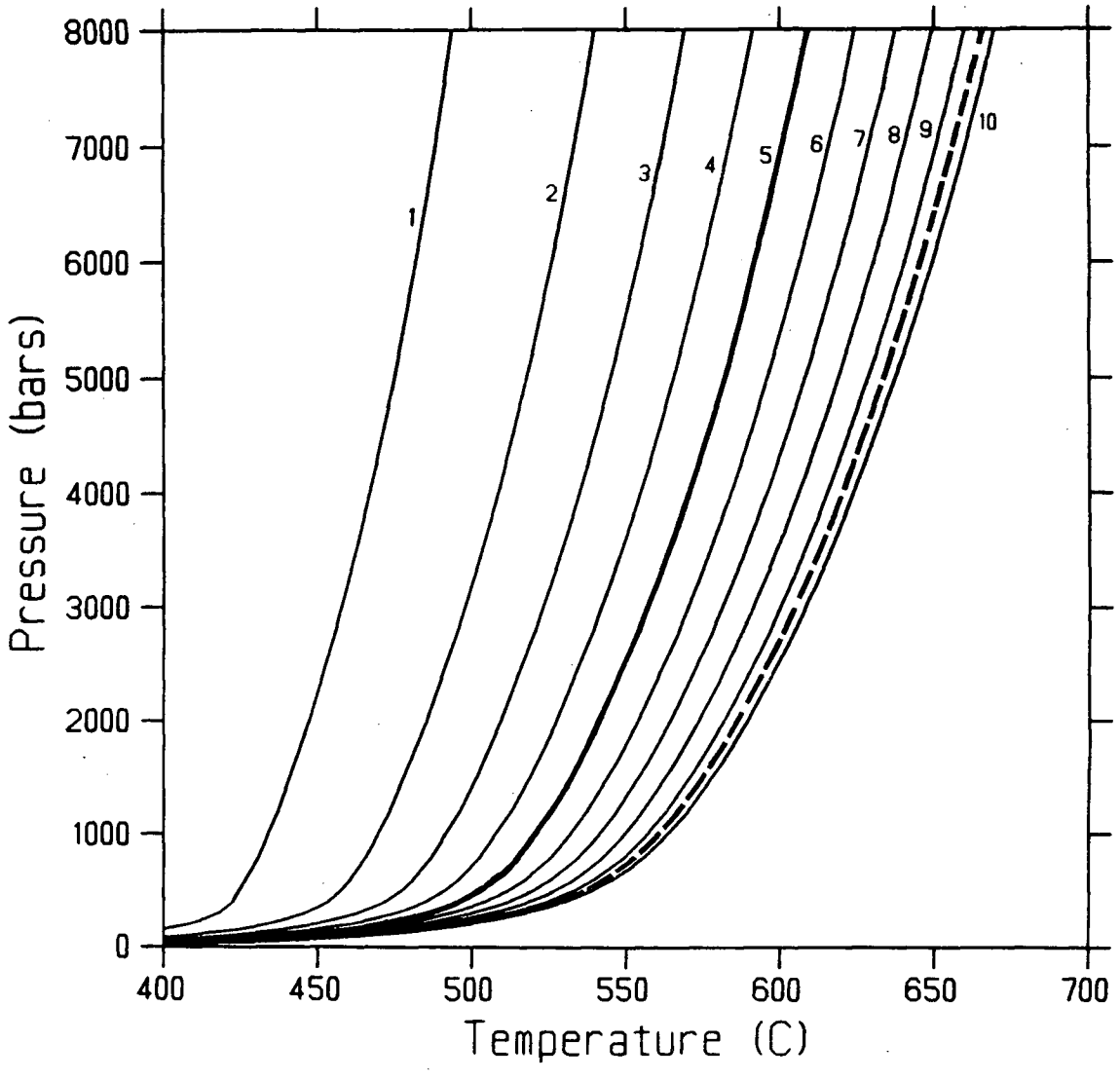

Fig 23 The displaced curves of equilibrium grossular + clinochlore = 3 diopside + 2 spinel + 4 H_2O with different diopside activities. Diopside activities increase from 0.1 (curve #1) to 1.0 (curve #10) by 0.1 each. Curve #5 (heavy solid line) corresponds to diopside activity (0.5) calculated from microprobe analysis data. The heavy dashed line is the equilibrium curve with diopside activity 0.96 calculated with the THERIAK program.

some Al^{3+} . We may calculate the diopside activity using simple site model by multiplying the values of Mg^{++} in M_1 sites, the Ca^{++} in M_2 sites and the square of Si^{4+} from the tetrahedral sites.

Based on this model, the diopside activities were calculated using the analysis data of microprobe (see Table IX). Because the aluminum values vary rather widely, the diopside activities also vary. The average value, however, is close to 0.5. Comparing Fig 23 for the equilibrium curve with 0.5 diopside activity, the equilibrium temperatures are 541.81°C and 520.92°C at 2000 bars and 1000 bars respectively, corresponding to a temperature decrease of 44°C at 2000 bars and 39°C at 1000 bars, from the curve calculated from pure diopside.

These calculations focus on an unsolved problem uncovered with the experiments. The equilibrium curve observed experimentally is close to the calculated curve using the equilibrium composition computed with THERIAK, using existing data on clinopyroxene solid solutions. This would be considered excellent agreement, except for the evidence that the experimental clinopyroxene is aluminous to a degree that should displace the equilibrium about 40°C to a lower temperature. The observed equilibrium curve has not, however, been displaced, leading to a conclusion that the experimental clinopyroxenes must contain undetected Al-rich inclusions or metastable Al-rich zones.

V. CONCLUSION

Experimental determination of the equilibrium grossular + clinochlore = 3 diopside + 2 spinel + 4 H_2O, an important reaction in the metamorphism of rodingite, indicates that this equilibrium deviates only slightly from what was theoretically predicted from thermodynamic data from UBCDATABASE. Experimental results show that the low temperature assemblage grossular + clinochlore is stable below temperature 502°C at 500 bars, 520°C at 1000 bars, 561°C at 2000 bars and 600°C at 4000 bars. The high temperature assemblage diopside + spinel is stable at temperatures higher than 560°C at 500 bars, 581°C at 1000 bars and 627°C at 2000 bars. Between these brackets there is a pressure-temperature region in which the assemblage diopside + clinochlore seems always to be found. Analysis for internal consistency by linear programming indicates that the new values of entropy and enthalpy constrained by the experiments are fully consistent with UBCDATABASE and Helgeson's database. Thus the experimental results from this study support the UBCDATABASE and the experiments, with UBCDATABASE may safely be used as an indication of the metamorphic conditions of metarodingites.

Diopside from the experimental assemblage diopside + clinochlore was proven by microprobe analyses to contain aluminum and is interpreted to be consistent with Tschermak substitution. Aluminum content varies greatly from one analysis to another. Some diopside grains contain a

significant amount of aluminum. Zonation of aluminum in diopside is probably the main cause for this although no zonation could been seen with SEM, microprobe, or optical microscope. The probable zonation of Al-bearing diopside may illustrate the fact that pyroxenes with aluminum are very difficult to equilibrate. It is easy to obtain imhomogeneous Al-bearing pyroxene crystals because of the slow diffusion of aluminum in pyroxene (Fujii, 1977; Gasparik, et al., 1980)

Theoretical thermodynamic prediction of the equilibrium allowing for solid solution in pyroxene indicates that diopside should be the dominant component, as high as 98mol%. Ca-Tschermak molecule and clinoenstatite ($Mg_2Si_2O_6$) make up the remaining 2mol%. Activity of diopside in the pyroxene thus should be very close to 1.0, which is consistent with the experiments in that the equilibrium curve according to the experimental brackets did not show measurable displacement caused by the low diopside activity. The average of diopside activities calculated from microprobe analysis data, however, is as low as 0.5, and this should lower the equilibrium temperature 44°C at 2000 bars and 39°C at 1000 bars respectively from the precalculated equilibrium. Because this activity is the average value and some of diopsides seem to contain a higher amount of aluminum, I believe that there are some undetected metastable aluminum-rich zones or even aluminum-rich inclusions in the diopside crystals.

The equilibrium studied presents itself as being an interesting area for further studies. In particular the composition of clinopyroxene from this reaction begs further research to clarify the nature of aluminum distribution in this pyroxene. This information, though it would not be significant for immediate geologic application, may contribute directly to a better understanding of crystal chemistry, thermodynamic modelling of pyroxene, and study of the equilibrium itself for research on metarodingites. Further study might be made by synthesizing a series of clinopyroxenes between the join Diopside - Ca-Tschermak pyroxene as starting materials to determine the stable composition of clinopyroxene coexisting with other phases from this equilibrium. It might be possible to trace the composition variation of the clinopyroxenes from runs at different conditions in this equilibrium. Futher experiments should use as high a pressure and temperature as possible to increase the aluminum diffusion rate in pyroxene and the reaction rate of experimental runs.

REFERENCES

Akasaka, M. and Onuma, K. (1980) The join $CaMgSi_2O_6$-$CaFeAlSiO_6$-$CaTiAl_2O_6$ and its bearing on the Ti-rich pyroxenes. Contributions to Mineralogy and Petrology, 71, 301-312.

Barth, T.F.W. and Posnjak, E. (1932) Spinel structures with and without variate atom equipoints. Zeitschrift fur Kristallographie, 82, 325-341.

Bell, J.M., Clark, E., and Marshall, P. (1911) The geology of the Dun Mountain subdivision, Nelson. New Zealand Geological Survey Bulletin, 12, 1-71.

Berman, R.G. and Brown, T.H. (1985) Heat capacity of minerals in the system Na_2O-K_2O-CaO-MgO-FeO-Fe_2O_3-Al_2O_3-SiO_2-TiO_2-H_2O-CO_2: Representations, estimation and high temperature extrapolation. Contributions to Mineralogy and Petrology, 89, 168-183.

Berman, R.G., Brown, T.H., and Greenwood, H.J. (1986) An internally-consistent thermodynamic data base for minerals in the system Na_2O-K_2O-CaO-MgO-FeO-Fe_2O_3-Al_2O_3-SiO_2-TiO_2-H_2O-CO_2. American Journal of Science.(in press)

Berman, R.G., Engi, M., Greenwood, H.J., and Brown, T.H. (1986) Derivation of internally-consistent thermodynamic data by the technique of mathematical propramming with application to the system MgO-SiO_2-H_2O. Journal of Petrology.(in press)

Benson, W.N. (1913, 1915, 1917, 1918) The geology of the grea s serpentine belt of New South Wales. Linnean Society of New South Wales, Proceedings, 38, 490-517; 569-596; 662-724; 40, 121-173; 540-624; 42, 222-283; 693-700; 43, 320-393; 593-690.

Bilgrami, S.A. and Howie, R.A. (1960) The mineralogy and petrology of a rodingite dike, Hindubagh, Pakistan. American Mineralogist, 45, 791-801.

Bloxam, T.W. (1954) Rodingite from the Girvan-Ballantrae complex, Ayrshire. Mineralogical Magzine, 30, 525-528.

Boyd, F.R. (1970) Garnet peridotites and the system $CaSiO_3$-$MgSiO_3$-Al_2O_3. Mineralogical Society of America, special paper, 3, 63-75.

Carter, F.W., Jr. and Wells, F.G. (1953) Geology and mineral resources of the Gasquet quadrangle, California-Oregon.

U.S. Geological Survey Bulletin, 995-C, 79-133.

Challis, G.A. (1965) The origin of New Zealand ultramafic intrusions. Journal of Petrology, 6, 322-364.

Chernosky, J.V. (1974) The upper stability of clinochlore at low pressure and the free energy of formation of Mg-cordierite. American Mineralogist, 59, 496-507.

Chesterman, C.W. (1960) Intrusive ultrabasic rocks and their metamorphic relationships at Leech Lake Mountain, Mendocino County, California. International Geological Congress, 21st Copenhagen, 1960, Proceeding, 13, 208-215.

Chinner, G.A., Boyd, F.R., and England, J.L. (1960) Physical properties of garnet solid solutions. Carnegie Institution of Washington, Annual Report of the Director of the Geophysical Laboratory, 59, 76-78.

Clark, J.R., Appleman, D.E., and Papike, J.J. (1969) Crystal-chemical characterization of clinopyroxene based on eight new structure refinements. Mineralogical Society of America, special paper, 2, 31-50.

Clark, J.R., Schairer, J.F., and de Neufville, J. (1962) Phase relations in the system $CaMgSi_2O_6$-$CaAl_2SiO_6$-SiO_2 at low and high pressure. Carnegie Institution of Washington, Annual Report of the Director of the Geophysical Laboratory, 61, 59-68.

Coleman, R.G. (1961) Jadeite deposits of the Clear Creek area, New Idria district, San Benito county, California. Journal of Petrology, 2, 209-247.

Coleman, R.G. (1966) New Zealand serpentinites and associated metasomatic rocks. New Zealand Geological Survey Bulletin, 76, 1-102.

Coleman, R.G. (1967) Low-temperature reaction zones and alpine ultramafic rocks of California, Oregon and Washington. U.S. Geological Survey Bulletin, 1247, 1-49.

Dal Piaz, G. (1967) Le "granatite" (rodingiti l.s.) nelle serpentine delle Alpi occidentali italiane. Memorie della Societa Geologica Italiana, 6, 267-313.

Dal Piaz, G. (1969) Filoni rodingitici e contatto tra serpentine e rocce incassanti nelle Alpi occidentali italiane. Soc. italiane min. pet. rendus, 25, 263-315.

De Neufville, J. and Schairer, J.F. (1962) The join diopside-Ca Tschermak's molecule at atmospheric pressure. Carnegie Institution Washington Year Book, 61, 56-59.

Engi, M. (1983) Equilibria involving Al-Cr spinel: Mg-Fe exchange with olivine. Experiments, thermodynamic analysis, and consequences for geothermometry. American Journal of Science, 283-A, 29-71.

Evans, H.T., Jr., Appleman, D.E., and Handwerker, D.S. (1963) The least squares refinement of crystal unit cells with powder diffraction data by an automatic computer indexing method. American Crystallographic Association Annual Meeting, Programs with Abstracts, 42p.

Evans, B.W., Trommsdorff, V., and Richter, W. (1979) Petrology of an eclogite-metarodingite suite at Cima di Gagnone, Ticino, Switzerland. American Mineralogist, 64, 15-31.

Fawcett, J.J. and Yoder, H.S. (1966) Phase relationships of chlorites in the system $MgO-Al_2O_3-SiO_2-H_2O$. American Mineralogist, 51, 353-380.

Flint, E.P., McMurdie, H.F., and Wells, L.S. (1941) Hydrothermal and x-ray studies and the relationship of the series to hydration products of portland cement. Journal of Research, United States, National Bureau of Standards, 26, 13-33.

Frost, B.R. (1975) Contact metamorphism of serpentinite, chloritic blackwall, and rodingite at Paddy-Go-Easy Pass, Central Cascades, Washington. Journal of Petrology, 16, 272-313.

Fujii, T. (1977) Pyroxene equilibria in spinel lherzolite. Carnegie Institution Washington Year Book, 76, 569-572.

Furuhashi, H., Inagaki, M., and Naka, S. (1973) Determination of cation distribution in spinels by x-ray diffraction method. Journal of Inorganic and Nuclear Chemistry, 35, 3009-3014.

Gasparik, T. (1980a) Mixing properties of clinopyroxenes in the system Di-En-Cats. Geological Society of America, Program with Abstract, 12.

Gasparik, T. (1980b) Role of aluminum in pyroxene equilibriua. Geological Society of America, Program with Abstract, 12.

Gasparik, T. (1984) Two-pyroxene thermobarometry with new experimental data in the system $CaO-MgO-Al_2O_3-SiO_2$. Contributions to Mineralogy and Petrology, 87, 87-97.

Gasparik, T. and Lindsley, D.H. (1980a) Experimental study of pyroxenes in the system $CaMgSi_2O_6-CaAl_2SiO_6-Ca_{0.5}AlSi_2O_6$. EOS, 16, 402-403.

Gasparik, T. and Lindsley, D.H. (1980b) Phase equilibria at high pressure of pyroxenes containing monovalent and trivalent ions. Reviews in Mineralogy, 7, 309-339.

Ganguly, J. and Kennedy, G.C. (1974) The energetics of natural garnet solid solution. I. Mixing of the aluminosilicate end-members. Contributions to Mineralogy and Petrology, 48, 137-148.

Gupta, A.K., Onuma, K., Yagi, K., and Lidiak, E.G. (1973) Effect of silica concentration on the diopsidic pyroxenes in the system diopside-$CaTiAl_2O_6$-SiO_2.Contributions to Mineralogy and Petrology, 41, 333-344.

Helgeson, H.C., Delany, J.M., Nesbitt, H.W., and Bird, D.K. (1978) Summary and critique of the thermodynamic properties of rock-forming minerals. American Journal of Science, 278-A, 1-229.

Hensen, B.J., Schmid, R., and Wood, B.J. (1975) Activity-composition relationships for pyrope-grossular garnet. Contributions to Mineralogy and Petrology, 51, 161.

Herzberg, C.T. (1972) Stability fields of plagioclase- and spinel-lherzolite. In: Progress in Experimental Petrology, D. 2, 145-148. Natural Environment Research Council Publications, London.

Herzberg, C.T. (1976a) The plagioclase spinel-lherzolite facies boundary; its bearing on corona structure formation and tectonic history of the Norweigian Caledonides. In: Progress in Experimental Petrology, D. 3, 233-235. Natural Environment Research Council Publications, London.

Herzberg, C.T. (1976b) The lowest pressure pyralspite garnet-forming reaction in CaO-MgO-Al_2O_3-SiO_2; the Seiland Ariegite subfacies boundary in simple spinel-lherzolites. In: Progress in Experimental Petrology, D. 3, 235-237. Natural Environment Research Council Publications, London.

Holland, T.J.B. (1977) Reversal hydrothermal determination of jadeite-diopside activities. EOS, 60, 405.

Holland, T.J.B., Navrotsky, A., and Newton, R.C. (1979) Thermodynamic parameters of $CaMgSi_2O_6$-$Mg_2Si_2O_6$ pyroxenes based on regular solution and cooperative disordering models. Contributions to Mineralogy and Petrology, 69, 337-344.

Holland, T.J.B., Navrotsky, A., and Newton, R.C. (1980) Thermodynamic parameters of $CaMgSi_2O_6$-$Mg_2Si_2O_6$ pyroxenes based on regular solution and cooperative disordering models. Reply, Contributions to Mineralogy and Petrology,

75, 305-306.

Jaffe, F.C. (1955) Les ophiolites et les roches connexes de la region du col des Gets. Schweizerische Mineralogische Petrographische Mitteilungen, 35, 1-150.

JCPDS (1980) Mineral Powder Diffraction File, Data Book, Card# 11-654.

Jenkins, D.M. and Newton, R.C. (1979) Experimental determination of the spinel peridotite to garnet peridotite inversion at 900°C and 1000°C in the system $CaO-MgO-Al_2O_3-SiO_2$, and at 900°C with natural garnet and olivine. Contributions to Mineralogy and Petrology, 32, 24-38.

Kushiro, I. and Yoder, H.S. (1965) The reactions between forsterite and anorthite at high pressure. Carnegie Institution Washington Year Book, 64, 89-94.

Kushiro, I. and Yoder, H.S. (1966) Anorthite-forsterite and anorthite-enstatite reactions and their bearing on the basalt-eclogite transformation. Journal of Petrology, 7, 337-362.

Lindsley, D.H. (1976) The crystal chemistry and structure of oxide minerals as exemplified by the Fe-Ti oxides. In: Rumble, D.(editor) Oxide Minerals, Mineralogical Society of America short course notes, 3, L1-L52.

MacGregor, I.D. (1965) Stability fileds of spinel and garnet peridotites in the synthetic system $MgO-CaO-Al_2O_3-SiO_2$. Carnegie Institution Washington Year Book, 64, 126-134.

McPhail, D.C. (1985) The upper thermal stability of Mg-chlorite. Unpublished M.Sc. thesis, University of British Columbia.

Miles, K.R. (1950) Garnetized gabbros from the Eulaminna district, Mt. Margaret goldfield. Western Australia Geological Survey Bulletin, 103, 108-130.

Muller, P. (1963) Kalksilikatfelse im serpentin des piz lunghin bei Maloja. Chemie der Erde, 23, 452-464.

Newton, R.C., Charlu, T.V., and Kleppa, O.J. (1977) Thermochemistry of high pressure garnets and clinopyroxenes in the system $CaO-MgO-Al_2O_3-SiO_2$. Geochimica et Cosmochimica Acta, 41, 369-377.

Nolan, J. and Edgar, A.D. (1963) An x-ray investigation of synthetic pyroxenes in the system acmite-diopside-water at 100Kg/cm^2 water-vapour pressure. Mineralogical Magzine, 33, 615-634.

O'Hara, M.J., Richardson, R.C., and Wilson, G. (1971) Garnet-peridotite stability and occurence in crust and mantle. Contributions to Mineralogy and Petrology, 32, 48-68.

Ohashi, y., Burnham, C.W., and Finger, L.W. (1975) The effect of Ca-Fe substitution on the clinopyroxene crystal structure. American Mineralogist, 60, 423-434.

Ohashi, Y. and Finger, L.W. (1976) The effect of Ca substitution on the structure of clinoenstatite. Carnegie Institution Washington Year Book, 75, 743-746.

Okamura, F.P., Ghose, S., and Ohashi, H. (1974) Structure and crystal chemistry of calcium Tschermak's pyroxene, $CaAlAlSiO_6$. American Mineralogist, 59, 549-557.

O'Neill, H.St.C. and Navrotsky, A. (1984) Cation distributions and thermodynamic properties of binary spinel solid solution. American Mineralogist, 69, 733-753.

Onuma, K. and Kimura, M. (1978) Study of the system $CaMgSi_2O_6$-$CaFeAlSiO_6$-$CaAl_2SiO_6$-$CaTiAl_2O_6$: II. The join $CaMgSi_2O_6$-$CaAl_2SiO_6$-$CaTiAl_2O_6$ and its bearing on Ca-Al-rich inclusions in carbonaceous chondrite. Journal of Faculty of Sciences, Hokkaido University, 18, 215-236.

Perkins, E.H., Brown, T.H., and Berman, R.G. (1986) Three programs which calculate pressure-temperature-composition phase diagrams. Computers and Geology. (in press)

Presnall, D.C. (1976) Alumina content of enstatite as a geobarometer for plagioclase and spinel lherzolites. American Mineralogist, 61, 582-588.

Rawson, S.A. (1984) Regional metamorphism of rodingites and related rocks from the North-Central Klamath Mountains, California. Unpublished Ph.D. thesis, University of Oregon.

Rice, J.M. (1983) Metamorphism of Rodingites: Part I. Phase relations in a portion of the system CaO-MgO-Al_2O_3-SiO_2-CO_2-H_2O. American Journal of Science, 283-A, 121-150.

Rutstein, M.S. and Yund, R.A. (1969) Unit-cell parameters of synthetic diopside-hedenbergite solid solutions. American Mineralogist, 54, 238-245.

Sakata, Y. (1957) Unit cell dimensions of synthetic aluminian diopside. Japanese Journal of Geology and Geography, 28, 161-168.

Saxena, S.K. (1968) Distributions of elements between

coexisting minerals and the nature of solid solution in garnet. American Mineralogist, 53, 994-1014, 2018-2024.

Saxena, S.K. and Ghose, S. (1971) Mg-Fe^2 order-disorder and the thermodynamics of the orthopyroxene crystalline solution. American Mineralogist, 56, 532-559.

Schlocker, J. (1960) Rodingite from Angel Island, San Francisco Bay, California. U.S. Geological Survey Professional Paper, 400-B, 311-312.

Seki, Y. and Kuriyagawa, S. (1962) Mafic and leucocratic rocks associated with serpentinite of Kanasak, Kanto Mountains, central Japan. Japanese Journal of Geology and Geography, 33, 15-32.

Shoji, T. (1974) $Ca_3Al_2(SiO_4)_3$-$Ca_3Al_2(O_4H_4)_3$ series garnet: composition and stability. Journal of Mineralogical Society, Japan, 11, 359-372. (in Japanese)

Suzuki, J. (1953) On the rodingite rocks within the serpentinite masses of Hokkaido. Journal of Faculty of Sciences, Hokkaido University, 8, 419-430.

Terry, R.D. and Chilingar, G.V. (1955) Comparison charts for visual estimation of percentage composition. Journal of Sedimentary Petrology, 25, 229-234.

Turner, F.J. (1930) The metamorphic and ultrabasic rocks of the low Cascade Valley, South Westland. New Zealand Institution Transaction, 61, 170-180.

Viswanathan, K. (1966) Unit cell dimensions and ionic substitutions in common clinopyroxenes. American Mineralogist, 51, 429-442.

Vuagnat, M. (1967) Quelques reflexious sur les ophispherites et les rodingites. Societa Italiana Mineralogia e Petrologia rendus, 23, 471-482.

Well, F.G., Hotz, P.E., and Carter, F.M.Jr. (1949) Preliminary description of the geology of the Kerby quadrangle, Oregon. Oregon Department of Geology and Mineral Industries, Bulletin, 40, 1-23.

Wilken, G. (1977) Scanning electron microscope study of synthetic pyrope-grossularite solid solution. Neues Jahrbuch fur Mineralogie, Abhandlungen, 130, 150-158.

Wood, B.J. (1979) Activity-composition relationships in $Ca(Mg,Fe)Si_2O_6$-$CaAl_2SiO_6$ clinopyroxene solid solutions. American Journal of Science, 279, 854-875.

Wood, B.J. and Banno, S. (1973) Garnet-orthopyroxene and

orthopyroxene-clinopyroxene relationships in simple and complex systems. Contributions to Mineralogy and Petrology, 42, 109-124.

Wood, B.J. and Holloway, J.R. (1984) A thermodynamic model for subsolidus equilibria in the system $CaO-MgO-Al_2O_3-SiO_2$. Geochimica et Cosmochimica Acta, 48, 159-176.

Wood, B.J. and Nicholls, J. (1978) The thermodynamic properties of reciprocal solid solutions. Contributions to Mineralogy and Petrology, 66, 389-400.

Yang, H,-Y. (1973) Synthesis of an Al- and Ti-rich clinopyroxene in the system $CaMgSi_2O_6-CaAl_2SiO_6-CaAlTiAlO_6$. Transaction of American Geophysical Union, 54, 478.

Yoder, H.S. (1950) Stability relations of grossularite. Journal of Petrology, 58, 221-251.

Yoder, H.S. and Chinner, G.A. (1960) Grossularite-pyrope-water system at 10,000 bars. Carnegie Institution of Washington, Annual Report of the Director of the Geophysical Laboratory, 59, 78-81.

Yoshikawa, K. (1977) Phase relations and the nature of clinopyroxene solid solutions in the system $NaFe^3Si_2O_6-CaMgSi_2O_6-CaAl_2SiO_6$. Journal of Faculty of Sciences, Hokkaido University, 17, 451-485.

APPENDIX 1

Microprobe analytic results of synthetic and equilibrium diopside

SAMPLE	MgO	Al_2O_3	SiO_2	CaO	Total	wt%Total
STD	1.0038	.0071	2.0017	0.9821	3.9947	91.10
	1.0033	.0074	2.0032	0.9995	4.0134	103.30
	1.0318	.0132	1.9595	1.0093	4.0338	83.30
	1.0517	.0106	1.9755	0.9858	4.0213	93.92
	0.9799	.0088	1.9731	1.0607	4.0223	92.95
	1.0696	.0196	1.9587	0.9841	4.0317	104.30
XRR-3	0.9338	.4863	1.7510	0.8345	4.0058	84.11
	0.8557	.7630	1.6199	0.7601	3.9987	93.07
	0.8482	.7521	1.6227	0.7781	4.0011	81.08
	0.8512	.7103	1.6870	0.7094	3.9579	104.25
	0.8809	.4053	1.7658	0.9796	4.0316	82.65
	0.8872	.5309	1.6885	0.9396	4.0462	85.65
	0.9625	.3776	1.8078	0.8555	4.0034	88.88
	0.9697	.3357	1.8147	0.8970	4.0173	90.52
	0.9118	.5394	1.7159	0.8474	4.0145	93.49
STD	0.9816	.0165	2.0031	0.9814	3.9886	90.77
	0.9804	.0063	1.9969	1.0164	4.0000	111.29
	0.9916	.0186	1.9640	1.0530	4.0269	102.67
XRR-3	0.9246	.3819	1.8032	0.8962	4.0059	99.84
	0.9787	.3275	1.8297	0.8707	4.0066	88.20
	0.9605	.3210	1.8366	0.8848	4.0029	82.08
	0.9157	.5816	1.6416	0.9288	4.0677	90.57
	0.8705	.4877	1.7772	0.8435	3.9789	109.62
	0.9893	.5576	1.6452	0.8929	4.0790	91.63

Microprobe results of synthetic and equilibrium diopside

SAMPLE	MgO	Al_2O_3	SiO_2	CaO	Total	Wt%Total
STD	0.9967	.0052	2.0063	0.9830	3.9912	98.27
	1.0488	.0017	1.9688	1.0111	4.0304	120.00
	0.9933	.0034	1.9891	1.0235	4.0093	104.36
	1.0214	.0061	2.0035	0.9626	3.9926	95.68
	0.9897	.0061	1.9894	1.0223	4.0075	118.48
	0.9676	.0069	1.9792	1.0623	4.0173	96.81
	0.9791	.0043	1.9862	1.0420	4.0118	113.61
	0.9596	.0039	2.0064	1.0217	3.9916	111.11
	1.0096	.0073	1.9709	1.0376	4.0254	84.87
	0.9746	.0049	1.9968	1.0245	4.0008	106.71
XRR-3	0.7589	.5156	1.7490	0.9696	3.9931	103.21
	0.9359	.4951	1.7341	0.8533	4.0184	86.14
	0.9621	.5251	1.6798	0.8906	4.0575	82.26
	0.7691	.4950	1.7692	0.9500	3.9833	92.49
	0.9805	.2939	1.8091	0.9603	4.0438	118.23
STD	1.0267	.0032	1.9541	1.0603	4.0443	83.03
	0.9992	.0081	1.9933	1.0021	4.0027	84.80
	1.0073	.0081	2.0028	0.9751	3.9932	83.24
	1.0014	.0040	1.9825	1.0276	4.0155	117.34
XRR-3	0.9339	.3603	1.7757	0.9743	4.0442	80.55
	0.9558	.4118	1.7726	0.8812	4.0214	94.42
	1.0388	.4161	1.7933	0.7504	3.9986	97.05
	0.9574	.3914	1.7783	0.8990	4.0260	82.60
	0.8866	.4782	1.7656	0.8650	3.9954	82.00
	0.9988	.5963	1.6307	0.8454	4.0712	99.06
	1.0151	.5526	1.6757	0.8045	4.0479	89.57
STD	1.0278	.0037	1.9822	1.0023	4.0160	90.55
	1.0182	.0021	1.9814	1.0158	4.0175	90.18
	0.9802	.0047	1.9669	1.0789	4.0307	116.49
	1.0670	.0038	1.9635	1.0004	4.0347	81.53
	0.9965	.0057	1.9944	1.0063	4.0029	112.49
XRR-3	0.9926	.2612	1.8628	0.8900	4.0066	106.50
	0.9891	.4389	1.7092	0.9343	4.0715	83.95
	0.9741	.4241	1.7805	0.8287	4.0075	96.53
	0.9568	.2868	1.7891	1.0349	4.0676	115.88
STD	1.0844	.0052	1.9325	1.0427	4.0648	105.83
	0.9523	.0213	2.0470	0.9218	3.9424	103.87
	1.0277	.0065	2.0101	0.9432	3.9866	84.93
	1.0610	.0040	1.9906	0.9518	4.0074	92.08
	1.0551	.0039	1.9826	0.9719	4.0145	102.84
	1.0188	.0050	1.9943	0.9849	4.0031	85.20

Microprobe analytic results of synthetic and equilibrium diopside

SAMPLE	MgO	Al_2O_3	SiO_2	CaO	Total	Wt%Total
STD	1.0218	.0055	1.9798	1.0103	4.0174	89.98
	0.9527	.0073	2.0455	0.9453	3.9508	111.38
	0.9349	.0262	2.0403	0.9453	3.9466	92.09
XRR-4	0.9328	.4783	1.6992	0.9514	4.0617	103.49
	0.8111	.5818	1.6552	1.0062	4.0520	119.92
	0.9350	.5240	1.6887	0.9016	4.0493	110.79
STD	0.9986	.0115	1.9455	1.0933	4.0489	85.81
XRR-4	0.8391	.4986	1.7013	1.0104	4.0494	90.38
	0.9009	.4281	1.7209	1.0152	4.0651	84.46
STD	0.9980	.0073	2.0005	0.9901	3.9959	102.30
	0.9557	.0199	2.0103	0.9937	3.9796	82.44
	1.0234	.0050	1.9757	1.0177	4.0218	89.68
XRE-10	0.9174	.3046	1.8339	0.9579	4.0138	107.41
	0.9629	.3823	1.7998	0.8641	4.0091	87.37
	0.8503	.4082	1.7674	1.0025	4.0284	116.60
	0.8266	.4969	1.7193	0.9875	4.0323	106.66
STD	1.0108	.0078	1.9413	1.0950	4.0549	83.22
	1.0319	.0064	2.0210	0.9163	3.9756	82.83
	0.9381	.0206	2.0095	1.0119	3.9801	96.67
	0.9747	.0038	2.0170	0.9856	3.9811	114.87

Microprobe analytic results of synthetic and equilibrium diopside

SAMPLE	MgO	Al_2O_3	SiO_2	CaO	Total	Wt%Total
STD	1.0669	.0060	1.9568	1.0106	4.0403	85.45
	0.9644	.0050	1.9786	1.0709	4.0189	102.36
	1.0128	.0064	1.9840	1.0095	4.0127	95.16
	0.9998	.0063	1.9935	1.0037	4.0033	98.98
XRR-4	0.8371	.5224	1.7176	0.9438	4.0213	104.63
	0.8648	.5097	1.7135	0.9437	4.0317	101.18
	0.7772	.5583	1.6946	0.9960	4.0261	90.89
	0.8928	.6965	1.6381	0.7962	4.0186	107.13
	0.8855	.5323	1.7008	0.9145	4.0331	95.31
	0.8259	.5524	1.6941	0.9573	4.0297	90.91
	0.9776	.6280	1.6669	0.7466	4.0191	98.19
STD	0.9655	.0050	2.0128	1.0013	3.9846	107.01
	0.9835	.0064	1.9906	1.0257	4.0062	80.07
XRR-3	0.9986	.2138	1.8856	0.9093	4.0073	87.91
	0.9699	.1947	1.9195	0.8990	3.9831	93.41
	0.9669	.3507	1.8421	0.8229	3.9826	89.26
	0.9588	.3196	1.8444	0.8730	3.9958	88.55
	0.9146	.3578	1.7978	0.9532	4.0234	96.87
	0.9720	.4223	1.7485	0.8976	4.0404	96.03
	0.9896	.3614	1.8040	0.8603	4.0153	93.84
	0.9901	.3281	1.8074	0.9029	4.0285	84.16
STD	1.0057	.0090	1.9975	0.9858	3.9980	81.71
	1.0053	.0121	1.9804	1.0156	4.0134	89.75
	0.9926	.0127	1.9491	1.0902	4.0446	91.25
XRE-10	0.8840	.5035	1.7011	0.9586	4.0472	86.12
	0.9119	.3869	1.8002	0.9074	4.0064	95.02
	0.8609	.4655	1.7687	0.9034	3.9985	91.34
STD	0.9737	.0062	1.9900	1.0354	4.0410	89.14
	1.0052	.0051	2.0105	0.9661	3.9869	84.35

APPENDIX 2

Mineral assemblages of rodingites and diopside compositions analyzed by Rawson (1984)

TABLE Assemblages in Rodingites*

Sample	Cc	Cte	Mi	Di	Gr	Sp	Tr	Zo	Sph	Opa
Huckleberry Mountain										
34	X	X					X	X		X
36	A	X‡		A			A	A	NA	NA
38	X	X		X			X	X	X	
39	X	X			X			X		
43A	X‡	A		A	A			A		A
43B	A	A		A			A	A		X
43C	A	A		A			X	A		
46A-EXT	A	A		A	A		A	A		
46A-INT	X‡	A		A	A		X‡	A		
46B-1		X		X	X			X	X	X
46B-2	A	X‡		A	A		A	A		
53	X	X		X	X			X		X
81A		X		X	X			X		
81B		A		A	A			A		
355B1	X‡	A		A	X‡			A		
355B2	A	X‡		A	A			A		
355D	X	X					X	X		X
402A1-2	X	X		X			X	X		
402B		A		A			X‡	A	NA	A
402E		X					X	X	X	X
Grider Ridge										
514B2-1		X					X	X		
515B2-2	X	X		X	X			X		X
522A1-1	X	X		X	X			X	X	X
522A1-2		X		X	X			X	X	X
522A1-3		X		X				X	X	X
522A2		X		X	X			X	X	X
522B1-1		X		X				X		
522B2-2		X		X	X					
522C		X		X	X			X	X	

TABLE Continued

Sample	Cc	Cte	Mi	Di	Gr	Sp	Tr	Zo	Sph	Opa
Tyler Meadow										
513B2-1T	X			X	X			X		X
513B2-1B		X				X	X	X		X
513C		X		X				X	X	
499A		A				NA	A	A	X‡	A
499B		X				X	X	X	X	X
Rattlesnake Ridge										
500B1-1G	X	X		X		X		X		
500B1-1	X	X		X	X			X		
K-2-B	A	A		A		A				
500E	A	X‡		A	A			X‡		
500F	A	A		A	A			A		
500H	X	X		X	X			X		
501C	X			X	X			X		
502-1-2		X		X		X				
528A1-MB	A	A	A	A	A			A		
528A1-MT		A	X‡	A		A				
27-4-E1		A	A	A		A		A		
27-4-E2	A	?		A	A			A		
27-4-C	A	A		A		A		A		
RB104C-T	A		A	A	A			A		
RB104C-B			A	A	A	A		A		

TABLE Continued

Sample	Cc	Cte	Mi	Di	Gr	Sp	Tr	Zo	Sph	Opa
Scott Bar Mountains										
494A1-1G		A		A		A	A	X‡		
494A1-1N		A		A			A	X‡		
494A1-2		A		A	A			A		
494C		A		A	A			A		
494D		A		A		A	A	A		
507B1-1		X	X	X	X			X		
507B1-2		X		X	X			X		
507E1-2		X	X	X	X			X		
508A1-1		X	X	X	X			X		
508A1-2		X	X	X	X			X		
508A1-4		X	X	X	X			X		
508A1-3		X	X	X	X	X				
510A		X		X		X	X			
510B1-1		X		X		X	X			
513A		X		X			X	X		
511A-B		X		X		X		X		
511A-T		X		X	X			X		

*Anorthite absent from all samples.
X = present in assemblage.
A = analyzed.
NA = present in probe section / not analyzed.
‡ = present in assemblage / absent from probe section.

	497A-2 n = 2	497A1 n = 12	481D n = 12	477A-3R n = 4
SiO_2	50.81(0.56)	51.54(0.60)	54.31(0.37)	51.92(0.49)
TiO_2	0.05(0.01)	0.08(0.06)	0.04(0.01)	0.04(0.00)
Al_2O_3	0.75(0.00)	1.07(0.42)	0.48(0.04)	0.64(0.06)
MnO	0.23(0.04)	0.17(0.04)	0.18(0.04)	0.25(0.12)
MgO	7.58(0.20)	10.24(0.40)	15.84(0.57)	7.63(0.55)
CaO	23.64(0.02)	23.71(0.32)	24.99(0.35)	23.13(0.27)
Na_2O	0.09(0.00)	0.11(0.08)	0.08(0.04)	0.14(0.01)
K_2O	0.03(0.00)	0.03(0.00)	0.03(0.00)	0.03(0.00)
FeO	16.27(0.34)	12.19(0.68)	3.57(0.85)	15.99(0.79)
Fe_2O_3	0.45(0.24)	0.38(0.43)	0.02(0.06)	0.00(0.00)
Total	99.89(0.00)	99.51(0.00)	99.54(0.00)	99.76(0.00)
Cations				
(Si)	1.973(0.007)	1.969(0.020)	1.997(0.006)	2.011(0.011)
(Ti)	0.001(0.000)	0.002(0.002)	0.001(0.000)	0.001(0.000)
(Al)	0.034(0.000)	0.048(0.019)	0.021(0.002)	0.029(0.003)
(Mn)	0.007(0.001)	0.005(0.001)	0.006(0.001)	0.008(0.004)
(Mg)	0.439(0.008)	0.583(0.020)	0.868(0.027)	0.441(0.031)
(Ca)	0.983(0.007)	0.970(0.009)	0.984(0.009)	0.960(0.013)
(Na)	0.007(0.000)	0.008(0.006)	0.006(0.003)	0.011(0.001)
(K)	0.001(0.000)	0.001(0.000)	0.001(0.000)	0.001(0.000)
(F_2)	0.528(0.007)	0.390(0.024)	0.110(0.027)	0.518(0.026)
(F_3)	0.026(0.014)	0.022(0.025)	0.001(0.003)	0.000(0.000)
Sum	4.000(0.000)	3.999(0.000)	3.995(0.000)	3.979(0.000)

	477A-3C n = 4	481C1-1R n = 5	481C1-1C n = 5
SiO_2	51.14(0.32)	53.94(0.36)	53.56(0.61)
TiO_2	0.04(0.00)	0.04(0.00)	0.04(0.00)
Al_2O_3	0.52(0.17)	0.47(0.19)	0.52(0.04)
MnO	0.36(0.13)	0.08(0.04)	0.15(0.09)
MgO	7.70(0.61)	13.97(0.73)	14.20(1.51)
CaO	23.14(0.42)	24.40(0.23)	24.65(0.30)
Na_2O	0.14(0.03)	0.13(0.06)	0.12(0.06)
K_2O	0.03(0.00)	0.03(0.00)	0.03(0.00)
FeO	16.13(1.44)	6.34(1.09)	6.14(2.11)
Fe_2O_3	0.00(0.00)	0.00(0.00)	0.00(0.00)
Total	99.20(0.00)	99.41(0.00)	99.41(0.00)
Cations			
(Si)	1.999(0.006)	2.007(0.008)	1.995(0.002)
(Ti)	0.001(0.000)	0.001(0.000)	0.001(0.000)
(Al)	0.024(0.008)	0.021(0.008)	0.023(0.002)
(Mn)	0.012(0.004)	0.003(0.001)	0.005(0.003)
(Mg)	0.448(0.033)	0.774(0.037)	0.788(0.076)
(Ca)	0.969(0.014)	0.973(0.010)	0.984(0.012)
(Na)	0.011(0.002)	0.010(0.004)	0.009(0.005)
(K)	0.001(0.000)	0.001(0.000)	0.001(0.000)
(F_2)	0.528(0.050)	0.197(0.035)	0.192(0.067)
(F_3)	0.000(0.000)	0.000(0.000)	0.000(0.000)
Sum	3.994(0.000)	3.987(0.000)	3.997(0.000)

	494A1-1 n = 13	494D n = 8	494A1-2-R n = 5	494A1-2-C n = 5
SiO_2	52.18(0.53)	50.72(0.79)	50.85(0.32)	51.52(1.03)
TiO_2	0.21(0.04)	0.10(0.03)	0.10(0.04)	0.10(0.03)
Al_2O_3	2.88(0.54)	5.38(0.74)	3.94(0.58)	3.88(0.63)
MnO	0.13(0.03)	0.10(0.02)	0.16(0.02)	0.16(0.02)
MgO	15.32(0.35)	14.66(0.28)	13.90(0.44)	14.01(0.45)
CaO	24.43(0.36)	25.04(0.28)	24.56(0.20)	24.48(0.27)
Na_2O	0.03(0.01)	0.04(0.02)	0.03(0.00)	0.03(0.01)
K_2O	0.03(0.00)	0.03(0.00)	0.03(0.00)	0.03(0.00)
FeO	3.37(0.62)	2.10(0.80)	4.25(0.75)	4.85(0.56)
Fe_2O_3	0.71(0.66)	1.30(1.01)	1.65(0.54)	0.85(0.92)
Total	99.28(0.00)	99.47(0.00)	99.48(0.00)	99.91(0.00)
Cations				
(Si)	1.917(0.022)	1.849(0.039)	1.868(0.015)	1.893(0.041)
(Ti)	0.006(0.001)	0.003(0.001)	0.003(0.001)	0.003(0.001)
(Al)	0.125(0.024)	0.231(0.031)	0.170(0.025)	0.168(0.027)
(Mn)	0.004(0.001)	0.003(0.001)	0.005(0.001)	0.005(0.001)
(Mg)	0.839(0.017)	0.797(0.019)	0.761(0.022)	0.767(0.025)
(Ca)	0.961(0.012)	0.978(0.007)	0.966(0.003)	0.964(0.009)
(Na)	0.002(0.000)	0.003(0.001)	0.002(0.000)	0.002(0.001)
(K)	0.001(0.000)	0.001(0.000)	0.001(0.000)	0.001(0.000)
(F_2)	0.104(0.019)	0.064(0.025)	0.131(0.024)	0.149(0.018)
(F_3)	0.039(0.036)	0.071(0.055)	0.091(0.030)	0.047(0.051)
Sum	3.997(0.000)	3.999(0.000)	4.000(0.000)	3.999(0.000)

	46A-EX1C n = 5	46A-EX1R n = 5	27-4-E1 n = 7	27-4-E2 n = 4
SiO_2	53.28(0.63)	53.76(0.91)	51.69(0.95)	49.50(0.51)
TiO_2	0.13(0.05)	0.11(0.04)	0.28(0.12)	0.18(0.02)
Al_2O_3	1.91(0.29)	2.23(1.02)	4.10(1.22)	5.80(1.42)
MnO	0.17(0.01)	0.22(0.07)	0.16(0.02)	0.20(0.07)
MgO	15.63(0.28)	15.79(0.44)	15.15(0.62)	13.43(0.45)
CaO	24.15(0.50)	23.29(1.12)	24.70(0.26)	24.41(0.09)
Na_2O	0.19(0.06)	0.14(0.08)	0.02(0.00)	0.02(0.00)
K_2O	0.03(0.00)	0.03(0.00)	0.03(0.00)	0.03(0.00)
FeO	3.77(1.12)	4.21(1.32)	2.93(0.49)	3.74(0.88)
Fe_2O_3	0.89(0.80)	0.56(1.25)	0.83(0.68)	1.53(0.38)
Total	100.16(0.00)	100.34(0.00)	99.89(0.00)	99.84(0.00)
Cations				
(Si)	1.940(0.022)	1.952(0.046)	1.884(0.040)	1.828(0.035)
(Ti)	0.004(0.001)	0.003(0.001)	0.008(0.003)	0.005(0.000)
(Al)	0.082(0.013)	0.095(0.043)	0.176(0.052)	0.252(0.059)
(Mn)	0.005(0.000)	0.007(0.002)	0.005(0.001)	0.006(0.002)
(Mg)	0.848(0.009)	0.855(0.018)	0.824(0.037)	0.740(0.028)
(Ca)	0.942(0.014)	0.906(0.047)	0.965(0.007)	0.966(0.009)
(Na)	0.014(0.005)	0.010(0.005)	0.002(0.000)	0.002(0.000)
(F_2)	0.115(0.034)	0.128(0.041)	0.089(0.015)	0.115(0.027)
(F_3)	0.048(0.044)	0.030(0.068)	0.045(0.037)	0.085(0.021)
Sum	3.999(0.000)	3.988(0.000)	3.999(0.000)	4.000(0.000)

	43B-R1 n = 5	43B-C n = 5	46A-I-R n = 4	46A-I-C n = 5
SiO_2	53.68(0.96)	53.70(0.83)	52.79(0.92)	52.11(0.74)
TiO_2	0.09(0.03)	0.12(0.03)	0.08(0.03)	0.07(0.04)
Al_2O_3	1.14(0.22)	1.60(0.35)	2.36(1.26)	2.44(1.31)
MnO	0.21(0.04)	0.20(0.03)	0.16(0.07)	0.15(0.08)
MgO	15.01(0.90)	14.81(1.04)	15.26(1.07)	15.96(0.48)
CaO	23.99(0.84)	23.73(0.61)	24.30(1.04)	24.61(1.04)
Na_2O	0.21(0.06)	0.23(0.06)	0.12(0.07)	0.11(0.09)
K_2O	0.01(0.01)	0.02(0.02)	0.01(0.02)	0.02(0.02)
FeO	5.14(1.23)	5.97(1.09)	4.08(0.99)	1.68(1.24)
Fe_2O_3	0.81(0.47)	0.39(0.59)	0.71(1.24)	2.13(1.08)
Total	100.28(0.00)	100.76(0.00)	99.87(0.00)	99.27(0.00)
Cations				
(Si)	1.963(0.027)	1.962(0.018)	1.933(0.038)	1.893(0.054)
(Ti)	0.002(0.001)	0.003(0.001)	0.002(0.001)	0.002(0.001)
(Al)	0.049(0.009)	0.069(0.015)	0.102(0.055)	0.104(0.055)
(Mn)	0.007(0.001)	0.006(0.001)	0.005(0.002)	0.005(0.003)
(Mg)	0.818(0.047)	0.807(0.055)	0.832(0.044)	0.864(0.030)
(Ca)	0.940(0.032)	0.929(0.026)	0.953(0.056)	0.957(0.032)
(Na)	0.015(0.004)	0.016(0.004)	0.008(0.005)	0.008(0.007)
(K)	0.000(0.000)	0.001(0.001)	0.001(0.001)	0.001(0.001)
(F_2)	0.157(0.038)	0.182(0.033)	0.125(0.031)	0.052(0.039)
(F_3)	0.045(0.026)	0.022(0.033)	0.038(0.067)	0.116(0.057)
Sum	3.996(0.000)	3.998(0.000)	4.000(0.000)	4.000(0.000)

	81BC n = 6	81BR n = 6	355B-2R n = 7	355B-2-C n = 5
SiO_2	53.16(1.02)	53.34(0.35)	54.77(0.64)	54.69(0.55)
TiO_2	0.08(0.06)	0.10(0.06)	0.04(0.00)	0.04(0.01)
Al_2O_3	1.23(0.92)	1.03(0.71)	0.17(0.11)	0.13(0.08)
MnO	0.19(0.05)	0.16(0.03)	0.15(0.04)	0.17(0.05)
MgO	15.51(0.57)	15.69(0.58)	15.03(0.96)	14.58(0.95)
CaO	24.21(0.85)	24.13(0.72)	25.23(0.16)	25.14(0.27)
Na_2O	0.14(0.12)	0.13(0.11)	0.04(0.05)	0.02(0.00)
K_2O	0.01(0.02)	0.00(0.01)	0.04(0.00)	0.04(0.00)
FeO	3.96(1.08)	4.09(1.17)	5.12(1.38)	5.31(0.48)
Fe_2O_3	1.09(1.01)	0.92(0.91)	0.85(2.06)	0.34(0.77)
Total	99.59(0.00)	99.59(0.00)	101.45(0.00)	100.47(0.00)
Cations				
(Si)	1.948(0.044)	1.956(0.024)	1.984(0.058)	2.004(0.032)
(Ti)	0.002(0.002)	0.003(0.002)	0.001(0.000)	0.001(0.000)
(Al)	0.053(0.040)	0.044(0.030)	0.007(0.005)	0.006(0.003)
(Mn)	0.006(0.001)	0.005(0.001)	0.005(0.001)	0.005(0.002)
(Mg)	0.847(0.033)	0.858(0.032)	0.811(0.038)	0.796(0.039)
(Ca)	0.950(0.035)	0.948(0.027)	0.979(0.024)	0.987(0.023)
(Na)	0.010(0.008)	0.009(0.008)	0.003(0.004)	0.001(0.000)
(K)	0.001(0.001)	0.000(0.001)	0.002(0.000)	0.002(0.000)
(F_2)	0.121(0.033)	0.126(0.037)	0.156(0.044)	0.163(0.017)
(F_3)	0.060(0.055)	0.050(0.049)	0.044(0.107)	0.018(0.041)
Sum	3.999(0.000)	3.999(0.000)	3.992(0.000)	3.984(0.000)

	355B-1 n = 7	46B-2 n = 5	36 n = 6	43CPORPH n = 4
SiO_2	52.62(0.51)	47.69(0.93)	53.13(0.79)	52.34(0.14)
TiO_2	0.07(0.07)	0.67(0.21)	0.11(0.04)	0.10(0.02)
Al_2O_3	0.41(0.22)	6.40(1.42)	1.11(0.33)	1.43(0.09)
MnO	0.19(0.03)	0.05(0.01)	0.24(0.03)	0.21(0.04)
MgO	15.02(0.46)	14.13(0.56)	14.60(0.87)	14.95(0.16)
CaO	24.44(0.58)	24.88(0.16)	24.20(0.35)	23.29(0.61)
Na_2O	0.02(0.00)	0.03(0.01)	0.16(0.13)	0.23(0.07)
K_2O	0.03(0.00)	0.03(0.00)	0.03(0.00)	0.04(0.01)
FeO	4.51(1.20)	0.46(0.60)	5.18(1.00)	4.82(0.45)
Fe_2O_3	2.36(1.26)	5.19(0.42)	0.93(1.05)	0.79(0.67)
Total	99.66(0.00)	99.50(0.00)	99.69(0.00)	98.19(0.00)
Cations				
(Si)	1.926(0.033)	1.707(0.040)	1.957(0.028)	1.953(0.018)
(Ti)	0.002(0.002)	0.018(0.006)	0.003(0.001)	0.003(0.000)
(Al)	0.018(0.009)	0.270(0.059)	0.049(0.015)	0.063(0.003)
(Mn)	0.006(0.001)	0.001(0.000)	0.008(0.001)	0.007(0.001)
(Mg)	0.819(0.018)	0.754(0.034)	0.801(0.031)	0.831(0.005)
(Ca)	0.958(0.016)	0.954(0.010)	0.955(0.023)	0.931(0.025)
(Na)	0.002(0.000)	0.002(0.000)	0.011(0.010)	0.016(0.005)
(K)	0.001(0.000)	0.001(0.000)	0.001(0.000)	0.002(0.000)
(F_2)	0.139(0.039)	0.014(0.018)	0.160(0.031)	0.150(0.015)
(F_3)	0.129(0.067)	0.279(0.022)	0.051(0.056)	0.044(0.037)
Sum	4.000(0.000)	4.000(0.000)	3.996(0.000)	4.000(0.000)

	402B-1-R n = 7	402B-1-C n = 5	42A-1PC n = 4	43A-1PR n = 4
SiO_2	51.00(1.27)	50.99(2.07)	53.37(0.62)	53.81(0.16)
TiO_2	0.80(0.33)	0.71(0.36)	0.13(0.03)	0.20(0.11)
Al_2O_3	4.31(1.06)	3.95(1.54)	1.80(0.25)	1.87(0.19)
MnO	0.27(0.03)	0.26(0.06)	0.20(0.02)	0.33(0.27)
MgO	14.73(0.76)	14.61(0.88)	14.34(0.65)	14.03(0.74)
CaO	24.01(0.57)	24.03(0.69)	23.49(0.62)	23.69(1.23)
Na_2O	0.02(0.01)	0.03(0.02)	0.26(0.24)	0.18(0.11)
K_2O	0.03(0.00)	0.03(0.00)	0.03(0.00)	0.03(0.00)
FeO	3.68(0.85)	3.82(1.24)	5.27(0.69)	5.47(0.47)
Fe_2O_3	0.86(0.88)	0.92(1.46)	0.05(0.10)	0.00(0.00)
Total	99.71(0.00)	99.35(0.00)	98.94(0.00)	99.60(0.00)
Cations				
(Si)	1.868(0.048)	1.876(0.071)	1.981(0.011)	1.986(0.012)
(Ti)	0.022(0.009)	0.020(0.010)	0.004(0.001)	0.006(0.003)
(Al)	0.186(0.046)	0.171(0.066)	0.079(0.012)	0.081(0.008)
(Mn)	0.008(0.001)	0.008(0.002)	0.006(0.001)	0.010(0.008)
(Mg)	0.804(0.038)	0.801(0.046)	0.793(0.029)	0.772(0.040)
(Ca)	0.942(0.016)	0.947(0.034)	0.934(0.020)	0.937(0.045)
(Na)	0.002(0.000)	0.002(0.001)	0.019(0.017)	0.013(0.008)
(K)	0.001(0.000)	0.001(0.000)	0.001(0.000)	0.001(0.000)
(F_2)	0.119(0.027)	0.118(0.039)	0.164(0.022)	0.169(0.015)
(F_3)	0.047(0.048)	0.051(0.080)	0.003(0.006)	0.000(0.000)
Sum	3.995(0.000)	3.995(0.000)	3.984(0.000)	3.975(0.000)

	494C-R n = 4	494C-C n = 5	500E n = 9	500F n = 6
SiO_2	50.65(0.78)	51.10(0.78)	54.37(0.57)	53.05(1.15)
TiO_2	0.10(0.01)	0.09(0.02)	0.04(0.01)	0.08(0.10)
Al_2O_3	6.42(0.86)	5.19(0.90)	1.27(0.57)	2.26(0.97)
MnO	0.04(0.01)	0.06(0.01)	0.04(0.00)	0.05(0.01)
MgO	14.63(0.37)	15.17(0.48)	16.82(0.64)	16.08(0.69)
CaO	24.65(0.20)	24.95(0.25)	24.95(0.35)	25.34(0.22)
Na_2O	0.05(0.02)	0.05(0.02)	0.08(0.07)	0.06(0.05)
K_2O	0.03(0.00)	0.03(0.00)	0.03(0.00)	0.03(0.00)
FeO	2.42(0.00)	1.79(0.00)	1.54(0.00)	1.81(0.00)
Fe_2O_3	0.00(0.00)	0.43(0.40)	0.04(0.13)	0.71(0.64)
Total	98.99(0.00)	98.86(0.00)	99.19(0.00)	99.48(0.00)
Cations				
(Si)	1.862(0.021)	1.873(0.024)	1.984(0.013)	1.934(0.032)
(Ti)	0.003(0.000)	0.003(0.001)	0.001(0.000)	0.002(0.003)
(Al)	0.278(0.037)	0.224(0.040)	0.055(0.025)	0.097(0.041)
(Mn)	0.001(0.000)	0.002(0.000)	0.001(0.000)	0.001(0.000)
(Mg)	0.802(0.020)	0.829(0.021)	0.915(0.032)	0.874(0.035)
(Ca)	0.971(0.003)	0.980(0.003)	0.976(0.011)	0.990(0.014)
(Na)	0.003(0.001)	0.004(0.002)	0.006(0.005)	0.004(0.004)
(K)	0.001(0.000)	0.001(0.000)	0.001(0.000)	0.001(0.000)
(F_2)	0.074(0.000)	0.055(0.000)	0.058(0.000)	0.057(0.000)
(F_3)	0.000(0.000)	0.024(0.020)	0.002(0.007)	0.039(0.035)
Sum	3.998(0.000)	4.000(0.000)	4.000(0.000)	4.000(0.000)

	528A1-MT n = 11	528A1-MB n = 8
SiO_2	47.30(0.97)	43.99(0.55)
TiO_2	0.45(0.07)	0.39(0.04)
Al_2O_3	8.21(0.86)	11.48(0.49)
MnO	0.17(0.03)	0.12(0.02)
MgO	13.15(0.52)	11.59(0.32)
CaO	24.33(0.20)	24.80(0.19)
Na_2O	0.04(0.01)	0.02(0.01)
K_2O	0.03(0.00)	0.03(0.00)
FeO	1.90(0.00)	0.21(0.00)
Fe_2O_3	4.06(0.83)	7.14(0.76)
Total	99.62(0.00)	99.48(0.00)
Cations		
(Si)	1.705(0.038)	1.561(0.028)
(Ti)	0.012(0.002)	0.010(0.001)
(Al)	0.349(0.036)	0.480(0.019)
(Mn)	0.005(0.001)	0.004(0.000)
(Mg)	0.707(0.029)	0.613(0.019)
(Ca)	0.940(0.008)	0.943(0.009)
(Na)	0.003(0.001)	0.002(0.001)
(K)	0.001(0.000)	0.001(0.000)
(F_2)	0.057(0.000)	0.006(0.000)
(F_3)	0.220(0.045)	0.382(0.038)
Sum	4.000(0.000)	4.000(0.000)

Mineral assemblages of rodingites and diopside compositions analyzed by Jack (personal communication)

Mineral assemblages of rodingites from Paddy-Go-Easy Pass, Washington. (all mineral assemblages have calcite, ±clintonite, and ±wollastonite.

	Di*	Tr	Gr	Zo	Pl	Ch	Sp
IR1.2	p		p	p	p	p	
IR2.1	p			p	p		
IR2.2	p		p	p			
IR3.1				p	p		
IR3.1R	p	p	p	p	p		
IR15.1	p			p	p		
IR15.2	p			p	p	p	p
IR18.1	p			p	p	p	p
IR20	p	p			p		p
IR25.2	p			p			
IR27.2	p			p			
IR29.3	p		p	p			
IR30.1	p	p		p	p		
IR36	p		p	p		p	
IR36.2	p			p			
IR36.3	p	p	p	p			
IR51.2A	p		p	p			
IR51.2B	p		p				
IR51.4B	p						
IR54.4	p						
IR57.2	p			p	p	p	p

---

* Di=diopside, Tr=trmolite, Gr=grossular, Zo=zoisite, Pl=plagioclase, Ch=chlorite, Sp=spinel.

	IR1.2 n = 2	IR2.1 n = 10	IR2.2 n = 2	IR3.1R n = 5
SiO_2	52.89(0.65)	53.59(0.20)	53.75(0.57)	52.36(0.81)
TiO_2	0.10(0.07)	0.08(0.02)	0.08(0.01)	0.07(0.07)
Al_2O_3	2.78(0.70)	1.47(0.22)	0.78(0.18)	0.89(0.31)
FeO*	3.26(0.11)	3.83(0.16)	3.09(0.00)	8.80(1.07)
CaO	0.13(0.01)	0.19(0.03)	16.55(0.08)	0.32(0.13)
MnO	16.70(0.81)	16.66(0.11)	24.29(0.33)	11.98(0.29)
MgO	24.49(1.43)	23.27(0.40)	0.18(0.03)	25.06(0.32)
Na_2O	0.13(0.14)	0.28(0.03)	0.03(0.01)	0.13(0.04)
K_2O	0.03(0.01)	0.03(0.02)	0.00(0.00)	0.00(0.00)
Total	100.50(0.00)	99.38(0.00)	98.75(0.00)	99.61(0.00)
Cations				
(Si)	1.929(0.007)	1.980(0.005)	2.147(0.008)	1.942(0.024)
(Ti)	0.003(0.002)	0.002(0.001)	0.002(0.000)	0.002(0.002)
(Al)	0.119(0.029)	0.064(0.010)	0.037(0.008)	0.039(0.014)
(Fe)	0.099(0.003)	0.118(0.005)	0.103(0.001)	0.273(0.034)
(Ca)	0.005(0.001)	0.007(0.001)	0.708(0.009)	0.013(0.005)
(Mn)	0.516(0.021)	0.521(0.003)	0.822(0.017)	0.377(0.009)
(Mg)	1.332(0.089)	1.282(0.028)	0.011(0.002)	1.386(0.015)
(Na)	0.009(0.010)	0.020(0.002)	0.002(0.001)	0.009(0.003)
(K)	0.001(0.001)	0.002(0.001)	0.000(0.000)	0.000(0.000)
Sum	4.014(0.000)	3.996(0.000)	3.833(0.000)	4.041(0.000)

	IR15.1 n = 5	IR15.2 n = 9	IR18.1 n = 7	IR20 n = 3
SiO_2	52.56(1.29)	52.52(0.83)	53.07(1.36)	53.03(1.41)
TiO_2	0.12(0.05)	0.18(0.09)	0.03(0.04)	0.35(0.10)
Al_2O_3	2.15(1.03)	2.68(0.78)	1.77(1.21)	3.04(2.39)
FeO*	4.73(1.10)	3.46(0.44)	2.94(0.61)	3.48(0.96)
CaO	0.12(0.02)	0.11(0.03)	0.08(0.03)	0.07(0.03)
MnO	14.87(0.63)	15.59(0.55)	16.32(0.66)	15.67(1.27)
MgO	25.27(0.17)	25.25(0.37)	25.57(0.15)	24.94(0.05)
Na_2O	0.14(0.13)	0.09(0.04)	0.04(0.04)	0.02(0.02)
K_2O	0.03(0.01)	0.00(0.00)	0.01(0.02)	0.02(0.01)
Total	99.99(0.00)	99.87(0.00)	99.83(0.00)	100.60(0.00)
Cations				
(Si)	1.927(0.032)	1.922(0.023)	1.943(0.038)	1.924(0.064)
(Ti)	0.003(0.001)	0.005(0.002)	0.001(0.001)	0.009(0.003)
(Al)	0.093(0.045)	0.116(0.034)	0.076(0.052)	0.129(0.101)
(Fe)	0.145(0.035)	0.106(0.014)	0.090(0.019)	0.105(0.028)
(Ca)	0.005(0.001)	0.004(0.001)	0.003(0.001)	0.003(0.001)
(Mn)	0.462(0.016)	0.483(0.017)	0.506(0.020)	0.482(0.042)
(Mg)	1.382(0.006)	1.377(0.017)	1.396(0.017)	1.349(0.012)
(Na)	0.010(0.009)	0.006(0.003)	0.003(0.003)	0.001(0.001)
(K)	0.002(0.001)	0.000(0.000)	0.000(0.001)	0.001(0.000)
Sum	4.029(0.000)	4.019(0.000)	4.019(0.000)	4.003(0.000)

	IR25.2 n = 12	IR27.2 n = 9	IR29.3 n = 8	IR30.1 n = 4
SiO_2	52.79(1.00)	53.38(0.62)	54.39(0.70)	52.67(0.14)
TiO_2	0.23(0.30)	0.14(0.42)	0.04(0.03)	0.12(0.13)
Al_2O_3	1.10(1.32)	1.17(0.35)	0.20(0.09)	0.74(0.29)
FeO*	8.81(1.13)	6.07(1.66)	5.58(1.64)	10.40(0.56)
CaO	0.29(0.08)	0.34(0.05)	0.29(0.03)	0.20(0.05)
MnO	12.70(0.62)	14.20(0.87)	14.94(1.01)	12.29(0.49)
MgO	24.21(0.51)	24.76(0.38)	24.49(0.46)	24.12(0.27)
Na_2O	0.08(0.04)	0.10(0.04)	0.04(0.05)	0.12(0.07)
K_2O	0.01(0.02)	0.03(0.03)	0.00(0.00)	0.00(0.00)
Total	100.24(0.00)	100.20(0.00)	99.97(0.00)	100.66(0.00)
Cations				
(Si)	1.949(0.041)	1.958(0.017)	1.997(0.016)	1.948(0.013)
(Ti)	0.007(0.008)	0.004(0.001)	0.001(0.001)	0.003(0.004)
(Al)	0.048(0.057)	0.051(0.015)	0.009(0.004)	0.032(0.013)
(Fe)	0.272(0.036)	0.186(0.052)	0.172(0.051)	0.322(0.018)
(Ca)	0.011(0.003)	0.014(0.002)	0.011(0.001)	0.008(0.002)
(Mn)	0.397(0.020)	0.441(0.026)	0.465(0.028)	0.385(0.013)
(Mg)	1.333(0.024)	1.354(0.016)	1.341(0.019)	1.330(0.018)
(Na)	0.006(0.003)	0.007(0.003)	0.003(0.004)	0.009(0.005)
(K)	0.001(0.001)	0.001(0.001)	0.000(0.000)	0.000(0.000)
Sum	4.024(0.000)	4.017(0.000)	3.999(0.000)	4.037(0.000)

	IR36 n = 10	IR36.2 n = 9	IR36.3 n = 7	IR51.2A n = 6
SiO_2	54.30(0.64)	53.36(0.25)	53.31(0.17)	54.52(0.40)
TiO_2	0.04(0.03)	0.06(0.04)	0.09(0.04)	0.00(0.01)
Al_2O_3	0.57(0.46)	0.27(0.23)	0.64(0.50)	0.10(0.05)
FeO*	8.15(0.80)	7.45(1.34)	7.16(1.00)	4.47(0.20)
CaO	0.25(0.06)	0.45(0.10)	0.21(0.02)	0.18(0.06)
MnO	13.03(0.61)	13.24(0.89)	13.39(0.41)	15.40(0.53)
MgO	24.30(0.52)	24.64(0.30)	24.52(0.27)	25.38(0.19)
Na_2O	0.07(0.04)	0.02(0.01)	0.06(0.02)	0.04(0.01)
K_2O	0.00(0.01)	0.00(0.00)	0.00(0.00)	0.01(0.01)
Total	100.70(0.00)	99.49(0.00)	99.37(0.00)	100.10(0.00)
Cations				
(Si)	1.986(0.012)	1.977(0.012)	1.974(0.012)	1.994(0.007)
(Ti)	0.001(0.001)	0.002(0.001)	0.002(0.001)	0.000(0.000)
(Al)	0.024(0.020)	0.012(0.010)	0.028(0.022)	0.004(0.002)
(Fe)	0.249(0.024)	0.231(0.041)	0.222(0.030)	0.137(0.006)
(Ca)	0.010(0.002)	0.018(0.004)	0.008(0.001)	0.007(0.002)
(Mn)	0.404(0.019)	0.415(0.027)	0.420(0.014)	0.477(0.015)
(Mg)	1.325(0.029)	1.361(0.017)	1.354(0.018)	1.383(0.014)
(Na)	0.005(0.003)	0.001(0.001)	0.004(0.001)	0.003(0.001)
(K)	0.000(0.000)	0.000(0.000)	0.000(0.000)	0.000(0.000)
Sum	4.004(0.000)	4.016(0.000)	4.012(0.000)	4.005(0.000)

	IR51.2B n = 6	IR51.4B n = 8	IR54.4 n = 10	IR57.2 n = 7
SiO_2	52.90(0.71)	51.01(0.29)	52.92(0.38)	54.59(1.03)
TiO_2	0.03(0.02)	0.03(0.01)	0.41(0.11)	0.10(0.05)
Al_2O_3	0.93(1.02)	0.36(0.25)	3.15(0.58)	1.45(0.52)
FeO*	7.02(1.98)	14.53(0.71)	4.05(0.28)	2.97(0.31)
CaO	0.47(0.05)	0.40(0.03)	0.14(0.02)	0.17(0.02)
MnO	13.37(1.14)	9.23(0.80)	15.55(0.35)	16.52(0.35)
MgO	24.84(0.75)	23.81(0.27)	22.47(0.45)	24.80(0.44)
Na_2O	0.04(0.04)	0.08(0.04)	0.54(0.04)	0.08(0.13)
K_2O	0.00(0.00)	0.02(0.02)	0.03(0.02)	0.00(0.00)
Total	99.58(0.00)	99.48(0.00)	99.25(0.00)	100.68(0.00)
Cations				
(Si)	1.957(0.034)	1.929(0.004)	1.951(0.014)	1.978(0.023)
(Ti)	0.001(0.001)	0.001(0.000)	0.011(0.003)	0.003(0.001)
(Al)	0.040(0.044)	0.016(0.011)	0.137(0.025)	0.062(0.022)
(Fe)	0.217(0.061)	0.459(0.023)	0.125(0.009)	0.090(0.009)
(Ca)	0.018(0.002)	0.016(0.001)	0.005(0.001)	0.007(0.001)
(Mn)	0.419(0.036)	0.296(0.025)	0.486(0.011)	0.507(0.014)
(Mg)	1.369(0.037)	1.342(0.017)	1.235(0.024)	1.340(0.031)
(Na)	0.003(0.003)	0.006(0.003)	0.039(0.003)	0.005(0.009)
(K)	0.000(0.000)	0.001(0.001)	0.001(0.001)	0.000(0.000)
Sum	4.024(0.000)	4.066(0.000)	3.989(0.000)	3.991(0.000)

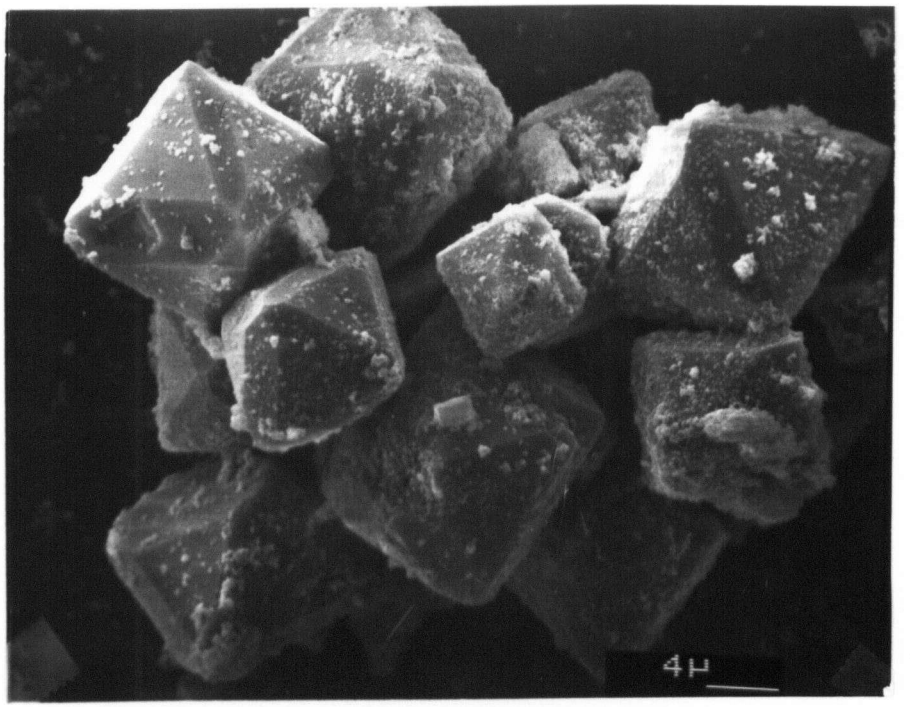

Plate 1 General view of synthetic spinel. The fine powder is also spinel according to E.D.S. analysis.

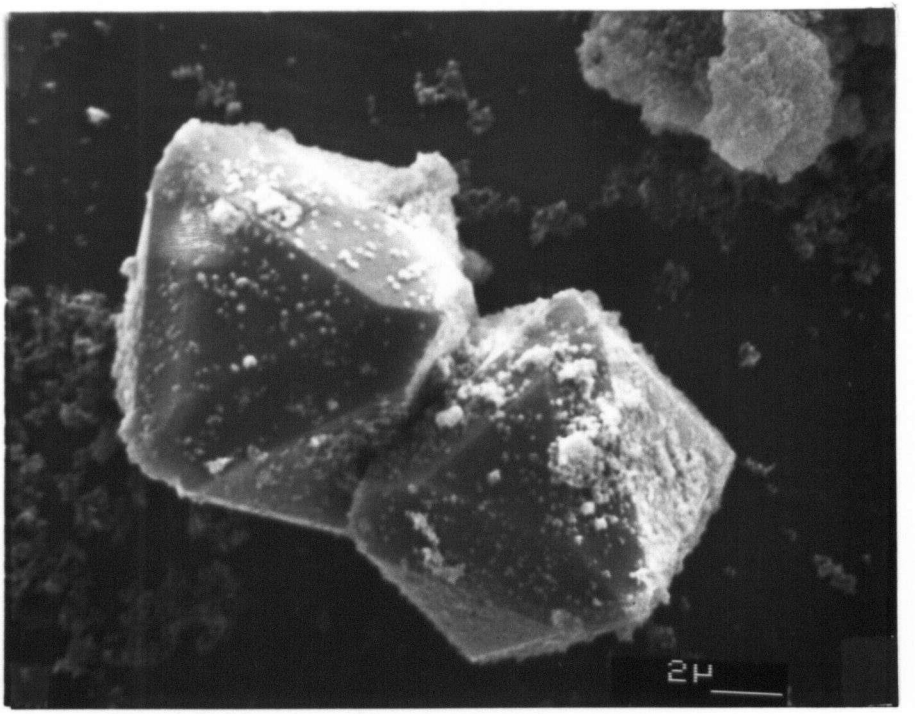

Plate 2 Euhedral crystals of synthetic spinel with surfaces of (1 1 1) and (1 1 0).

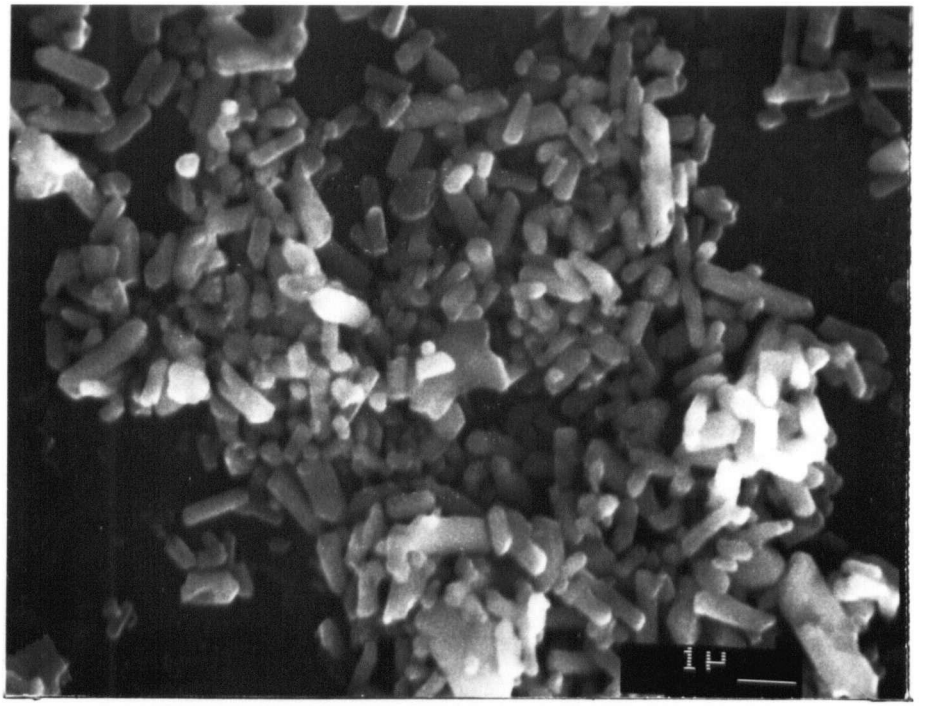

Plate 3 Subhedral to euhedral crystals of synthetic diopside.

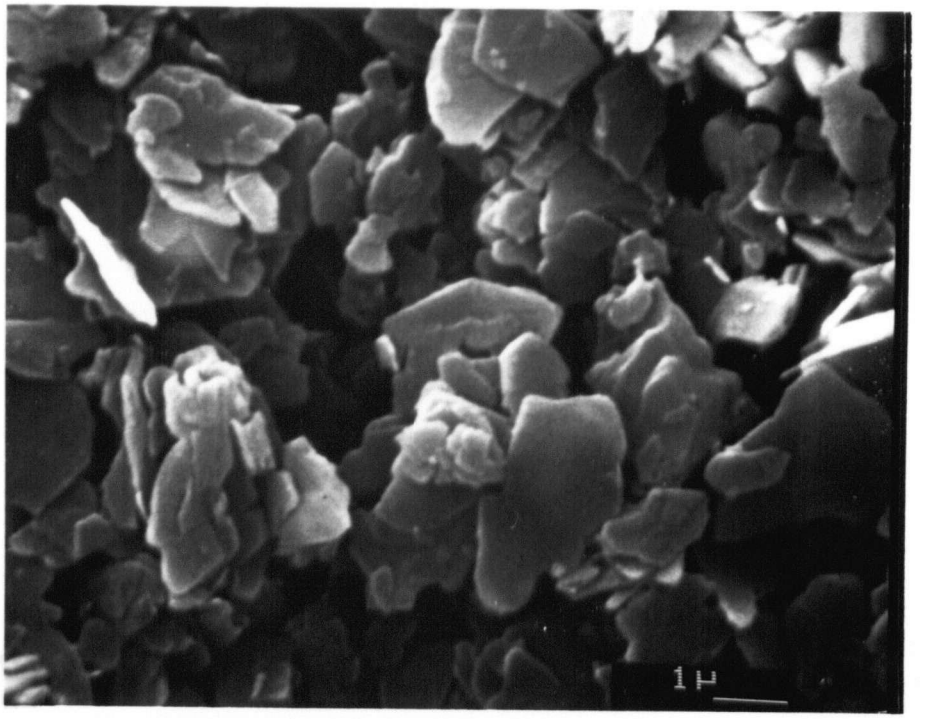

Plate 4 Synthetic clinochlore with subhedral crystals.

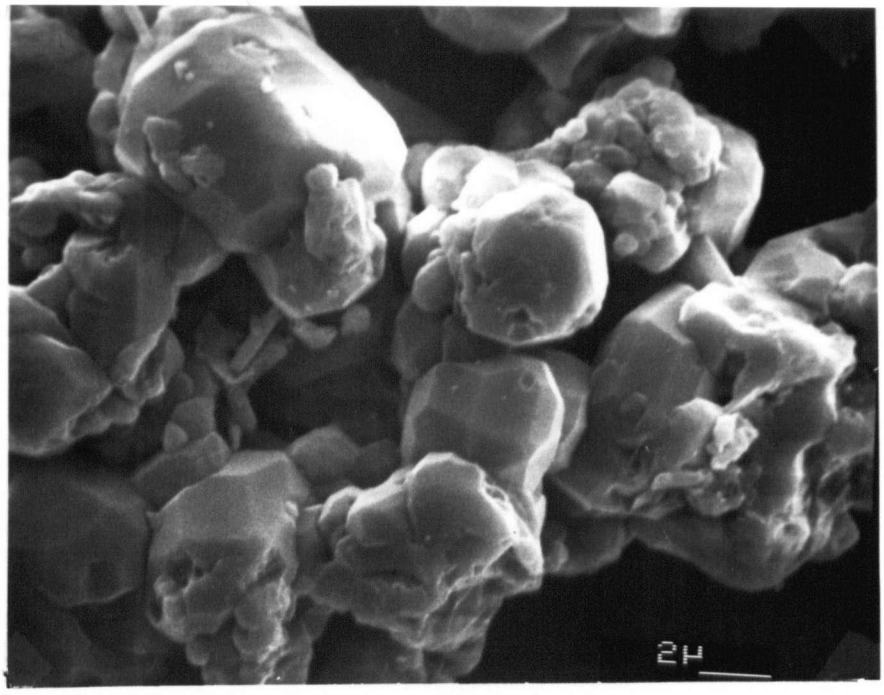

Plate 5 Synthetic grossular with euhedral to subhedral crystals and some fine short prismatic wollastonite as impurities.

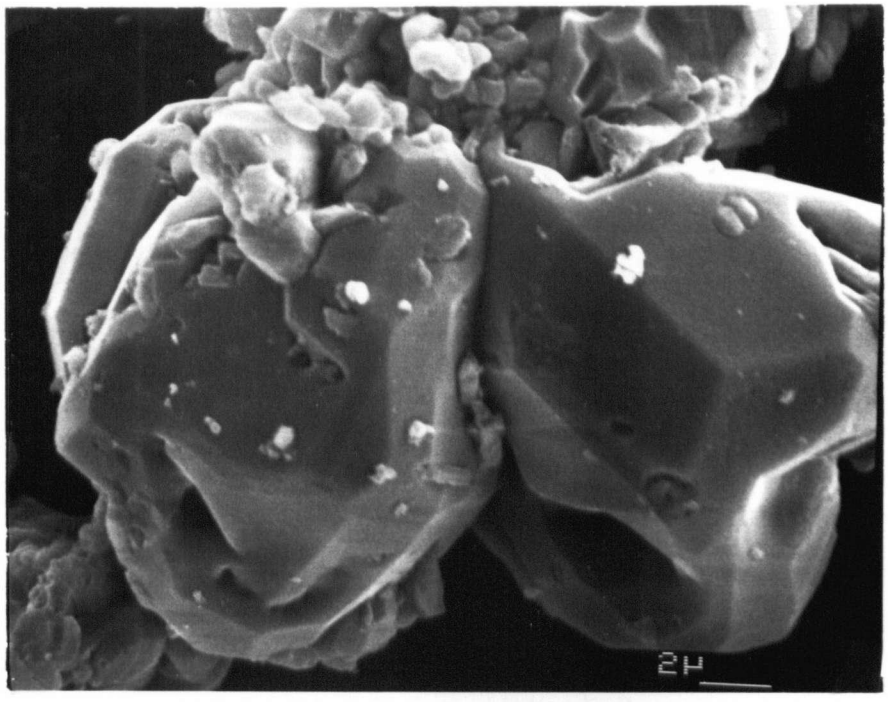

Plate 6 Close view of synthetic grossular crystals with some inclusions of oxides(?).

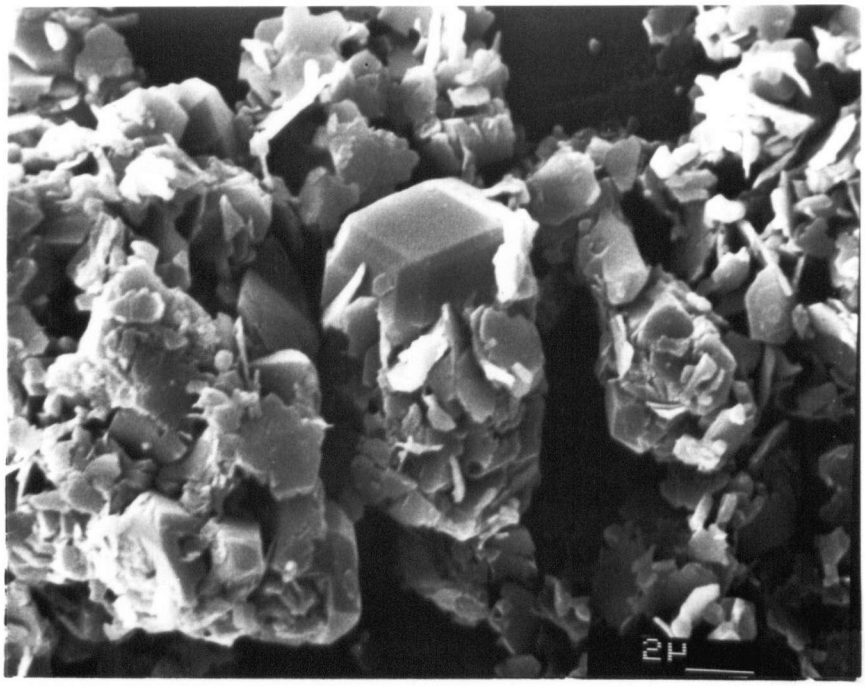

Plate 7 Low temperature stable assemblage of clinochlore + grossular. Notice the euhedral grossular crystals with surfaces of (1 1 1) and (1 1 0).

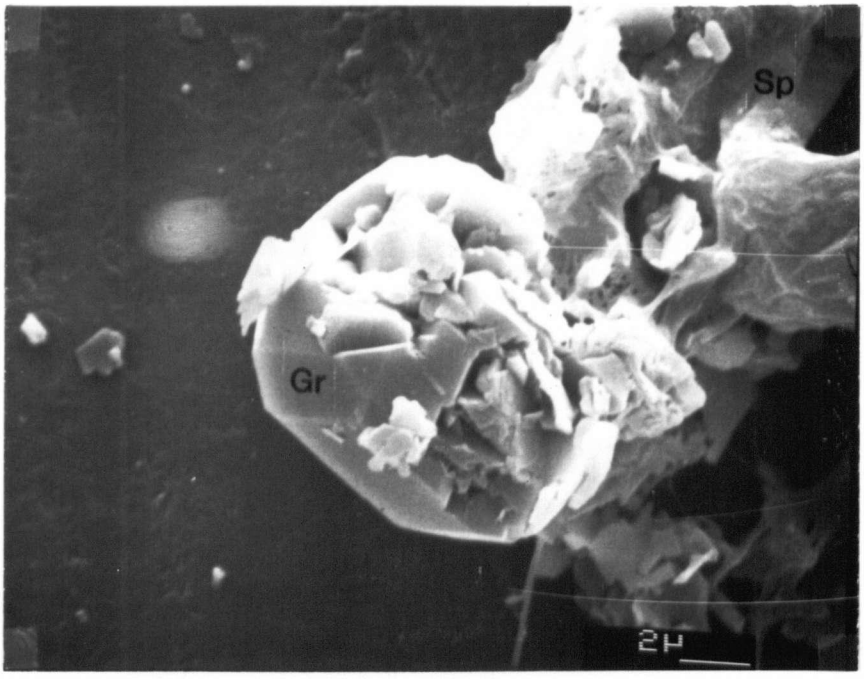

Plate 8 Grossular crystal growing near spinel crystals that were dissolved during equilibrium run. (Gr = grossular, Sp = spinel)

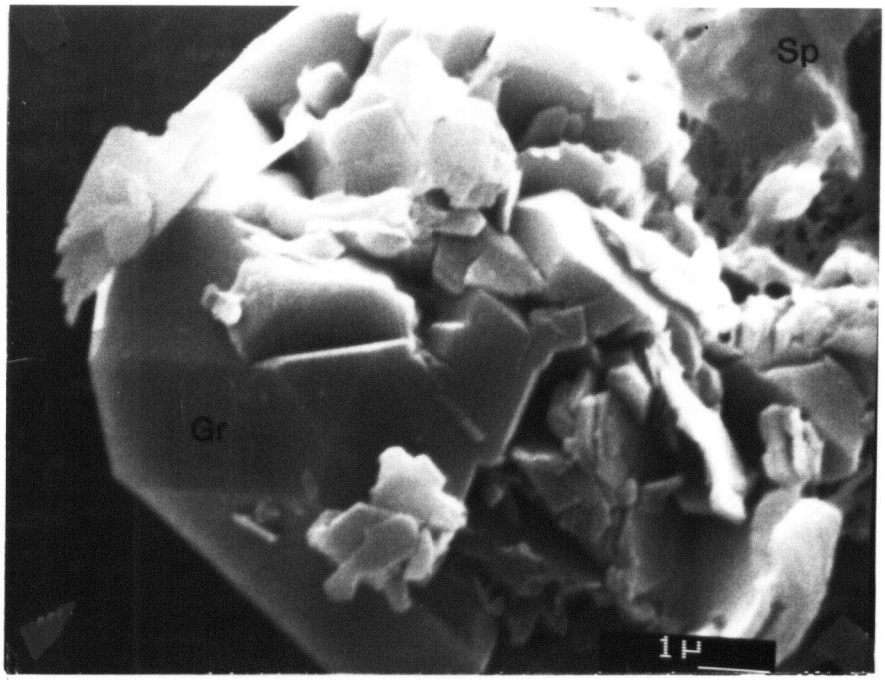

Plate 9 Grossular crystal and residual spinel crystals with many small holes.(Gr = grossular, Sp= spinel)

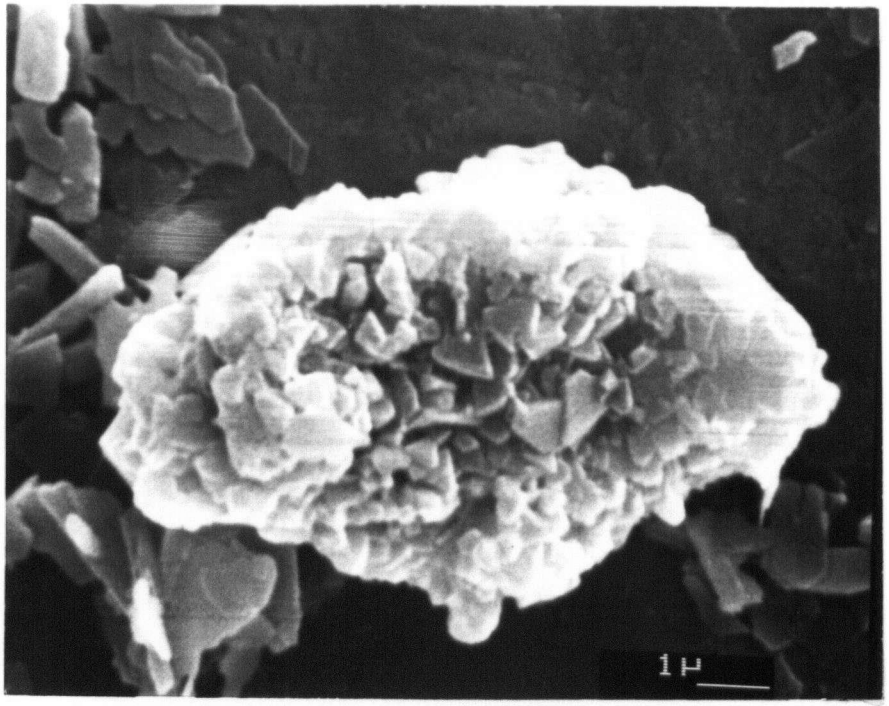

Plate 10 The aggregate of fine spinels from high temperature stable assemblage diopside + spinel. Plates of residual clinochlore are visible.

Plate 11 The abnormal assemblage of diopside + clinochlore from starting material 80wt% diopside + spinel with 20wt% grossular + clinochlore. Notice the euhedral crystals of both minerals.

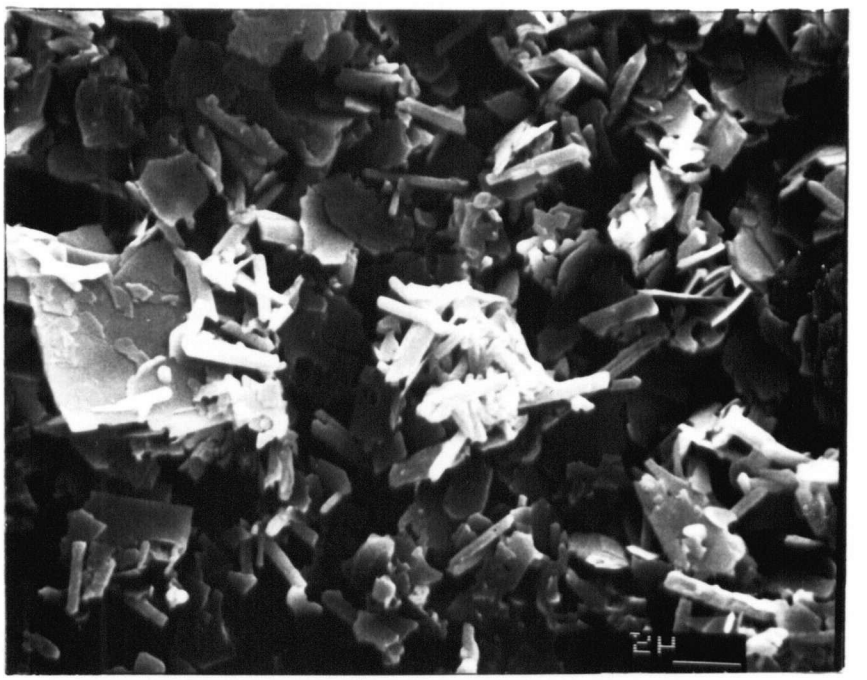

Plate 12 The abnormal assemblage diopside + clinochlore from starting material 80wt% grossular + clinochlore with 20wt% diopside + spinel. Notice that most crystals are subhedral.